ANALYSIS OF GLOBAL GENE EXPRESSION PROFILES AND INVASION RELATED GENES OF COLORECTAL LIVER METASTASIS

DISSERTATION

Zur Erlangung des akademischen Grades

doctor rerum naturalium

(Dr. rer. nat.)

im Fach Biologie

eingereicht an

Mathematisch-Naturwissenschaftlichen Fakultät I

der Humboldt-Universität zu Berlin

von
MSc.Biotechnology. Obul Reddy Bandapalli
geboren am 01.06.1977 in Madanapalli, Indien

Präsident der Humboldt-Universität zu Berlin
Prof. Dr. Christoph Markschies

Dekan der Mathematisch-Naturwissenschaftlichen Fakultät I
Prof. Dr. Christian Limberg

Gutachter
PD. Dr. Karsten Brand
Prof. Dr. Wolfgang Uckert
PD. Dr. Glen Kristiansen

Tag der mündlichen Prüfung: 31.08.2007

SELBSTSTÄNDIGKEITSERKLÄRUNG

Hiermit versichere ich, dass ich die vorliegende Arbeit selbstständig und nur unter Verwendung der angegebenen Literatur und Hilfsmittel angefertigt habe.
Desweiteren erkläre ich meine Kenntnisnahme der dem angestrebten Verfahren zugrunde liegenden Promotionsverordnung. Ich habe mich anderwärts nicht um einen Doktorgrad beworben und bin nicht im Besitz eines entsprechenden Doktorgrades.

Berlin, den……

Obul Reddy Bandapalli

To my Father (“Appa”)

For his self-set values and the wisdom with which

he raised me; always make a big difference in my life

CONTENTS

LIST OF FIGURES

LIST OF TABLES

Acknowledgements

I am indebted to my supervisor PD. Dr.Karsten Brand, not only for introducing me to the exciting field of genomics but also for his motivating words, constructive criticism day after day, help, financial support and friendship.

I would like to thank Prof. Peter Schirmacher for all his support and encouragement during my work at the Institute of Pathology.

I am very grateful to Prof. Wolfgang Uckert and PD.Dr.Wolfgang Kemmner for hosting me at MDC.

I would like to thank Olaf, Kerstin, Sefer and all the CUSTOSians for a good start to my research in Germany with their friendly gesture at Custos Biotechnolgie GmbH.

Many thanks to Victoria, Nawid, Heiko, Christoph and all the colleagues whose friendship and support have made it more than a working place at Pathology institute in Heidelberg.

I am thankful to Dr. Ralf Weiskirchen, Dr. Dieter Beule, Dr.Susanne Dihlmann, Prof.Jürgen Weitz and Dr.Hanspeter Herzel for embarking with me on this thesis journey. Their contributions, in immunohistochemistry, bioinformatics and human liver metastasis samples have been of great value to the success of my thesis.

I also owe a lot to Mrs. Bonn at MDC and Mrs. Annette Weninger at DKFZ for their help in scanning the microarray chips.

I have to say 'thank-you' to: all my dear friends and well-wishers for all the emotional support, entertainment and caring they provided me over the past years. You are so many that to thank you all personally would take another thesis, but you know who you are and I am ever grateful to you all. Thanks to Shilpa for proofreading the thesis and for everything. Schoeppler´s family is a true substitute for my home in Germany; I am blessed to have met you.

Thanks to the European Union for financial support under frame work 6 “Cancer Degradome”.

Finally, I thank my family for everything. It is their love and support for what I am today.

Abbreviations

^0C	Degree Centigrade
A	Adenosine
Apaf-1	Apoptosis protease activating factor 1
Apof	Apolipoprotein
APS	Ammoniumpersulphate
ATP	Adenosine Triphosphate
bp	Base pair
CO2	Carbon dioxide
cDNA	Complementary DNA
CXCL1	Canonical Cysteine-any amino acid Cysteine Ligand 1
CXCL2	Canonical Cysteine-any amino acid Cysteine Ligand 2
CXCL3	Canonical Cysteine-any amino acid Cysteine Ligand 3
CXCL5	Canonical Cysteine-any amino acid Cysteine Ligand 5
DMSO	Dimethyl Sulphoxide
DNA	Deoxyribonucleic Acid
dNTP	Deoxyribonucleosidetriphosphate
DTT	1, 4-Dithiothreitol
ECL	Enhanced Chemiluminescence
EDTA	Ethylenediaminetetraacetate
et al	et alii (and others)
EtBr	Ethidium Bromide
FCS	Fetal Calf Serum
g	Gram
GO	Gene Ontology
GCOS	Gene Chip Operating Software
h	Hour
IHC	Immunohistochemistry
IL-8	Interleukin-8
IgG	Immunoglobulin G
IVT	*In vitro* Transcription
Kb	Kilobase
kDa	Kilo Dalton
l	Liter
LB	Luria Bertoni Broth Medium
LSB	Lamaelli Sample Buffer
M	Molar
mM	MilliMolar
mA	Milliampere
mg	Milligram
min	Minute
ml	Milliliter
µg	Microgram
µl	Microliter
µM	Micromolar
mM	Millimolar
mRNA	Messenger RNA
ng	Nanogram
N_2	Nitrogen

PAGE	Poly Acrylamide Gel Electrophoresis
PBS	Phosphate Buffered Saline
PBS-T	Phosphate Buffered Saline with 0.1% Tween 20
PCR	Polymerase Chain Reaction
qPCR	Quantitative Polymerase Chain Reaction
RNA	Ribonucleic acid
RNAsin	RNAase inhibitor
RPM	Rotations per Minute
RT	Room Temperature
RT-PCR	Reverse Transcriptase- Polymerase Chain Reaction
SDS	Sodium Dodecyl (lauryl) Sulphate
Sec	Second
TAE	Tris-Acetate-EDTA
Taq	Thermophilus aquaticus
TBS	Tris Buffered Saline
TBS-T	Tris Buffered Saline with 0.1% Tween 20
TE	Tris EDTA
TEMED	N,N,N,N -Tetramethyl-Ethylenediamine
Tris	Tris Hydroxymethylaminoethane
U	Unit
UV	Ultraviolet
V	Volt

Abstract

The liver is the organ, which is most frequently populated by metastases and may therefore serve as a model organ for metastatic invasion. For this reason, it was the aim of this thesis to understand the gene expression profiles and identify metastasis and invasion related genes.

Differential gene expression was examined in three systems: A syngeneic mouse model (CT26/Balb/C mouse), a xenograft model (LS174/nude mouse) and five clinical specimens.

Gene expression profiles of a syngenic mouse model (CT26) and human clinical specimen revealed that the invasion front should be considered as a whole instead of separating it into histologically defined liver invasion and tumor invasion to find more overlapping potential target genes. This indicates that gene expression patterning may aid in the assessment of the suitability of an animal model for target gene determination.

Global gene expression studies focussed on the host part of the invasion front, using gene ontology terms and GOSSIP software revealed a pronounced overrepresentation of GO-terms (e.g. “extracellular matrix”, “cell communication”, “response to biotic stimulus”, “structural molecule activity” and “cell growth”). On the single gene level hepatic stellate cell (HSC) activation markers were over-represented in this region demonstrating the feasibility of a differential gene expression approach on a genome wide scale.

Global gene expression studies focusing on the tumor cells *in vitro, in vivo* and tumor part of the invasion front revealed an overall increase of cellular specialization from *in vitro* to the *in vivo* situation and a further increase of specialization from tumor to invasion front. Secreted angiogenic cytokines (Invasion specific pattern) were found to be up regulated in the invasion front compared to the inner parts of the tumor. ß -catenin gene of “cell adhesion” GO term was elevated 9.6 fold in invasion front compared to *in vitro*. Evaluation of transcriptional up-regulation of ß-catenin by promoter activity showed an 18.4 fold increase in the tumor cells of the invasion front as compared to the tumor cells in the inner parts of the tumor. In addition, promoter activity as assessed by soluble human placental alkaline phosphatase reporter gene mRNA was 3.5 fold higher in the inner parts of the tumor than in cells growing in cell

culture indicating a transcriptional mechanism of β-catenin regulation in addition to the well described posttranslational regulatory mechanisms.

In summary, application of high throughput Oligonucleotide microarray analysis in combination with real time PCR technology allowed the identification of genes, which might play a role in proliferation, invasion and angiogenesis of tumors in colorectal liver metastasis.

Key words

Tumor-stromal cell interactions, invasion and metastasis, gene expression profiling, xenograft models, liver, β-catenin, cross-species.

Zusammenfassung

Die Leber ist das am häufigsten von Metastasen betroffene Organ und kann daher als Modellorgan für metastatische Invasion dienen. Aus diesem Grund war es das Ziel dieser Dissertation Genexpressionsprofile zu verstehen und metastasierungs- sowie invasionsassoziierte Gene zu identifizieren.

Differentielle Genexpression wurde in drei Systemen überprüft: Einem syngenen Mausmodell (CT26/Balb/C Maus, einem Xenograftmodell (LS 174/Nacktmaus) sowie in fünf Gewebeproben von Patienten.

Genexpressionprofile des syngenen Mausmodells (CT26) und der Patientenproben zeigten, dass man die Invasionsfront als Ganzes betrachten sollte und sie nicht in einen histologisch naheliegenden Leberteil und Tumorteil separieren sollte, um möglichst viele überlappende Gene zu finden. Diese Daten zeigen, dass die Ermittlung von Genexpressionsmustern bei der Prüfung der Eignung eines Tiermodells für die Ermittlung von Targetgenen helfen kann.

Globale Genexpressionstudien, die auf den Wirtsteil der Invasionsfront fokussiert sind zeigten bei Nutzung von „gene ontology terms“ und der „Gossip“ Software eine bemerkenswerte Überrepräsentation z. B. der „GO-terms“ „extrazelluläre Matrix“, Zellkommunikation“, „Antwort auf biotischen Stimulus“, Strukturmolekülaktivität“ und „Zellwachstum“. Auf der Einzelgenebene waren in dieser Region Marker der Aktivierung hepatischer Sternzellen (HSCs) überrepräsentiert, was die Durchführbarkeit einer Analyse differentieller Genexpression im genomweiten Rahmen anzeigt.

Globale Genexpressionsstudien, mit Fokus auf den Tumorzellen in der in vitro Situation, in vivo und in der Invasionsfront zeigten insgesamt einen Anstieg zellulärer Spezialisierung von der in vitro- zur in vivo Situation und einen weiteren Anstieg vom Tumorinneren zur Invasionsfront. Sezernierte proangiogenetische Chemokine (invasionsspezifisches Muster) zeigten eine Hochregulation in der Invasionsfront im Vergleich zum Tumorinneren. Das β-catenin -Gen (GO-term „cell adhesion“) war in der Invasionsfront 9.6 fach erhöht im Vergleich zur in vitro Situation. Die Überprüfung der transkriptionellen Aktivierung von β-catenin über die Prüfung der Promotoraktivität zeigte einen 18.4 fachen Anstieg in den Tumorzellen der Invasionsfront verglichen mit den Tumorzellen im Tumorinneren. Weiterhin war die

Promotoraktivität (an Hand der Aktivität der mRNA des Alkalischen Phosphatase Reportergens) im Tumorinneren 3.5 fach höher als in der Zellkultur, was für einen transkriptionellen Mechanismus der β-catenin Regulation zusätzlich zu den bereits gut beschriebenen posttranslationalen Mechanismen spricht.

Zusammenfassend kann man festhalten, dass die Hochdurchsatz-Oligonukleotid Mikroarray-Analyse in Kombination mit der real time PCR Technologie die Identifikation von Genen ermöglicht hat, die eine Rolle in Proliferation, Invasion und Angiogenese in kolorektalen Lebermetastasen spielen könnten.

Schlagworte

Tumor-stroma Zelle interaktionen, Invasion und Metastasierung, Gene Expression Profiling, genograft modelle, leber, β-catenin, Inter-spezies

1 Introduction

1.1 Epidemiology of colon cancer

Colorectal cancer, also called **colon cancer** or **bowel cancer**, includes cancerous growths in the colon, rectum and appendix. It is the third most common form of cancer and the second leading cause of death among cancers in the Western world. Many colorectal cancers are thought to arise from adenomatous polyps in the colon. These mushroom-like growths are usually benign, but some may develop into cancer over time. The majority of the time, the diagnosis of localized colon cancer is through colonoscopy. The most common colon cancer cell type is adenocarcinoma which accounts for 95% of cases. Other, rarer types include lymphoma and squamous cell carcinoma.Colon cancer incidence is not much different between males and females, however colon cancer is slightly more prevalent in women compared to men (ratio of 1.2:1) but the rectal cancer is more common in males (ratio of 1.7:1). Colon cancer is more common among elderly persons compared to younger persons. The risk of developing colon cancer begins to increase from the age of 40 and goes up with every passing year. The median age of presentation of colon cancer varies according to the country. In the United States the median age at presentation is 72 years. Colon cancer is more common in African Americans compared to the Caucasian population in the United States. The incidence of colon cancer has been on the increase in African Americans since 1973 and the incidence in this ethnic group has gone up by about 30 percent during the last 3 decades. Incidence of colorectal cancer varies widely from country to country. Countries which are more industrialized like United States, Canada, UK, Western Europe, Australia have a much higher incidence of colorectal cancer compared to less industrialized parts of the world like Asia, Africa, and South America. The American Cancer Society estimates that about 145,000 cases of colorectal cancer will be diagnosed and about 56,000 people will die from the disease in 2005. The death rate from colon cancer has declined over the past 15 years due to improved screening methods and advances in treatment.

1.2 Etiology of colon caner

Age is the primary risk factor. Incidence of the disease increases significantly after the age of 50. Some people have a **genetic** predisposition to carcinogenic (i.e., cancer causing) effects of the diet on the digestive tract, which increases the risk for

colorectal cancer. When this predisposition is combined with a high dietary intake of fat and red meat and a low dietary intake of fiber (e.g., bran), vitamins (e.g., folate), and minerals (e.g., calcium), the risk is even higher. **Ashkenazi Jews** have a higher incidence of a specific genetic mutation (called I1307K) that increases the risk for colorectal cancer. Daily alcohol use (may double the risk), eating a high-fat, low-fiber diet, obesity, sedentary lifestyle, Smoking. A **family history** of intestinal polyps or colorectal cancer (especially before the age of 60) results in an increased risk for the disease. Other diseases and medical conditions that increase the risk include diabetes, genetic disorders such as familial polyposis syndromes and hereditary non-polyposis colon cancer syndrome (HNPCC), inflammatory bowel disease (e.g., ulcerative colitis, Crohn's colitis, granulomatous colitis). (**Familial polyposis syndromes** are rare genetic (i.e., inherited) conditions characterized by early onset of multiple intestinal polyps (called **polyposis**) and a very high (virtually 100%) risk for colorectal cancer. Familial adenomatous polyposis (characterized by as many as thousands of polyps throughout the entire colon), **Hereditary nonpolyposis colon cancer (HNPCC) syndrome** is a genetic condition characterized by early-onset colorectal cancer (i.e., develops before age 50) and multiple colorectal cancers).

1.3 Prognosis of colon caner

Colorectal cancer can be asymptomatic (i.e., it may not cause symptoms). **Blood in the stool** is a common sign of the disease. Blood may be bright red or dark in color, and may not be noticeable. Chronic bleeding may result in iron deficiency **anaemia**, which may cause fatigue and pale skin. Other symptoms include: Abdominal discomfort (e.g., pain, bloating, cramping, fullness), change in bowel habits, Constipation or diarrhoea, narrow stools, nausea and vomiting, unexplained weight loss and hepatomegaly (enlargement of the liver) due to spreading of the tumor. The survival rate for people with colorectal cancer depends on the extent of the cancer at the time of diagnosis and the individual’s response to treatment. In addition, many new discoveries have the potential for improving the treatment of colorectal cancer, as well as the prognosis. Prognosis depends on the stage of the disease and the overall health of the patient. Overall, colorectal cancer patients have a 5-year survival rate of about 61%. The 5-year survival rate is about 92% when the disease is treated before it has spread (metastasized); 64% when the cancer has spread to nearby

organs or lymph nodes; and 7% when it has spread to other parts of the body (e.g., liver, lungs).

1.4 Colorectal liver metastasis

The liver is the most common site of distant metastasis from colorectal cancer for two main reasons.

A. The liver filters the venous drainage from the intra-abdominal viscera, including the distal oesophagus, stomach, spleen, small bowel, colon, rectum, adrenals, pancreas, gallbladder, and biliary tree. Furthermore, the liver receives 30% of the cardiac output. Thus, the volume of blood filtered by the liver is second only to that filtered by the lungs.

B. Physiologically, the liver is occupied by numerous cell types capable of providing a rich milieu for tumor cell growth. Tumor cells that survive the systemic circulation may eventually reach the liver. If the tumor cells express the appropriate phenotype allowing progression through all stages of the metastatic cascade, then the result is a metastasis. The liver microenvironment consists of not only organ- specific cells, such as hepatocytes, but also endothelial cells, pericytes, inflammatory cells, Kupffer cells, fibroblasts, and the extracellular matrix, all of which provide a favourable milieu for tumor cell implantation and initiation of angiogenesis. (Radinsky et al., 1996)

1.5 Therapeutic approaches for colorectal liver metastasis

Clinical experience suggests that patients with colorectal liver metastases have heterogenous tumor biology. The ongoing trend is to include a surgical approach for more patients with liver metastases from colorectal carcinoma. With the addition of newer chemotherapeutics, survival has improved in patients treated both medically and surgically for metastatic colorectal cancer. The role of neoadjuvant chemotherapy is being clarified. The current approach is upfront surgery unless a lesion is considered unresectable. Neoadjuvant therapy may soon be recommended more frequently, however, as more predictable responses from the intervention occur. During the preoperative evaluation, attention needs to be focused on considering sufficient liver parenchyma and assessment for extra hepatic disease. Survival

benefits in patients undergoing a second liver resection have similar outcomes as those undergoing a primary resection. Regardless of the surgical resection, patients benefit most when tumor-free margins greater than 1 cm are achieved. If the margins are close, RFA or cryotherapy can be added to ensure an adequate depth. Resection remains a critical treatment modality for patients with colorectal liver metastases since it provides the only significant chance for cure or long-term survival. With the extraordinary advances made in chemotherapeutics as well as newer surgical techniques, metastatic colon cancer remains a potentially curable disease. Patients are best treated in a multimodality environment where a medical oncologist, a radiologist, and those skilled in hepatobiliary surgery plan and execute optimal therapy.

1.6 Physiopathology of Liver Metastasis

Spreading of cancer cells from their site of origin to distant organs, named metastasis is a major cause of therapy failure (Mareel et al., 1993). In colorectal cancer half of the cancer deaths are due to loco-regional extension and the other half due to distant metastasis. In order to metastasise, cancer cells must acquire the capability to invade into the vascular system, to survive and to proliferate at the place of metastasis. Invasion marks the onset of malignancy; cells are released from their normal epithelial context, lose polarity, perforate the basement membrane and finally migrate into the stroma. There, they meet with the vessels that provide a route for transport to distant sites such as the liver. Then, metastases emerge through proliferation of cancer cells that have left the vessel and lodged in the liver parenchyma or have formed an embolus in the vessel lumen and grown from that site. All these activities are intimately linked with alterations of a variety of host cells that are in continuous cross talk with the cancer cells (Mareel et al., 1993). The liver is a frequent site of metastasis from many types of primary tumours (Debois et al., 2002). Such high frequency and liver specificity cannot be explained solely by the blood flow in the efferent vessels, portal vein and hepatic arteries respectively.

Organ specificity of metastasis, as exemplified by the liver, is best explained by the “seed” and “soil” hypothesis by Paget in 1889 (Paget 1889). He raised the question “What is it that decides what organ shall suffer in a case of disseminated cancer?”. His answer was “The microenvironment of each organ (the soil) influences the survival and growth of tumour cells (the seed)”. This hypothesis is still valid and

serves as a rich source of inspiration for clinical and experimental analysis of metastasis. What modern research has added to Paget's seed and soil hypothesis mainly concerns the cellular and molecular mechanisms that underpin the cross talk between the cancer cells and their host.

A current definition of the "seed and soil" hypothesis consists of three principles. First, neoplasms are biologically heterogeneous and contain subpopulations of cells with different angiogenic, invasive, and metastatic properties. Second, although some of the steps in this process contain stochastic elements, metastasis as a whole favors the survival and growth of a few subpopulations of cells that pre-exist within the parent neoplasm. Thus, metastases can have a clonal origin, and different metastases can originate from the proliferation of different single cells. Third, the outcome of metastasis depends on multiple interactions ("cross talk") of metastatic cells with homeostatic mechanisms.

The cancer cells are the seed

Before cancer cells produce metastases, they undergo a series of genetic alterations, conveying upon them uncontrolled growth, loss of differentiation, acquisition of invasion and ectopic survival (Mareel et al., 2002).

The liver is the soil

1.6.1 The role of the host in metastasis

Numerous clinical and experimental observations support the role of host factors in the development and the malignancy of tumours. Pathologists have since a long time recognized that tumours contain not only cancer cells but also host cells. This host participation is described as desmoplasia, consisting of fibroblastic cells and extracellular matrix, as inflammation and immune response, represented by lymphocytes, macrophages and dendritic cells, and as angiogenesis evidenced by newly formed blood and lymph vessels (Mareel et al., 2003).

1.6.2 Specific growth or specific homing

The question whether cancer cells can home everywhere and grow only at distinct sites or whether they home only at specific sites but can grow everywhere is too simple. Metastasis is a multifactorial event including molecular crosstalking between cancer cells and host cells as well as the blood flow, carrying colorectal cancer cells

to the capillary bed of the liver via the portal vein. Growth is currently best explained in terms of neoangiogenesis (Carmeleit et al., 2000). When the balance between positive and negative angiogenic factors switches to the positive side, endothelial cells are stimulated to leave the constraints of the vessel wall; much like invasive cancer cells leave the epithelium. These endothelial cells migrate towards the cancer cell nest, proliferate and finally differentiate to make new vessels. Such vessels constitute not only a source of nutrients, growth factors and invasion factors but also provide access for host cells from distant sites, initiate further spread of the cancer cells and establish a link between the primary tumour and its metastases (O´Reilly et al., 1994). Homing of cells implicates a stepwise interaction between the circulating cancer cells and the endothelium that is regulated by the cross talk of cell adhesion molecules and chemokines with their respective receptors. Two molecular explanations have been forwarded for specific homing: expression of specific receptors on the surface of endothelial cells or release of specific chemokines, molecules exerting an attractive force on circulating cancer cells that bear specific receptors. Such chemo-attractants have been demonstrated for breast cancer (Müller et al., 2001).

Metastasis is a hallmark of malignancy in cancers of the gastrointestinal tract. In colorectal cancers as well as in cancers of many other organs, the liver is a predilection site for metastasis. This predilection is explained by the seed and soil theory, launched by Paget in 1889 (Paget 1889). The seed, cancer cells, need a series of genomic alterations in oncogenes and tumour-suppressor genes to invade, survive and grow in distant organs. The soil, the liver, produces attractants and growth factors that undertake molecular cross talk with the metastatic cancer cells. Understanding of the mechanisms of metastasis may assist in the treatment.

Besides unrestricted proliferation and reduced apoptosis, unbalanced invasion is the third major prerequisite of malignant behaviour of the tumor cell. Invasion of tumor cells depends on a permissive host environment at the invasive site of the primary tumor as well as at the site of metastasis. The host participates in the induction, selection and expansion of neoplastic cells to an extent that researchers are even raising the question of “who is invading whom?”(Liotta et al., 2001). Likewise, the tumor cells of the invasion front display features, which differ from those in the inner parts of the tumor. The increased knowledge about this host environment and

possible therapeutic advantages of targeting this compartment like reduced capability to acquire resistance and easy access have led to the development of several therapeutics (Liotta et al., 2001). Prominent examples of this group of drugs are synthetic metalloprotease inhibitors, which have received much attention although only recently one trial proved clinical therapeutic efficacy (Bramhall et al., 2002& Evans et al., 2001). The difficulty in the design of stromal therapeutics may in part be due to the huge number of potential target molecules and the complicated not yet resolved interactive pathways. As an adjunct to focussed mechanistic studies which are usually performed *in vitro*, understanding of the biological processes could be increased by global *in vivo* gene expression studies. Several interesting studies towards this direction have been reported (Ryu et al., 2001,Roesch et al., 2003, Paweletz et al., 2001, Mariani et al., 2001& Brazma et al., 2001) but studies with a clear focus on the gene expression patterns of the host tissue excluding the tumorous epithelial compartment have not yet been published.

1.7 Microarray technologies for global gene expression profiles and identification of invasion related genes

Patterns in the invasion front as compared to the inner parts of the tumor have been published (Mariani et al., 2001, Roesch et al., 2003 & Iacobuzio-Donahue et al., 2002). However, none has specifically focussed on angiogenesis or on liver metastases nor has there been a distinction between tumor genes and host genes. This distinction is of particular interest if tumor cell/host cell interaction which is the initiating and probably crucial interaction during angiogenesis is studied *in vivo*.

In particular, the microenvironment has a significant effect on tumor development and progression (Bissell et al., 2001). Tumor cell lines have been considered an important resource for cancer investigations because of their limited cellular complexity compared with human tumors and the ease with which they can be grown and manipulated under controlled conditions. However, as the *in vitro* microenvironment is substantially less complex than the environment in which cancer cells proliferate *in vivo*, the conclusions reached from cancer cell line investigations, although informative, may not be directly applicable to the natural setting in which human tumors arise, progress, and are treated. Given that the consequences of particular genetic alterations in cancer may be highly context dependent and governed by the

spatial and temporal involvement of multiple interacting components, identification of gene expression differences between *in vitro* proliferation and *in vivo* tumor growth potentially may uncover genes that play an important role in tumor formation.

Global RNA expression profiling of xenograft tumors from human-derived cells grown in immune-compromised mice makes it possible to determine the extent to which cancer cells modify their expression profile in response to the local microenvironment. Gene expression profiling using oligonucleotide arrays represents an excellent means to study such tumor-host relationships in this setting because the potential background due to cross-species hybridization is minimal (bandapalli et al., 2006).

In this thesis, transcriptional changes in human LS174T colon adenocarcinoma cells grown orthotopically in the liver of nude mice were investigated to better mimic the environment of human liver metastasis. Potential host tissue response to the implantation of cancer cells were also examined using a mouse oligonucleotide array to measure the expression of mouse genes in liver tissue adjacent to tumor. To gain further insight into the contributions of various factors in the microenvironment of liver metastasis, transcriptional profiles of cells grown *in vitro* with profiles of orthotopically implanted tumors were compared. Furthermore the role of CXC chemokines and ß-catenin genes was studied that were found to be up regulated in the invasion front.

1.8 CXC chemokines

The CXC chemokines are a unique family of cytokines for their ability to behave in a disparate manner in the regulation of angiogenesis. CXC chemokines have four highly conserved cysteine amino acid residues, with the first two cysteine amino acid residues separated by one nonconserved amino acid residue (i.e., CXC). A structural domain within CXC chemokine family dictates their functional activity. The NH_2 terminus of the majority of the CXC chemokines contains three amino acid residues (Glu-Leu-Arg: the ELR motif), which precedes the first cysteine amino acid residue of the primary structure of these cytokines (Strieter et al., 1995). Members that contain the ELR motif (ELR^+) are potent promoters of angiogenesis (Luster et al., 2000& Belperio et al., 1998). In contrast, members that are inducible by interferons and lack the ELR motif (ELR^-) are potent inhibitors of angiogenesis (Strieter et al., 2004). The

angiogenic members of the CXC chemokine family include CXCL1, CXCL2, CXCL3, CXCL5 and CXCL8. The best described member is probably CXCL8 (IL-8). The ability of CXCL8 to promote endothelial cell survival and proliferation has been substantiated by a number of studies (Nor et al., 2001 & Li et al., 2003). Induction of the expression of CXCL8 in cancer cells by diverse signals and subsequent tumor-associated angiogenesis has been shown (Strieter et al., 2004& Dong et al., 2001). The other pro-angiogenic members of the CXC chemokine family have been less extensively described (Strieter et al., 2004).

The fact that all ELR+ CXC chemokines mediate angiogenesis highlights the importance of identifying a common receptor that mediates their biological function in promoting angiogenesis. The candidate CXC chemokine receptors are CXCR1 and/or CXCR2. Only CXCL8 and CXCL6 specifically bind to CXCR1, whereas all ELR+ CXC chemokines bind to CXCR2 (Addison et al., 2002). The ability of all ELR+ CXC chemokine ligands to bind to CXCR2 supports the notion that this receptor mediates the angiogenic activity of ELR+ CXC chemokines. While CXCR1 and CXCR2 are detected in endothelial cells (Addison et al., 2000, Murdoch et al., 1999 & Salcedo et al., 2000), the expression of CXCR2, but not CXCR1, has been found to be the primary functional chemokine receptor in mediating endothelial cell chemotaxis (Addison et al., 2000 & Murdoch et al., 1999et al.,) Another receptor which binds at least to CXCL1, CXCL5 and CXCL8 (Addison et al., 2004) and is expressed on endothelial cells is the Duffy antigen receptor for chemokines (DARC).

The angiostatic members of the CXC chemokine family include CXCL4, 9, 10 and 11 (Strieter et al., 2004). They are interferon-inducible. The putative receptor for angiostatic chemokines is CXCR3 (Strieter et al., 2004). Angiostatic effects of chemokines seem to be mainly attributable to immunologic effects involving T lymphocytes, and the paradigm of immunangiostasis has been postulated (Strieter et al., 2004).

1.9 β-catenin

β-catenin is involved in cell-cell adhesion as well as in signal transduction and transcriptional activation of a huge number of target genes

(http://www.stanford.edu/~rnusse/pathways/targets.html).

For its action as transcriptional activator it has been shown to localize to the nucleus and associate to members of the TCF/LEF family of transcription factors (Brembeck et al., 2006 & Huelsken et al., 2002). During cancer development this nuclear accumulation as well as overall increased protein levels seem to be caused by either stabilizing mutations of the gene itself or by mutations affecting components of the ß-catenin degradation complex including the APC*, AXIN1 or AXIN2* tumor suppressor genes (Brembeck et al., 2006 & Huelsken et al., 2002). In colorectal cancer, the second most common cancer in both sexes (Grem et al., 2001), nuclear localization has been mainly observed at the invasion front of primary tumors as well in liver metastases (Brabletz et al., 2001). One current concept interprets this finding as mechanism within the epithelial mesenchymal transition which takes place preferably at the invasive margin and leads to the acquisition of a less differentiated and more mesenchymal appearance (Brabletz et al., 2005). Posttranslational regulation is generally believed to be the main regulatory mechanism for β-catenin activity. However, increased mRNA levels have occasionally been reported in some types of cancers including colorectal (El-Bahrawy et al., 2001& Mann et al., 1999), gastric (Ebert et al., 2002), hepatocellular (Cui et al., 2001) and desmoid (Saito et al., 2002) cancer indicating at least some influence of transcriptional or posttranscriptional regulation.

1.10 Aim of the thesis

Global RNA expression profiling of xenograft tumors from human-derived cells grown in immune-compromised mice makes it possible to determine the extent to which cancer cells modify their expression profile in response to the local microenvironment. Gene expression profiling using oligonucleotide arrays represent an excellent means to study such tumor-host relationships in this setting because the potential background due to cross-species hybridization is minimal.

The thesis is majorly focused on two themes. Chapter 1 deals with the degree of interspecies overlap of genes between the syngenic model CT26 and human clinical specimen.

Chapter 2, 3 deal with the analysis of global gene expression profiles and invasion front related genes in xenograft model.

1. Interspecies comparison of gene and gene expression profiles in a mouse model of colorectal liver metastasis and in clinical specimens

A. What is the degree of interspecies overlap on the single-gene level?

B. How similar are gene expression patterns and single-gene expression in an interspecies comparison and can relations between these parameters in addition to histological assessment be used to explain interspecies overlap?

C. Which gene expression patterns and selected marker genes can be considered typical for the different compartments?

2. Global gene expression profiles of host tissue at the invasive front of colorectal liver metastases

A To examine whether a xenograft nude mouse model of colorectal liver metastases would deliver reliable and valid data

B To provide comprehensive and unbiased study of the components of the host reaction upon tumor invasion and

C To deliver potential target genes for the development of host cell directed therapeutics.

3. Gene expression profiles of tumor cells *in vitro*, *in vivo* and at the invasion front of colorectal liver metastases

A To explore the gene expression changes in tumor invasion front during confrontation with host tissue

B Gain insight in the activation of the β-catenin promoter in the invasion front of colorectal liver metastases.

2 Materials

2.1 Instruments

Autoclave	Systec V-95 (Systec GmbH)
Centrifuges	MiniSpin & 5804R (Eppendorf)
CO_2-Incubator	Hera-Cell 150 (Heraeus)
Laminar Air- flow	HeraSafe (Hearaeus)
Microscope	Axiovert 40 C (Carl Zeiss)
Multi^{TM} Image Light Cabinet	Alpha Innotech
PALM® MicroBeam-Laser-System	P.A.L.M. Microlaser Technologies AG, Bernried, Germany
PCR Machine	Cyclone Gradient (PeQlab)
pH Meter	Meter SevenEasy (Mettler Toledo)
Precisions Balance	ABS 104-S (Mettler Toledo)
Spectrophotometer	Bio photometer (Biorad)
UV Transilluminator	Benda Laboratories
Vacuum pump	VaccuSafe (Integra Biosciences)
Vortexer	Reax Top (Heidolph)

2.2 Chemicals and reagents

1Kb Ladder	Invitrogen
dNTP	Invitrogen
ECL	Amersham Pharmacia
FCS	Sigma Aldrich
Lipofectamine 2000	Invitrogen
Rainbow Protein Marker	Amersham Pharmacia
RNAsin	Promega
RPMI	Invitrogen
Skimmed Milk Powder	Carl Roth

2.3 Special Material

Biomax Light Film	Kodak
Cell Culture Material	Falcon, Greiner and Nunc Nalgene
Membrane Slides for LCM	Molecular Machines&Industries
Microarray chips	Affymetrix
Nitrocellulose Membrane Hybond	Amersham Pharmacia
Whatmann Paper	Whatmann

2.4 Plasmids

pSM2C Plasmid **containing** CXCL-1, IL-8 & non-silencing shRNAmir construct from Open Biosystems USA

pSEAPBhBCTNf1, pSEAPBhBCTNf2, pSEAPBhBCTNf3 containing fragment 1, 2&3 of β-catenin promoter from BCCM/LMBP Plasmid&DNA Library collection, Belgium

pBabe Puro containing puromycin resistance marker.

Sh RNAmir Clone Sequences

CXCL-1 (Accession No: NM_001511)

Clone 1 (RHS1764-9681692)

TGCTGTTGACAGTGAGCGCCCTGCACACTGTCCTATTATATAGTGAAGCCACAGA
TGTATATAATAGGACAGTGTGCAGGTTGCCTACTGCCTCGGA

Clone 2 (RHS1764-9193979)

TGCTGTTGACAGTGAGCGCCCTGCACACTGTCCTATTATATAGTGAAGCCACAGA
TGTATATAATAGGACAGTGTGCAGGTTGCCTACTGCCTCGGA

CXCL-8 (Accession No: NM_000584)

Clone 1 (RHS1764-9502516)

TGCTGTTGACAGTGAGCGAGGGAGAATATACAAATAGCAATAGTGAAGCCACAGA
TGTATTGCTATTTGTATATTCTCCCGTGCCTACTGCCTCGGA

Clone 2 (RHS1764-9210951)

TGCTGTTGACAGTGAGCGCCGGAATAATGAGTTAGAACTATAGTGAAGCCACAGA
TGTATAGTTCTAACTCATTATTCCGTTGCCTACTGCCTCGGA

2.5 Kits

ECL Plus Western Blotting Detection Kit	Amersham Pharmacia
Fast Plasmid™ Mini kit	Eppendorf
Light Cycler RNA Master SYBR Green I	Roche

Megascript™ High Yield Transcription Kit	Ambion
Phospha-Light™ System	Applied Biosystems
Plasmid Maxi Kit	Qiagen
RiboAmp™ HS RNA Amplification Ki	Arcturus
RNA 6000 Pico LabChip Kit	Agilent Technologies
RNA Transcript Labelling Kit	Affymetrix
RNeasy® mini Kit	Qiagen

2.6 Cell Lines

LS174T Human colon adenocarcinoma cell line

CT26 Mouse colon carcinoma cells

2.7 Reagents

50x TAE-Buffer (1l)

242g	Tris Base
57.1ml	Glacial Acetic acid
37.2g	Na_2 EDTA, pH 8,0

TE Buffer

0.040M	Tris-acetate
0.1%	Acetic acid
0.002M	EDTA.2H_2O pH 8.0

Gel loading Buffer

5%	Glycerin
166. 7 µM	EDTA
0.0025%	Bromophenol Blue

PBS 10X, pH 7,4

80g	NaCl
2g	Kcl
14.4g	Na2HPO4-7H2O
2.4g	KH2PO4
make upto 1l with H2O	

LB-Agar medium

20 g/l	Peptone
10 g/l	Yeast extract
5 g/l	NaCl

15 g/l	Agar

2x-LB broth (low-salt) Medium

20 g/l	Peptone
10 g/l	Yeast extract
5 g/l	NaCl
50µg/ml	Chloramphenicol

10X Laemmli running Buffer

250mM	Tris base
1.92M	Glycine
1%	SDS

2X Laemmli sample buffer

pH 6.8 0.12M	Tris-HCl
20% V/V	Glycerine
4% V/V	SDS
10%V/V	B-Mercaptoethanol

Stacking Gel (5%)

1.1ml	H2O
2.5ml	30% Acrylamide Mix
1.3ml	1.0M Tris pH6.8
0.05ml	10% SDS
0.05ml	10% Ammonium Persulphate
0.002ml	TEMED

Separating Gel (15%)

0.68ml	H2O
0.17ml	30% Acrylamide Mix
0.13ml	1.5M Tris pH6.8
0.01ml	10% SDS
0.01ml	10% Ammonium Persulphate
0.001ml	TEMED

Transfer Buffer I

36.33g	Tris Base in 600ml water (pH 10.4)
200ml	Methanol
Make upto 1l with water	

Transfer Buffer II

3.03 g	Tris base in 600ml of water (pH 10.4)
200ml	Methanol
Make upto 1l with water	

Transfer Buffer III

5.25g	Norleucin
3.03g	Tris Base in 600ml of water (pH 9.4)
200ml	Methanol
Make upto 1l with water	

Z-Buffer+EDTA

60mM	Na2HPO4
40mM	NaH2PO4
10mM	KCl
1mM	MgSO4
2.5mM	EDTA pH 8.3
50mM	b-mercaptoethanol (3µl/ml)
Make upto 1l with water	

Special Primers

T7 Primer	MBI Fermentas
Oligo dT	Invitrogen

Human Specific Primers

Gene	Primer sequence	Ann. temp T(°C)	Product size (bp)
APAF1		60	124
	For: 5'- AACCAGGATGGGTCACCATA -3' Rev: 5'- ACTGAAACCCAATGCACTCC -3'		
APOF		62	110
	For: 5'- TTCTGCACCCAAAGTCACTG -3' Rev: 5'- ATCAGCCTGACAACCAGCTT -3'		
CDH1		65	110
	For: 5'-AGGCCAAGCAGCAGTACATT-3' Rev: 5'-ATTCACATCCAGCACATCCA-3'		
CXCL1		55	-
	For: 5'-Qiagen Quantitech Primer-3' Rev: 5'- Qiagen Quantitech Primer -3'		
CXCL2		55	-
	For: 5'- Qiagen Quantitech Primer -3' Rev: 5'- Qiagen Quantitech Primer -3'		
CXCL3		55	-
	For: 5'- Qiagen Quantitech Primer -3' Rev: 5'- Qiagen Quantitech Primer -3'		
CXCL5		55	-
	For: 5'- Qiagen Quantitech Primer -3' Rev: 5'- Qiagen Quantitech Primer -3'		
COL5A2		58	105
	For: 5'- TGGAGAAGGTGGAAAACCAG -3' Rev: 5'- TCTCCTCTTTCCCCAGGATT -3'		
CTNNB1		55	268
	For: 5'- TTGGTAGGGTGGGAGTGGTTTA-3' Rev: 5'- CAGGCCAATCACAATGCAAG-3'		
EpHB2		60	110
	For: 5'- AGCATTACCCTGTCGTGGTC -3' Rev: 5'- TTTATGGCTGTGGCGTTGTA -3'		
EREG		60	186
	For: 5'- TTTGCTCTCAGCTGATGTGTCC -3' Rev: 5'- TGGCCTTGGTTGAAGACCAT -3'		
IL-8 8CXCL8)		60	85
	5'-CTC TTG GCA GCC TTC CTG ATT-3' 5'-TAT GCA CTG ACA TCT AAG TTC TTT AGCA-3'		

MARCKS		58	189
	For: 5'- CACCTTCTTCCTCTGCCTTG -3' Rev: 5'- CCCATTGTGACCCCTATCAC -3'		
MARK3		58	120
	For: 5'- TTCCGTTACCCTGAGAGTCG -3' Rev: 5'- GCCAGTGTAGGGAGATGCTT -3'		
MPZL1		58	128
	For: 5'- AAGGAAGCTGCTCACACTGA -3' Rev: 5'- TCTGCAACCAGGAAAGGAGT -3'		
RHOB		60	106
	For: 5'- ACAGCTTCAGCACAGCCTCT -3' Rev: 5'- CGCTTATGGCAAAAACAACC -3'		
THBS2		58	124
	For: 5'- TATTCCCGAGACCAACGAAG -3' Rev: 5'- ACATCATCGTCACTCCCACA -3'		
18s RNA		60	
	For: 5'-AAACGGCTACCACATCCAAG -3' Rev: 5'-CCTCCAATGGATCCTCGTTA -3'		

Mouse specific primers

Gene	Primer sequence	Ann temp T (^{o}C)	Product size (bp)
Apof		62	124
	For: 5'- ATACAGCCCAGCCGTCTAAA-3' For: 5'- CCAGGGACAGAAAGGTTCAA-3'		
cRBP		58	229
	For: 5´- GAGGCATGGTTCTGCACTGA -3` Rev: 5´- CCGTGGCTTCTGATCCTTGT -3`		
Col5a2		58	210
	For: 5'- ACACACGTGCCCAGTAATGA-3' For: 5'- GGAAATCTATCCCAGCTTGC-3'		
cstb		58	151
	For: 5'- TGAAGTCCCAGCTTGAATCG -3' Rev: 5'- AGGGGTTGAAACACCCTCAA -3'		
ctsc		60	223
	For: 5'- GGCAGTTGCCTTTGAAGTCC -3' Rev: 5'- TCCTCTGCGGATACGGAAGT -3'		

ctss		60	178
	For: 5'- ATTCAGCTCCCCTTTGGTGA -3'		
	Rev: 5'- TCCCATAGCCAACCACAAGA -3'		
Dfy		62	173
	For: 5'- GCCTCATGGGATGGTTCTCA -3'		
	Rev: 5'- TGGTCTGATGGCAGAACAGG -3'		
Efnb2		59	176
	For: 5'- TGTCATCGGTTGGCTACGTT -3'		
	Rev: 5'- CCAAAGCTGAACCAACTCCA -3'		
Eng		58	197
	For: 5'- ATATGGCTGCCCGGGATTAC -3'		
	Rev: 5'- CCAACCGAAGTTGTGCCAGT -3'		
Flt1		60	176
	For: 5'- CAGTGCAATCCCCACTGAGA -3'		
	Rev: 5'- ACACACTGCAGCCGACAAGA -3'		
GapDH		62	-
	For: 5'-TGC ACC ACC AAC TGC TTA-3'		
	For: 5'-CCT GCT TCA CCA CCT TCT T-3'		
Gbp1		60	114
	For: 5'- AGGGCAGCTGTCTTTGGGTA -3'		
	Rev: 5'- GCCAATCCCAGCTTAGAGCA -3'		
Gbp2		60	127
	For: 5'- CGACTCCATTTTGGGGTCAC -3'		
	Rev: 5'- GCATGATGAAGGCCGAGAGT -3'		
Gbp3		60	171
	For: 5'- CATAGCAGCTGAGCGGACAA -3'		
	Rev: 5'- TCCCTCAGCAGCATCTCCTT -3'		
α-SMA		58	280
	For: 5'-CCTGACTGAGCGTGGCTATT-3'		
	Rev: 5'-CGCTGACTCCATCCCAATGA-3'		
Thbs2		58	108
	For: 5'- GGGACCACACAAATTGATCC-3'		
	For: 5'- CCCAAACTCGTCGAAACCTA-3'		
Tie1		58	173
	For: 5'- AGCCTCGAAACTGCGATGAC -3'		
	Rev: 5'- GATGCCCGCATAGGTGAAGT -3'		

2.8 Antibodies

Actin	ICN Biomedicals
α-Smooth Muscle Actin (Clone ASM-1)	Cymbus Biotech
ß-catenin	BD Biosciences
cRBP	Santhacruz Biotechnology
CXCL-1	R&D (Gift from Dr.Wente)
Desmin (Clone D33)	Dako Cytomation
Hep Par-1 (M7158)	Dako Cytomation
Interleukin-8	Santacruz Biotechnology
Transgelin (SM 22 α)	Abcam

3 Methods

3.1 Cell Culture and Animal Experiments

Cell Culture

LS174T human colon adenocarcinoma and CT 26 Mouse colon carcinoma cells were cultured in RPMI (PAA Laboratories GmbH) supplemented with 10% FCS (Sigma–Aldrich GmbH), 2 mM glutamine, 100 IU/ml penicillin, and 50 mg/ml streptomycin (PAA Laboratories GmbH). Medium renewal was done two times per week.

Cells were detached using Trypsin-EDTA (0.05% Trypsin/0.02% EDTA; PAA Laboratories GmbH) following standard protocols (Freshney et al., 1987). In order to freeze cells, cultures were detached and resuspended in 5 ml culture medium. Cells were pelleted by centrifugation at 1000 rpm for 10 min at 4°C. Pellets were resuspended in culture medium containing 10% DMSO (Sigma) to a concentration of $1x10^6$ cells/ml and stored at -80^0C

For cell counting, cells were stained with one volume trypan blue (Sigma–Aldrich GmbH) to visualize apoptotic cells and counted using a haemocytometer (Neubauer chamber), according to standard protocols (Freshney et al., 1987).

Animal Experiments

For animal experiments we modified a previously described model in which tumor cells are injected into the spleen of nude mice, resulting in extensive liver metastasis (Dunnington et al., 1987). Six to eight week old female, athymic nude mice (NMRI-*nu/nu*) (Möllegard and Bomholdgard Laboratories, Ry, Denmark) were anesthesized using Ethomidat (Radenarkon, Asta Medica Frankfurt, Germany) at a concentration of 40 µg/g bodyweight. They were subjected to a lateral abdominal incision extending just below the last left rib in a sickle shape of about 1 cm. The spleen was luxated and 50 µl of $5x10^6$ LS174T-cells were injected into the tip of the spleen using a 30.5 gauge needle. Alternatively, mice were subjected to a midline abdominal incision extending from the xiphoid process to just above the urinary bladder. The liver and its major blood vessels were exposed and 50 µl of $5x10^6$ LS174T-cells were injected into the upper mesenteric vein using a 30.5 gauge needle. In a third model, 50 µl of $5x10^6$ LS174T-cells were injected along the margin of the large liver lobe. All three

models produce extensive liver colonization after a period of 2 to 4 weeks. At that time, animals were euthanized, livers were removed and 10 mm thick pieces containing tumor areas and liver were embedded in TissueTek OTC medium (Sakura, Tokyo, Japan), snap frozen in methyl butane, pre-cooled in liquid nitrogen, and stored at -80°C.

3.2 Tissue preparation and laser microdissection (LMD)

Frozen tissue blocks were cut into 8 µm sections using a cryostat (Leica, Wetzlar, Germany) and stained using Cresyl Violet. Briefly, the staining consisted of sequential incubations in 70% ethanol (1 min), Meyer's hematoxylin (Sigma, Taufkirchen, Germany, 1 min), DEPC treated tap water (1 min), 2% eosin (10 s), 70% ethanol (30 s), 95% ethanol (2 x 30 s), and 100% ethanol (2 x 30 s). Thereafter, the sections were left to air-dry for 5-10 minutes. After microscopic control of staining quality and tissue preservation, the sections were used for microdissection using Leica AS LMD (Leica, Wetzlar, Germany), MMI (Molecular Machines & Industries, Eching, Germany) or PALM laser microdissection instrument (PALM Microlaser Technologies GmbH). Two distinct cell populations were separately microdissected for comparison between liver and invasion front liver: a) invasion front tissue extending 3 cell rows into the liver and 3 cell rows into the tumor, b) normal liver tissue at least 3 rows away from the invasion front. Microdissection was performed separately by three different scientists yielding material for three separate experiments (experiments 2-4, subject for RNA amplification). In addition, material for a fourth experiment was generated by the concerted action of all scientists (experiment 1, no RNA amplification). Four different distinct cell populations were microdissected for interspecies comparison and tumor versus tumor invasion comparison. a) Liver tissue atleast 3 cell rows away liver invasion front, b) liver invasion front 3 cell rows adjacent to the tumor invasion front, c) tumor invasion front 3 cell rows adjacent to the liver invasion front and d) tumor atleast 3 cell rows away from the tumor invasion front. After microdissection the slices were collected in tubes, added 50µl of Buffer RLT (Qiagen) and stored at -80°C.

3.3 RNA extraction, quality control and quantification

3.3.1 Extraction of total RNA from cell lines

To extract RNA for microarray experiments, cells were quickly thawed at 37°C and pelleted at 1000 rpm for 10 min at 4°C prior addition of RLT Buffer (Qiagen). For quantitative RT-PCR experiments cells were detached by directly adding RLT Buffer (Qiagen) to the culture vessel. Total RNA was extracted according to the instructions given in the RNeasy mini kit manual. Briefly 1 volume of 70% ethanol (350µl) was added to the homogenized lysate and mixed well by pipetting slowly. 700 µl of the sample, including any precipitate that may have formed was transfer to an RNeasy spin column in a 2 ml collection tube and centrifuged for 15 seconds at10,000 rpm. Flow-through was discarded, 350 µl Buffer RW1 was added to the RNeasy spin column and centrifuged for 15 seconds at 10,000 rpm to wash the spin column membrane. 80ml of DNase was added to the centre of the column and incubated at RT for 15 min. 350µl o of RW1 was pipetted onto the spin column and centrifuged at 10,000 rpm for 15 Sec. Flow-through was discarded and 500 µl Buffer RPE was added to the RNeasy spin column, centrifuged for 15 seconds at 10,000 rpm to wash the spin column membrane. 500 µl Buffer RPE was added to the RNeasy spin column, centrifuged for 2 min at 10,000 rpm. RNeasy spin column was placed in a new 2 ml collection tube and centrifuged at full speed for 1 min. RNA was eluted with 30-50 µl RNase-free water by centrifuged for 1 min at 10,000 rpm to elute the RNA in a new 1.5 ml collection tube.

3.3.2 Extraction of total RNA from snap-frozen and microdissected tissues

H&E and Cresyl violet stained histological sections were prepared from each tissue prior to RNA extraction. Representative tissue areas, identified on the H&E stained histological sections, were microdissected as described in the Tissue preparation and laser microdissection section and used for RNA extraction. 350µl final volume of RLT Buffer (Qiagen) was added to 3-5 frozen tubes of each sample and total RNA was extracted as described above.

(http://www1.qiagen.com/literature/handbooks/PDF/RNAStabilizationAndPurification/FromAnimalAndPlantTissuesBacteriaYeastAndFungi/RNY_Mini/1035969_HB_Bench

Protocol.pdf). To eliminate contaminating DNA, RNA was treated using the DNAse I system of Qiagen.

3.3.3 Evaluation of RNA quantity and quality

Total RNA concentrations were determined using a spectrophotometer. To assess the quality of total RNA from cells, 0.5–1 µg RNA was separated on conventional 0.8% agarose (Applichem GmbH) gels using 1 X TAE (prepared from 50 X TAE stock solution, see Appendix) as a running buffer (Ausubel et al.,1994.). Total RNA concentrations from microdissected samples were determined using RNA 6000 pico kit on an Agilent Bioanalyser instrument (Agilent technologies Deutschland GmbH) as described below

Principle of Lab-on-a-Chip

The electrophoretic assays are based on traditional gel electrophoresis principles that have been transferred to a chip format. The chip format dramatically reduces separation time and sample consumption. The system provides automated sizing and quantitation information in a digital format. On-chip gel electrophoresis is performed for the analysis of DNA, RNA and proteins.

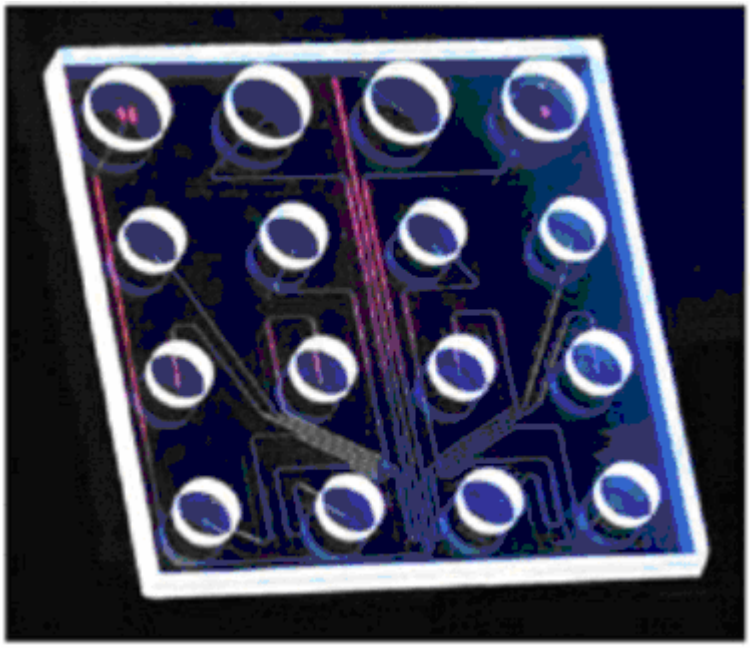

Figure 1: Lab-on-a-chip (Source: Agilent Technologies)

The chip accommodates sample wells, gel wells and a well for an external standard (ladder). Micro-channels are fabricated in glass to create interconnected networks among these wells. During chip preparation, the micro-channels are filled with a sieving polymer and fluorescence dye. Once the wells and channels are filled, the chip becomes an integrated electrical circuit. The 16-pin electrodes of the cartridge are arranged so that they fit into the wells of the chip. Each electrode is connected to an independent power supply that provides maximum control and flexibility. Charged biomolecules like DNA or RNA are electrophoretically driven by a voltage gradient-similar to slab gel electrophoresis. Because of a constant mass-to-charge ratio and the presence of a sieving polymer matrix, the molecules are separated by size. Smaller fragments are migrating faster than larger ones. Dye molecules intercalate into DNA or RNA strands or Protein-SDS micells. These complexes are detected by laser-induced fluorescence. Data is translated into gel-like images (bands) and electrophorograms (peaks). With the help of a ladder that contains fragments of known sizes and concentrations, a standard curve of migration time versus fragments size is plotted. From the migration times measured for each fragment in the sample, the size is calculated. Two marker fragments (for RNA only one marker fragment) are run with each of the samples bracketing the overall sizing range. The "lower" and "upper" markers are internal standards used to align the ladder data with data from the sample wells. This is necessary to compensate for drift effects that may occur during the course of a chip run.

For RNA assays, quantitation is done with the help of the ladder area. The area under the ladder is compared with the sum of the sample peak areas. The area under the "lower" marker is not taken into consideration. For total RNA assays, the ribosomal ratio is determined, giving an indication on the integrity of the RNA sample. The 2100 expert software plots fluorescence intensity versus migration time and produces an electrophorogram for each sample.

Protocol

Briefly; RNA 6000 Pico dye concentrate was equilibrated to room temperature for 30 min, vortexed for 10 seconds, spun down and added 1 µl of dye into a 65 µl aliquot of filtered gel. The solution was vortexed well and centrifuged at 14000 rpm for 10 min at room temperature. A new RNA 6000 Pico chip was placed on the Chip Priming

Station and 9.0 µl of gel-dye mix was pipetted in the well marked G. Chip Priming Station was closed and the plunger was pressed until it is held by the clip. Waited for exactly 30 seconds then released the clip. 9.0 µl of gel-dye mix was Pipetted in the wells marked G. 9.0 µl of the RNA 6000 Pico Conditioning Solution (yellow) was pipetted in the well marked CS. 5 µl of RNA 6000 Pico marker (green) was pipetted in all 11 sample wells and in the well marked Ladder. 1 µl of diluted ladder was loaded in well marked Ladder symbol and1 µl of sample in each of the 11 sample wells. Chip was placed in the adapter and vortexed for 1 min. at the set-point of the IKA vortexer (2400rpm). The chip was run in the Agilent 2100 bioanalyzer within 5 min.

3.4 RNA Amplification (In Vitro transcription)

3.4.1 Amplification of RNA for host-tumor interactions studies

Microarray technology provides high-throughput analysis of gene expression profiles. However, using standard protocols, a substantial amount of RNA (50-100ug) is needed in order to apply this powerful technology. This molecular approach is thus rendered useless for many purposes if this limitation is not overcome.

The increasing need to broaden the use of microarray technology has resulted in approaches to amplify the target RNA. Amplification of RNA has been developed and used in gene expression analysis before the microarray technique appeared. RNA amplification, unlike PCR amplification, is linear and not biased by the size of the template. In this method, mRNA is reverse transcribed with an oligo dT/T7 promoter primer. After synthesis of double stranded cDNA, antisense RNA is transcribed *in vitro* generally resulting in a 1000-fold amplification of the original amount. If necessary, a second round of amplification was performed simply by repeating the procedure. Amplified RNA was labelled with biotinylated NTPs and analyzed using microarrays.

3.4.2 Reverse transcription (RT) of RNA and second strand synthesis

RT was performed as previously described (Luo et al., 1999) with some modifications: 10 µl of the purified total RNA from RT was mixed with 2 µl dT_{24}-T7-Primer (20 µM (5'-GGC CAG TGA ATT GTA ATA CGA CTC ACT ATA GGG AGG CGG- $(dT)_{24}$3', TibMolBiol, Berlin, Germany) to initiate first strand synthesis. Primer

and RNA were incubated for 5 min at 70 °C, followed by incubation for 2 min at 42 °C. Next, 4 µl of 5x first-strand reaction buffer, 2 µl 0,1M DTT, 1 µl 10 mM dNTPs, 1 µl 40 U/µl RNAsin (Promega, Mannheim, Germany) and 1 µl 200 U/µl Superscript II (Invitrogen, Karlsruhe, Germany) were added and incubated for 1 hour at 42 °C. Next, 91 µl RNase-free water, 30 µl 5x second-strand synthesis buffer, 3 µl 10mM dNTPs, 1 µl 10U/µl *E. coli* Ligase, 4 µl 10U/µl DNA-polymerase I und 1 µl 2U/µl *E. coli* RNase H were added and the mixture was incubated for 2 hours at 16° C, followed by a 5 min incubation step at 16°C after the addition of 2 µl 5U/µl T4-DNA-polymerase. The reaction was stopped by the addition of 10 µl 0.5M EDTA at pH 8. cDNA was extracted with phenol-chloroform and NH_4-acetate precipitation. The pellet was re-suspended 12 µl RNase-free water.

3.4.3 T7-based RNA amplification

First round T7-based RNA amplification was performed using the T7-Megascript-Kit (Ambion, Huntingdon, UK). 12 µl cDNA were mixed at room temperature with 2 µl T7-buffer, 2 µl 40 mM NTPs and 2 µl enzyme-mix and incubated for 9 hours at 37°C. The aRNA was extracted with phenol-chloroform and NH_4-acetate precipitation. The pellet was re-suspended in 10 µl RNase-free water.

3.4.4 Subsequent rounds of aRNA amplification

10 µl of aRNA from the first-round amplification were mixed together with 2 µl 50 ng/µl random hexamers (Invitrogen, Karlsruhe, Germany), incubated for 10 min at 70°C, and then chilled on ice and equilibrated at room temperature for 10 min. Then, 4µl 5x first-strand buffer, 2 µl 0.1 M DTT, 1 µl 10 mM dNTPs, 1 µl 40 U/µl RNasin und 1 µl 200 U/µl Superscript II were added and incubated for 1 hour at 37°C. Subsequently, 1 µl RNase H was added and incubated at 37° C for 20 min, after which the reaction mix was heated to 95° C for 2 min and chilled on ice. For the second-strand synthesis, 1 µl T7-$(dT)_{24}$-primer was added and incubated at 70°C for 5 min and at 42°C for 10 min. Next, 92 µl RNase-free water, 30 µl 5 x second-strand buffer, 3 µl 10 mM dNTPs, 4 µl DNA-Polymerase I and 1 µl RNase H were added and incubated at 16°C for 2 hours. 2 µl T4-DNA-polymerase were added and incubated at 16°C for 10 min. The clean up of the double-stranded cDNA was performed as described for the first round of amplification. cDNA was then ready for second-round T7 *in vitro* transcription and RT which were performed as described for the first

round. Then, a third-round of aRNA amplification/labelling was performed as described in the Biotin labelled cRNA transcription section.

3.4.5 Amplification of RNA for interspecies comparison studies

RNA was amplified according to the instructions given in the RiboAmp™ HS RNA amplification kit manual (Arcturus GmbH;

http://www.arctur.com/research_portal/images/pdf/riboamp_HS_userguide_verC.pdf and MessageAmp™ II-Biotin *Enhanced* Single Round aRNA Amplification Kit; Ambion (Europe) LtD. http://www.ambion.com/techlib/prot/fm_1791.pdf)

3.5 Microarray hybridization and data analysis

3.5.1 Generation of Oligonucleotide array probes

Biotinylated cRNA target was generated[15] from both, amplified and non-amplified cDNAs (2µg) using the Bioarray high yield transcription kit (ENZO, New York, NY) following the manufacturer's protocol. After a 5-hour incubation period at 37°C, the final biotin-labelled cRNA product was purified using RNeasy spin columns (Qiagen, Hilden, Germany) and eluted in 30 µl of RNase-free water. The concentration of biotin-labelled cRNA was determined by UV absorbance. In all cases 20 µg of each biotinylated cRNA preparation were fragmented, assessed by gel electrophoresis and placed in a hybridization cocktail containing four biotinylated hybridization controls (BioB, BioC, BioD, and Cre) as recommended by the manufacturer.

3.5.2 Hybridization

Prior to hybridization to an Affymetrix microarray, a hybridization cocktail was prepared by using fragmented cRNA, probe array controls (hybridization control bio B, bio C, bio D, cre at a final concentration of 1.5, 5, 25 and 100 pMoles/l respectively; Control Oligonucleotide B2 50pmol/l), acetylated BSA 0.5mg/ml, 2X Hybridization Buffer (Final 1X concentration is 100 mM MES, 1M [Na+], 20 mM EDTA, 0.01% Tween-20) and Herring Sperm DNA 0.1mg/ml. The target was then hybridized to a Gene chip array as described in the affymetrix manual (http://www.affymetrix.com/support/downloads/manuals/expression_s2_manual.pdf). Labelled samples were hybridized for 16 hours with Gene Chip® Murine MGU74Av2

for liver and liver invasion front comparison; Gene Chip® Mouse Expression set 430 and Gene Chip® Human Genome U133 set for interspecies comparison and Gene Chip® Human Genome U133 set (Affymetrix, Santa Clara, CA) for tumor and tumor invasion front comparison. A complete list of probe sets analysed in this arrays can be found at Affymetrix´s NetAffyx™ analysis center.

(https://www.affymetrix.com/site/login/login.affx).

The Affymetrix Gene chip technique makes use of a conjugate of Biotin-Streptavidin-Phycoerythrin (Biotin-SAPE) for labelling. The Biotin-SAPE conjugation is modified in the staining step after hybridisation. Hybridisation and staining is followed by scanning and storage of the image data. The information from a gene expression experiment (Affymetrix) is stored in several data files: an image file (*.dat), and a *.cel file which store the intensity data calculated from the *.dat file. The *cel file contains a single intensity value for each cell. The cell intensity data is then analysed and saved as a *.chp file, which contains qualitative and quantitative analysis for every probe set. In addition, an experiment information file and a report file are created. The report file summarises the data quality information from each single experiment from the *.dat file and contains a single intensity value for each probe cell delineated by the grid. The intensity data from the *.cel file is then analysed. Hybridisation controls (a mixture of fragmented cRNA from *E. coli* and P1 bacteriophage), that are spiked into the hybridisation cocktail, evaluate the sample hybridisation efficiency and can also be used to indirectly assess RNA sample quality among replicates. All hybridisation controls should be scored “present” in samples that show good hybridisation efficiency. Internal control probe sets are included in all arrays and are used to assess RNA sample and assay quality. House keeping genes like GAPDH and β-actin are commonly used. The ratio of the signal values between the 3´ probe set and the 5´ probe set (see above) should not exceed 3 for good quality assays.

3.5.3 Percent Present

The “Percent Present” (%P) is a measurement of the number of present probe sets in relation to the total number of probe sets on the array. The %P depends on a number of factors including cell origin, array type and RNA quality. Replicate samples should have similar %P values.

3.5.4 Scaling/normalisation

There are many sources of systemic variation in a microarray experiment that affect the measured gene expression levels. The overall intensity between arrays should be similar and global scaling/normalisation is performed to minimise technical variation between arrays. Differences in overall intensity are most likely due to assay variables including pipetting error, hybridisation, washing and staining efficiencies, which are all independent of relative transcript concentration. For replicates and comparisons the scaling/normalisation factors should be comparable. Large discrepancies (e.g. three-fold or greater) may indicate significant assay variability or sample degradation leading to noisier data.

3.5.5 Data analysis

In this study image analysis was performed with Affymetrix Gene Chip Operation Software version 4.0 (GCOS) to analyse the scanned images, convert intensities to a numerical format and obtain a detection call. This call indicates whether a transcript is reliably detected (Present) or not detected (Absent). The scanned images from the chips were processed using Affymetrix Microarray Suite 4.0, (Affymetrix Inc. Santa Clara, CA), NetAffyx, Microarray Database software, Excel (Microsoft, Seattle; USA) and GOSSIP (Microdiscovery, Berlin, Germany).

3.5.6 Pair-wise comparison

GCOS was used for pair-wise comparisons. During a comparison analysis, each probe set on the experiment array is compared to its counterpart on the baseline array (e.g. Invasion tumor will be assigned as “experiments” and tumor as “baseline”), and a change p-value is calculated indicating a Change call that is either: “Increase”, “Marginal Increase”, “Decrease”, “Marginal Decrease” or “No Change” in gene expression. First, comparisons yielding a “No Change” call were removed. Second, a Detection call, “Present” or “Absent” transcript, for each probe set was assigned. Then, probe signals that were “Absent” in both base line sample and experiment sample were excluded. The third metric was to sort on the relative change, fold change, in transcript abundance. GCOS uses a “Signal Log Ratio”. A fold change of 2 for increases or decreases corresponds to a Signal Log Ratio of 1 or -1 respectively.

3.6 RT-PCR and Gel Electrophoresis

3.6.1 First-Strand cDNA Synthesis

To 500 ng to 1µg of RNA in a 0.5-ml tube 1µl of 50 µM oligo (dT) 12-18, 1 µl of 10 mM dNTP mix were added, total volume was made upto 10µl with sterile distilled water and incubated at 65°C for 5 min., quick chilled on ice and the contents of the tuber were collected to the bottom of the tube by brief centrifugation.

4µl of 5X First Strand Buffer, 2 µl of 0.1M DTT and 1µl of RNaseOUT were added, the contents of the tube were mixed gently and incubated at 42°C for 2 min. 1µl of Superscript II was added to the tube, mixed by pipetting up and down and incubated for 50 min. at 42°C. The reaction was inactivated by heating the tube at 70°C for 15 min. and cooled down to 4°C The cDNA was used as template for PCR reactions or stored at -20°C.

3.6.2 Polymerase Chain Reaction (PCR)

Polymerase chain reaction was performed to standardize protocols for qPCR and to check for specificity of the primers. A master mix was prepared containing all required reagents and aliquoted to PCR tubes according to the following protocol

Master Mix:

10X PCR Buffer	2.5µl
10Mm dNTP mixture	0.5µl
50mM MgCl2	0.75µl
Primer Mix (10µM each)	1.25µl
Template DNA (cDNA)	1.0µl
Taq DNA polymerase	0.1µl

Sterile DEPC treated water to a final volume of 25µl

24µl master mix was aliquoted to each tube and 1µl of appropriate cDNA was added.

Tubes were placed into PCR machine and required programme was chosen

Initial Denaturation Step – 94^0C 3min

Cycle Step 1 - Denaturation94^0 C 1min

Cycle Step 2 – Annealing 55-60^0C 45 min (dependent upon primers used)

Cycle Step 3 - Elongation 74^0C 1min

Final Elongation Step - 74^0 C 3min

PCR products were either stored at 4^0 C or ran on a 1% agarose gel for analysis of the product.

3.6.3 Gel Electrophoresis

For the horizontal electrophoresis 0.6 to 3% agarose in 1X TAE with 0.2µg/ml EtBr was dissolved by heating. The probes were diluted with 1/5 volume of gel loading buffer and loaded into the wells along with ladder. The electrophoresis was run with a constant volume between 80-120v for 60-90 min. The bands were visualized under UV transilluminator and documented with Multi Image light cabinet.

3.7 Quantification of mRNA expression levels using Light Cycler

3.7.1 General principle of quantitative PCR

PCR starts with a background phase followed by an exponential (or log) phase and ends in a plateau phase. Increase of PCR product during an amplification reaction can be detected by using the fluorochrome SYBR green, which binds to double stranded DNA, by the LightCycler system.

During amplification, the number of PCR products present at a certain PCR cycle is described by the equation:

$$N_n = N_0 \, x \, E^n$$

where N_n is number of products at PCR cycle n; N_0 is initial number of product (template); E is amplification efficiency; n is number of PCR cycle

Accurate DNA quantification is only possible in the log-phase of a PCR in which E is constant. In theory, the maximal amplification efficiency in log-phase is 2 so that every PCR product is replicated once per cycle. In practice amplification efficiencies in this phase are generally less than 2 due to many factors that could inhibit PCR reactions (suboptimal primers, PCR inhibitors in sample material etc.).

To determine amplification efficiencies for individual PCRs, serial template dilutions have to be amplified on the LightCycler instrument. Standard curves and their slopes

are determined using the software provided by the LightCycler system. Amplification efficiencies are described by the equation:

$$E = 10^{-1/\text{slope}}$$

where E is amplification efficiency; slope is slope of standard curve.

The easiest way to determine absolute mRNA copy numbers of a gene of interest is to use an external standard, which is prepared from serial dilutions of RNA with known concentrations. Standard curves can be generated by amplification of the standard gene products on the LightCycler system (one-step RT-PCR). Based on these standard curves, concentrations of a target sample can be determined. However, quantification of mRNA copy numbers using this method do not necessarily reflect the actual and physiological expression level of a gene due to differences in isolation and storage of RNA. For these reasons, it makes sense to determine mRNA expression level of a gene of interest relative to a housekeeping/reference gene to adjust for alterations in mRNA copy numbers induced by experimental treatment. If this approach is used, separate standard curves have to be generated to determine the mRNA concentrations of the gene of interest and the reference gene in a given sample.

Total RNA samples used in qRT-PCR were from the same preparations as described for the Affymetrix GeneChip experiments. However, to minimize any cross reaction artefacts, the liver part of the invasion front was microdissected separately from tumor; thereby defining new types of tissues (liver and liver invasion without tumor, Tumor Invasion without liver and Tumor). For each of the gene of interest identified from the GeneChip, primers were designed from the target sequences retrieved from the Affymetrix Probe Sequence Database using Primer3 software. Quantitative PCRs were carried out in duplicates using equal amounts of each RNA sample. Each reaction contained the fluorescent indicator SYBR Green I dye and 0.5μM of each respective forward and reverse primer in a total volume of 20 μL. Amplification PCR and monitoring of the fluorescent emission in real-time were done in Light Cycler as recommended by the manufacturer (Light Cycler RNA Master SYBR Green I protocol). The data collected from these quantitative PCRs defined as threshold cycle (Ct) of detection for the target or the housekeeping genes in each RNA sample. To convert the Ct value into a relative abundance of target and housekeeping gene per

sample, a standard curve was generated for the housekeeping gene using serial dilutions of RNA sample: an arbitrary value of template was first assigned to the highest standard and then corresponding values were assigned to the subsequent dilutions and these relative values were plotted against the Ct value determined for each dilution resulting in the generation of the standard curve. The relative amount of target and housekeeping genes in each sample was then determined using the comparative Ct method. The relative quantity of target, normalized to an endogenous reference (usually 18s RNA gene).

3.8 Immunohistochemistry

For immunohistochemistry, formalin fixed pieces of tumor bearing livers were paraffin embedded. 1.5 µm sections were deparaffinized with xylene and passaged through decreasing concentrations of ethanol. Subsequently antigen retrieval was performed by heating the slides in 10 mM citric acid in a microwave oven (two times 5 min, 560 W) at pH 6.0. Sections were blocked against endogenous peroxidases using 3% H_2O_2 and were incubated with anti-ß-catenin, diluted 1:200 in PBS, at 4°C overnight. After washing and incubation with secondary antibody (anti-mouse/anti-rabbit; Vector, Burlingame, CA, USA) for 30 min. staining reaction was done using DakoCytomation AEC Chromogen (Dako GmbH, Hamburg, Germany) as substrate. For α-smooth muscle actin (α-SMA) staining, α-SMA detection was performed with a 1:100 diluted monoclonal mouse anti α-SMA antibody (clone asm-1, Cymbus Biotech, Chandlers Ford, UK), procollagen type I with a polyclonal antibody (Santa Cruz, sc-25974) at 1:100 dilution, transgelin (SM22α) with a polyclonal antibody (ABCAM, ab 10135) at 1:50 dilution and cellular retinol binding protein (cRBP-1) with a polyclonal antibody (Santa Cruz, sc-17145) at 1:100 dilution. As a secondary antibody, 1:300 diluted biotinylated anti-mouse IgG (Vector Laboratories, Buringame, CA) was used according to established protocols (Borkham-Kamphorst et al., 2004). The antibody reaction procedures were followed by treatment with an avidin-conjugated peroxidase (Vectastain ABC-Elite Kit, Vector Laboratories). Peroxidase activity was detected with diaminobenzidine (DAKO, Hamburg, Germany) and tissue sections were briefly counterstained with methyl green. For Hep-Par-1 and desmin staining, deparaffination and heat mediated antigen retrieval in 0.05 M citrate buffer of pH 6 of 2 µm thin sections were followed by incubation with monoclonal antibodies. Hep-Par-1 (DAKO, #M7158) is an antibody reacting specifically with hepatocytes in routinely

processed specimen (Wennerberg et al., 1993) and identifies an antigen unique to hepatocellular mitochondria (Lamps et al., 2003). Anti-desmin antibody (Clone D33; DAKO #M0760) was used to visualize HSC in quiescent as well as activated states (Geerts et al.; 2001) The primary antibodies were detected according to the alkaline phosphatase anti-alkaline phosphatase (APAAP) method using a rabbit-anti mouse secondary antibody (DAKO, #Z0259), a mouse monoclonal APAAP complex (DAKO, #D0651), and the Fast Red chromogenic substrate system (DAKO, #K0699). Haemalaun was used as a counterstain.

3.9 shRNA

A short sequence of RNA which makes a tight hairpin turn and can be used to silence gene expression. The use of specially designed vector constructs for inducing RNA interference has numerous advantages over oligonucleotide-based techniques. The most significant advantage is stability. Promoter regions in the vector ensure that shRNA transcripts are constantly expressed, maintaining cellular levels at all times. Thus, the duration of the effect is not as transient as with injected RNA, which usually lasts no longer than a few days. And by using expression constructs instead of oligo injection, it is possible to perform multi-generational studies of gene knockdown because the vector can become a permanent fixture in the cell line.

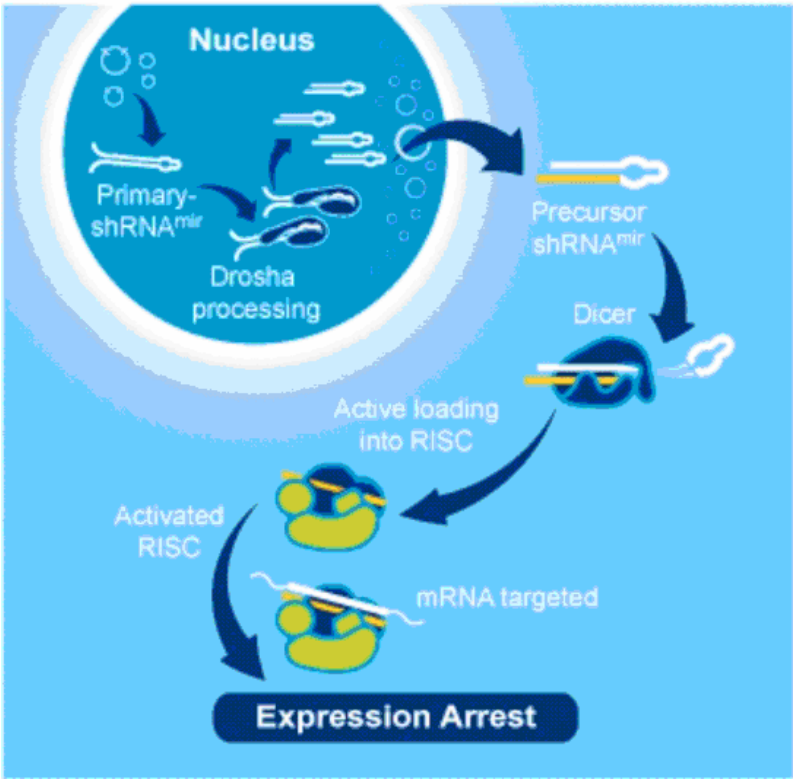

Figure 2: MicroRNA processing pathway utilized for shRNAmir (Source: Open Biosystems)

3.10 shRNAmir design

Expression Arrest shRNAmir triggers have been designed to mimic a natural microRNA primary transcript and each target sequence has been selected based on thermodynamic criteria for optimal small RNA performance (Silva et al., 2005) and cloned into pSM2 Vector. The clones were readily supplied in Bacterial stocks by Biocat GmbH for the gene of interest.

Advantages of shRNAmir design

Replaced mature microRNA sequence in mir-30 with gene specific duplexes

Adding mir-30 loop and context sequences adds endogenous processing by Drosha which increases subsequent Dicer recognition and specificity

Dicer processing promotes active loading into the RISC complex

Rules based design include destabilizing the 5"end of the antisense strand for strand specific incorporation into RISC

Increased Drosha/Dicer processing=More siRNA=Greater knockdown

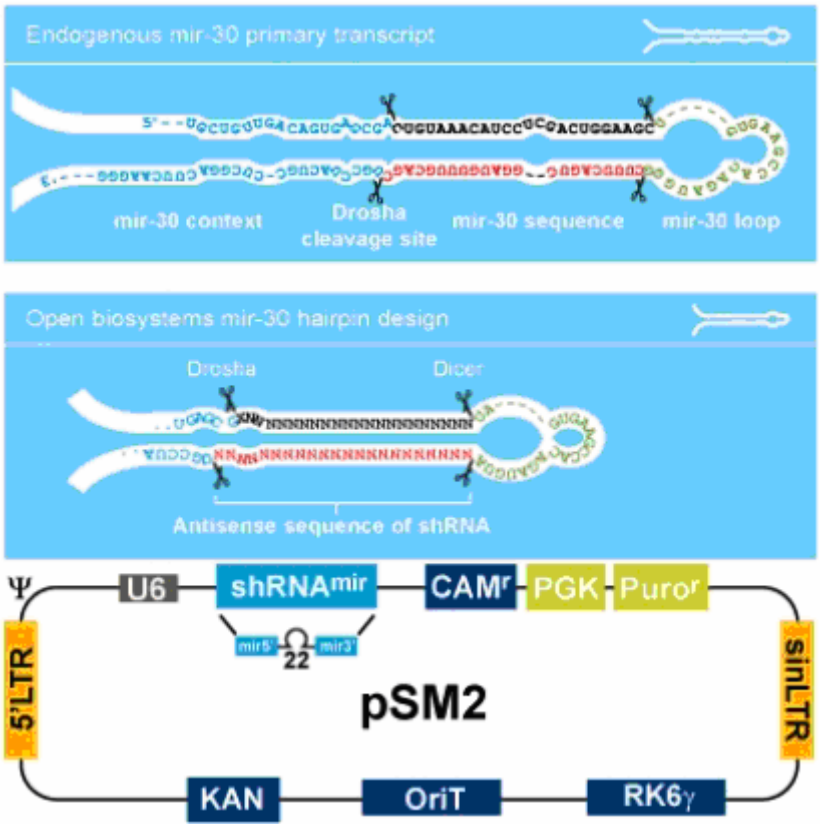

Figure 3: Unique microRNA adapted design (Source: Open Biosystems)

3.11 Extraction of Plasmid DNA

3.11.1 Mini-Preparation

Mini-preparation was usually performed to screen the recombinants following the isloation of plasmids from pSM2 vectors containing shRNA.

The plasmid extraction was done according to manufacturer's instructions. (Eppendorf Fast Plasmid Mini. Cat No 0032007.653). A single colony was grown overnight in 3 ml of 2X LB medium containing chloramphenicol to a final concentration of 50 µg/ml. The culture was incubated overnight at 37°C with vigorous shaking at approximately 250 rpm.

An aliquot (1.5 ml) of the overnight culture was transferred to 2 ml culture tube, and centrifuged at max. speed for 1min. The pellet was resuspended in 400 µl of *ice-cold complete* lysis solution, mixed thoroughly by constant vortexing at the highest setting for a full 30 sec. and incubated at room temperature for 3 min. The supernatant was transferred to a spin column assembly and centrifuged for 30–60 sec. at maximum

speed. 400 µl of diluted wash buffer was added to the spin column assembly and centrifuged for 30–60 sec. at max. speed. Filtrate was decanted from the spin column assembly waste tube and the spin column was placed back into the waste tube and centrifuged at max. speed for 1 min. to dry the spin column. Column was transferred into a collection tube and 50 µl of elution buffer was added directly to the centre of the spin column membrane and centrifuged at max. speed for 30–60 sec. The extracted plasmid DNA was further used to check for any uneventful recombinants in the clones. The remaining bacterial suspension was either stored as glycerol stock (15 %) or used for Maxi-prep.

3.11.2 Maxi-Preparation

Maxi-prep was typically done according to the protocol of the manufacturer. One hundred millilitres of 2x LB medium containing 50 µg/ml chloramphenicol was inoculated with either the bacterial glycerol stock or rest of the bacterial culture from the mini-prep. The culture was incubated over night at 37°C with vigorous shaking at approximately 250 rpm.The entire suspension was centrifuged at 12000rpm, 4°C for 10 min in an Eppendorf B007 rotor. The pellet was resuspended in 10 ml of resuspension buffer containing 100 µg/ml of RNase A. Further a volume of 10 ml of lysis buffer was added. The sample was gently mixed and left for 5 min at RT to allow bacterial cell lysis. A volume of 10 ml of ice-cold neutralisation buffer was added and kept on ice for another 20 min. The suspension was centrifuged at 12000 rpm 4°C for 1hr. The resultant supernatant was passed through a previously equilibrated Qiagen Tip 500 column. Once the solution was filtered, the column was washed twice with 30 ml of wash buffer. Finally the DNA was eluted with 15 ml of elution buffer into a centrifuge tube. An additional 10.5 ml of isoproponal was added slowly to elute along the walls of the centrifuge tube. Immediately, the DNA precipitate could be visualised forming a white ring at the interface of the two solutions. The DNA was pelleted by ultra centrifugation for 1 hr at 12000rpm, and 4°C. The pellet was subsequently washed with 5 ml of 70 % ice-cold ethanol. Finally the pellet was air dried, and resuspended in appropriate amount of TE-buffer (pH 7.6). The purified DNA was stored at -20°C for further use.

3.12 Puromycin Dose-Response

In order to generate stable cell lines expressing the shRNA of interest, it is important to determine the minimum amount of puromycin required to kill non-transfected cells. A simple procedure to quickly test this was used. Cells were plated at 25% confluence in 18 wells of a 24-well plate and grown overnight. The wells were labelled to reflect the concentration of antibiotic to be applied (in duplicate). Medium containing 0, 0.5, 1, 1.5, 2, 4, 6, 8, 10 µg/ml puromycin was prepared. Growth media was aspirated from the cells and medium containing appropriate dilutions of the antibiotic was applied to the wells. Plate was returned to the incubator. Every 3 days the old medium was aspirated and replaced with freshly prepared selective medium. The cells were monitored daily and the percentage of surviving cells was observed. Optimum effectiveness was reached in 5-7 days with puromycin. The minimum antibiotic concentration to use is the lowest concentration that kills 100% of the cells in 5–10 days from the start of antibiotic selection.

3.13 Transfection

3.13.1 Transfection of Cells with Plasmid DNA containing shRNA constructs

The day before transfection, cells were plated in a 6 well plate so that they were approximately 2-3x10^6 confluent on the day of transfection. Arrest-In™ reagent was warmed to ambient temperature (approximately 10-15 minutes at room temperature) and mixed well by vortexing prior to use. For each well in transfection, plasmid DNA (4µg) and Arrest-In™ (10µg) were diluted in 50µl of serum-free medium each. Diluted DNA was added to the diluted Arrest-In™ reagent, mixed rapidly and incubated for 10 minutes at room temperature. 100µl complex was added directly to cells in culture with existing growth medium and gently rocked back and forth. After 6 h incubation the transfection medium was aspirated and replaced with the standard culture medium. The cells were returned to the CO_2 incubator at 37^0C. After 48 hrs of incubation, the cells were transferred to medium containing Puromycin (2µg/ml) for selection.

3.13.2 Co-transfection of pSEAP plasmid with pBabe Puro

LS174T were transfected with pSEAP plasmid DNA carrying different fragments of □-catenin promoter along with pBabe Puro plasmid harbouring puromycin selection

marker in 9:1 ratio. One day before transfection, 2-3 x 10^6 cells were plated in 2000 µl of growth medium so that cells were 90-95% confluent at the time of transfection. For each transfection 3.5µg of pSEAP and 0.5µg of pBabe puro Plasmid DNA was diluted in 50 µl of Opti-MEM® I Reduced Serum Medium and mixed gently. 10µl of Lipofectamine™ 2000 was diluted in 50 µl of Opti-MEM® I Medium, incubated for 5 minutes at room temperature. The diluted DNA was combined with diluted Lipofectamine™ 2000 (total volume = 100 µl), mixed gently and incubated for 20 minutes at room temperature. 100 µl of complexes were added to each well containing cells and medium. Mixed gently by rocking the plate back and forth and returned to 37°C in a CO_2 incubator for 18-48 hours prior to testing for transgene expression. Medium was changed after 6 hours. For stable cell lines: cells were passaged at a 1:10 dilution into fresh growth medium 48 hours after transfection with 2µg/ml puromycin.

3.14 Protein preparation and quantification

LS174T clones of CXCL1, IL-8, non-specific shRNA and mock-transfected LS174T cells were each plated in tissue culture flasks. After reaching confluency the cells were washed thrice with PBS and 200µl lysis buffer was added to the flasks and incubated for 10 min on ice with shaking and at -80^{0}C for 10 min. The lysate was transferred into eppendorf tubes, centrifuged for 5 min. at 4^{0}C and the supernatant was collected in new tubes. The protein content was measured by using Bio photometer and stored at -20^{0}C.

3.15 Sodium dodecylsulphate polyacrylamide gel electrophoresis (SDS-PAGE) and Western blotting (WB)

Appropriate volumes (10µg) of the samples were mixed with equal volumes of 2x Laemmli buffer containing SDS and mercaptoethanol, boiled for 10 min. at 100^{0}C to denature the proteins and snap cooled on ice. Briefly centrifuged and Vertical mini gels was performed in a Biorad gel apparatus employing 5% stacking gel and 15% separating gel at 100 V (stacking gel) and 180 V (separation gel) in Laemmli discontinuous buffer. For WB performance, separated proteins were electro transferred onto nitrocellulose membrane (pore size 0.45 µm) for 60 minutes at 230 mA by semi-dry transfer system (Scie-Plas, UK) using the buffer (Towbin et al.1979) After confirming the transfer of proteins by staining with 0.5% Ponceau solution, the membrane was destained with TBST. Unspecific binding sites were blocked with

TBST in 5%skimmed milk powder for 1h and the membranes were washed once with TBST. All steps of assay were performed by shaking at room temperature. After that, respective antibodies in TBST with 5%skimmed milk powder (CXCL-1 2µg/ml; IL-80.2µg/ml R&D systems, Minneapolis, USA) were added to the membrane and incubated overnight at 4^0C. After washing four times for 15 min. each with TBST, the membranes were incubated for 60 minutes with Goat anti-mouse IgG-HRP; at 1:2000 dilution (Santha Cruz Biotechnology, Santha Cruz, USA) or rabbit anti-goat IgG -HRP (Sigma, St. Louis, USA) at 1:4,000 dilution in TBST with 5% skimmed milk powder. Membranes were washed 6 times as before for 10 min. each. Excess buffer was drained off from the membrane and placed on a saran wrap facing the protein side up and ECL detection reagent was added on to the membrane and incubated for 5 min. Excess detection reagent was drained off from the membrane and placed on a new saran wrap and exposed to autoradiography film for suitable time in an x-ray cassette.

3.16 Reporter gene activity (SEAP) measurement

The Tropix® Phospha-Light™ system is a chemiluminescent reporter gene assay system designed for the rapid, sensitive, and non-isotopic detection of secreted human placental alkaline phosphatase in cell culture media. The Phospha-Light™ assay incorporates Tropix CSPD® chemiluminescent substrate and Emerald™ luminescence enhancer for high sensitivity and wide dynamic range. CSPD® substrate has been used for detection of secreted placental alkaline phosphatase in cell culture media (Cullen, B. et al.; 1992). The alkaline phosphatase assay is simple and rapid. Secreted placental alkaline phosphatase is measured from 48 to 72 hr after cell transfection. Cell culture medium or cell lysate is incubated with Reaction Buffer until maximum light emission is reached (approximately 20 min for culture media). Light output is then measured in a luminometer. Chemiluminescent assays for placental alkaline phosphatase may be conducted in cells that have endogenous alkaline phosphatase activity. Endogenous non-placental enzyme activity is significantly reduced by a combination of heat inactivation and differential inhibition that does not significantly inhibit the placental isozyme. It is important to determine the level of endogenous enzyme in media or extracts from non-transfected cells to establish assay background.

Protocol

Sufficient CSPD® substrate was diluted to 1:20 with reaction buffer diluent to make reaction buffer (100µl/tube). Assay buffer and reaction buffer were equilibrated (100 µl/sample) to room temperature. Sufficient 5X dilution buffer was diluted to 1X (300 µL/sample) with H_2O. Samples were prepared by diluting 100 µL of culture medium with 300 µL of 1X dilution buffer in a microfuge tube. Samples were heated at 65°C for 30 min. and then cooled on ice to room temperature.100 µL of sample and 100 µL of assay buffer were added to a luminometer tube and incubated for 5 min. To this 100 µL of reaction buffer was added, incubated 20 min and measured in a luminometer for 1 sec/tube. All the assays were performed in triplicates.

4 Results

4.1 Interspecies comparison of gene and gene expression profiles in a mouse model of colorectal liver metastasis and in clinical specimens

Invasion-related genes over-expressed by tumor cells as well as by reacting host cells represent promising drug targets for anti-cancer therapy. Such candidate genes need to be validated in appropriate animal models. This study examined the suitability of a murine model (CT26/ Balb/C) for the representation of clinical colorectal liver metastasis on a global gene expression scale. Interspecies similarity was examined through overlap of up-regulated genes, gene expression patterns (gene ontology-terms) and condensed pattern families between the respective compartments. In order to acquire cross-compartmental patterns and to generalize findings obtained in distinct animal models with respect to the clinical situation, global gene expression patterns were examined in a syngenic immunocompetent mouse model and in a set of five clinical samples of colorectal liver metastases. Histology and global gene expression data from four compartments namely liver, distant from the invasion front (L), liver adjacent to the invasion front (LI), tumor adjacent to the invasion front (TI) and tumor distant from the invasion front (T) were analyzed particularly concentrating on the following three questions:

What is the degree of interspecies overlap on the single-gene level?

How similar are gene expression patterns and single-gene expression in a interspecies comparison and can relations between these parameters in addition to histological assessment be used to explain interspecies overlap?

Which gene expression patterns and selected marker genes can be considered typical for the different compartments?

4.1.1 Intraspecies cross-compartmental correlation of histology and gene expression

To examine the degree of correlation of global gene expression changes to the histology within each species, the four compartments (liver, liver invasion, tumor invasion and tumor) were compared with each other on the gene expression scale separately for each species prior to interspecies comparisons. The number and percentage of differentially regulated genes (increase calls plus decrease calls)

between each of the four defined compartments was determined (Table 1). The comparison of tumor and tumor invasion compartments showed the lowest number of differentially regulated genes, followed by the comparison of pure liver and liver invasion compartments (Table 1, upper panel). Comparison of compartments of different histological origin displayed higher values (Table 1, lower panel) than compartments of identical histologic origin. These data indicate that the fact of different histological origin (e.g. tumor versus liver) is reflected on the level of global gene expression and is not clouded by background noise in this model. On the other hand, the observation that there are differentially regulated genes between L versus LI and T versus TI argues for a number of invasion specific processes in both species responsible for these differentially regulated genes.

Table 1: Percentage of genes present (in at least one of two compartments) and total number of differentially regulated genes (increase plus decrease calls)

	Human		*Murine*	
Compartmental Comparisons	*%*	*no*	*%*	*no*
T/TI	9.1±0.1	1519±9	22.5±0.9	3452±144
L/LI	23.8±5.0	3785±797	25.6±3.5	3790±519
TI/LI	28.8±4.4	5310±819	35.1±4.2	5683±675
LI/T	34.4±4.8	5871±80	28.6±2.4	4327±363
L/TI	37.8±0.1	6817±13	34.9±0.9	5458±138
L/T	40.8±0.8	6555±127	35.0±0.9	5034±124

L= liver, LI=liver invasion, TI=tumor invasion, T=tumor.

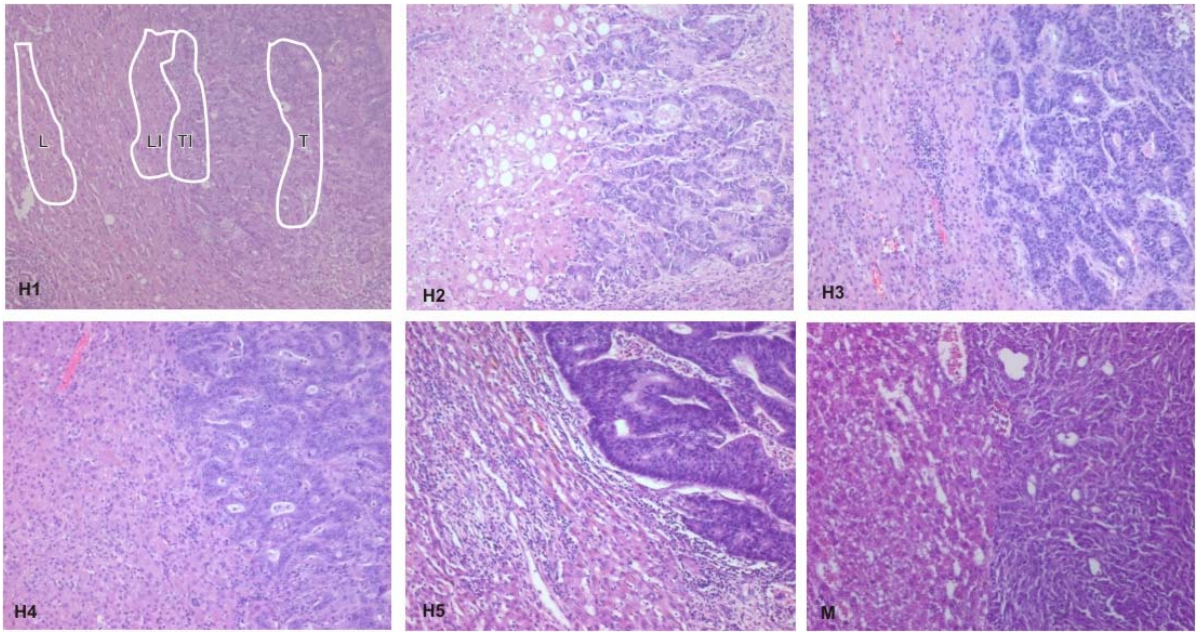

Figure 4: Histology of invasion fronts of liver metastases from the clinical specimen and from the murine model.

HE staining of the invasion front of five clinical specimens (H1-H2) and murine tumors (M, CT26) growing in the livers of Balb/C mice. The human tumors were moderately to lowly differentiated adenocarcinomas with moderate stroma production and stroma reaction by a mild lymphocytic infiltrate. The tumor part of the invasion front did not differ strikingly from the inner parts. The liver displays an orderly structure with some fibrosis and a mild to moderate lymphocytic infiltrate in the portal tracts, no major pigments and mild to moderate fatty degeneration. The liver part of the invasion front contains mainly hepatocytes, but, in addition, an increased number of inflammatory and fibroblast like cells as well as sporadically ECM-like deposits. The murine tumor is a lowly differentiated to undifferentiated adenocarcinoma with little stroma production and little stromal reaction. As in the clinical samples the tumor does not significantly differ from the tumor part of the invasion front. The livers are of orderly structure with no apparent abnormalities. The liver part of the invasion front does not display gross differences to the liver except that the hepatocytes appear to be slightly flattened.

Areas of microdissection are displayed exemplarily (H1).

4.1.2 *Interspecies overlap of compartment-specific up-regulated genes, gene expression patterns and histological similarity*

The extent of interspecies overlaps of up-regulated genes were examined, which, in the invasion front, would represent potential target genes for tumor invasion. In addition, these findings were evaluated to see whether they would be paralleled by the histopathology and gene expression patterns.

To determine the single-gene overlaps, files of IDs were created, which included all genes present in one particular compartment within one species that display an “increase call” (up-regulation) as compared to all other three compartments of the same species.

Gene expression patterns were determined using the Gene Ontology tree with its branches “biological process”, molecular function” and “cellular component”. Thereby, those GO-terms which were “typical” for any of the 4 compartments were defined. To obtain these compartment specific GO-terms, the following algorithm was applied:

Compartment specific up-regulated genes were selected as described above (test file).

A reference file was created including all genes which are present in at least one of the four compartments.

The distribution of the respective test files was compared to the distribution of the reference files in the GO-matrix (GOSSIP software).

Interspecies syn-compartmental comparisons revealed that pure liver compartments showed the highest values among the species with a gene expression pattern overlap of 28% and a single-gene overlap of 16.4% (Table 2). Tumor invasion showed values of 10.9% (patterns) and 8.2% (single gene). Liver invasion compartments and tumor compartments displayed very low overlap-values (Table 2). These data indicate marked differences in the biological processes even in compartments of the same histologic origin.

Although from different tissues of origin, cross-compartmental overlap was surprisingly high between human liver invasion and murine tumor invasion compartments (pattern: 16.5%, single-gene 6.3%). This result indicates that genes involved in invasion may overlap between the species independent from

histologically defined compartments. If up-regulated genes from both human invasion compartments were added and compared to both murine invasion compartments resulted in 9.0% overlapping genes as compared to only 4.6% of syn-compartmental comparisons (data not shown). Similarly, if up-regulated genes from both murine invasion compartments were added and compared to both human invasion compartments resulted in 5.6% overlapping genes as compared to only 2.9% of syn-compartmental comparisons (data not shown).

Relaxation of inclusion criteria dramatically increased overlapping genes in syn-compartmental as well as cross-compartmental comparisons (Table 2, third panel). E.g., more than half of exclusively up-regulated genes in human liver (52.7%) were at least present (but not necessarily up-regulated) in the murine counterpart. However, syn-compartmental specificity was nearly lost (e.g. overlap of liver and tumor: 43.8%). These data indicate that the number of overlapping genes can be increased by relaxing criteria but at the cost of compartmental specificity.

Table 2: Interspecies gene expression pattern overlap

Murine / *Human*	*L*	*LI*	*TI*	*T*
Gene expression pattern overlap				
	% (277±2)	*% (5±4)*	*% (76±26)*	*% (51±1.4)*
L (458±42)	28 (128±7.8)	0.28 (1±1.4)	2 (9±6.4)	1.7 (8±1.4)
LI (133±11)	24.8 (33±0)	0 (0±0)	16.5 (22±1.4)	0.8 (1±0)
TI (46±31)	19.5 (9±3.5)	0 (0±0)	10.9 (5±7)	10.9 (5±1.4)
T (11±15)	27.2 (3±4)	0 (0±0)	45.5 (5±0)	0 (0±0)
Single-gene overlap: up-regulated versus up-regulated				
	% (635±5)	*% (440±88)*	*% (402±4)*	*% (440±8.5)*
L (999±156)	16.4 (164±8.5)	3.0 (30±0.7)	1.0 (10±0)	1.1 (11±0.7)
LI (352±104)	5.1 (18±3.5)	2.8 (10±6.4)	6.3 (22±9.2)	2.6 (9±2.8)
TI (170±84)	1.8 (3±0.7)	0.6 (1±0)	8.2 (14±11.3)	5.3 (9±3.5)
T (320±81)	0.9 (3±0)	1.3 (4±0.7)	4.7 (15±7.8)	1.6 (5±4.2)
Single-gene overlap: up-regulated versus present				
	% (11754±347*)*	*% (13127*±700*)*	*% (13962*±190*)*	*% (11562*±131*)*
L (999±156)	52.7(527±32.5)	51.7(517±45.3)	50.4(504±14.8)	43.8(438±41)
LI (352±104)	41.2(45±52.3)	50.3 (177±68)	54.8(193±53)	48 (169±52)
TI (170±84)	57.6(98±53.7)	60 (102±57.3)	71.8(122±67.2)	61.2(104±55.9)
T (320±81)	29.4(94±24)	35.6(114±29.7)	37.2(119±35.3)	30.6(98±38.1)

First panel: percentage and total number (in brackets) of human GO-terms overlapping with murine) and single-gene overlap (lower two panels, percentage and total number (in brackets) of human genes overlapping with 1. up-regulated genes. Second panel or 2. genes present (third panel) in mouse). The total number of up-regulated genes or over-represented patterns for each compartment is indicated in the first column (human) and the first line (murine) of each panel.

4.1.3 Gene expression patterns and pattern families

Inorder to know the biological mechanisms responsible for the observed interspecies similarities and gene expression overlaps, GO-terms (biological processes, molecular functions and cellular compartments) fulfilling the following criteria were included into further analysis:

Number of underlying genes per GO-term >9

No terms of lower hierarchy clearly contributing to a significant higher node (e.g. exclusion of “collagen V” if “collagen” is significant)

Only one out of two or more alternate and significant terms (either “steroid binding” or “steroid metabolism”)

No very general GO-terms of highest hierarchical levels (e.g. “membrane”, “extracellular”).

Application of these criteria resulted in 52 “core” GO-terms (Figure 2). For each GO-term, a diagram was constructed based on the p-values for the four different compartments in both species (Figure 5). Such a diagram allows one to directly visualize in which compartment one particular GO-term is over-represented. Comparing the four bars to the left (human) with the ones to the right (murine) allows one to directly compare significant GO-terms between the two species. GO-term-diagrams displaying the same compartmental distributions were grouped and the statistically significant compartments were indicated (Figure 5, framed). In principle, the 8 (2x4) examined compartments with significant p-values could be combined in 256 possible ways (all possible combinations of 2-8 compartments=binomial coefficient n over k =n!/(k!(n-k)!)). However, only 10 combinations were actually found, indicating a non-random and probably biologically meaningful distribution of over-represented GO-terms among the different compartments. These 10 groups of GO-term diagrams with identical compartmental distribution were ordered into columns and were named according to the significant compartments (e.g. Lh or LIh

TIm, Figure 5, framed). Subsequently, GO-terms were grouped into pattern families by biological reasoning. 46 out of 52 GO-terms were assigned to 4 larger pattern families: Secondary metabolism, invasion, immune response and primary metabolism (Figure 5, different grey scales).

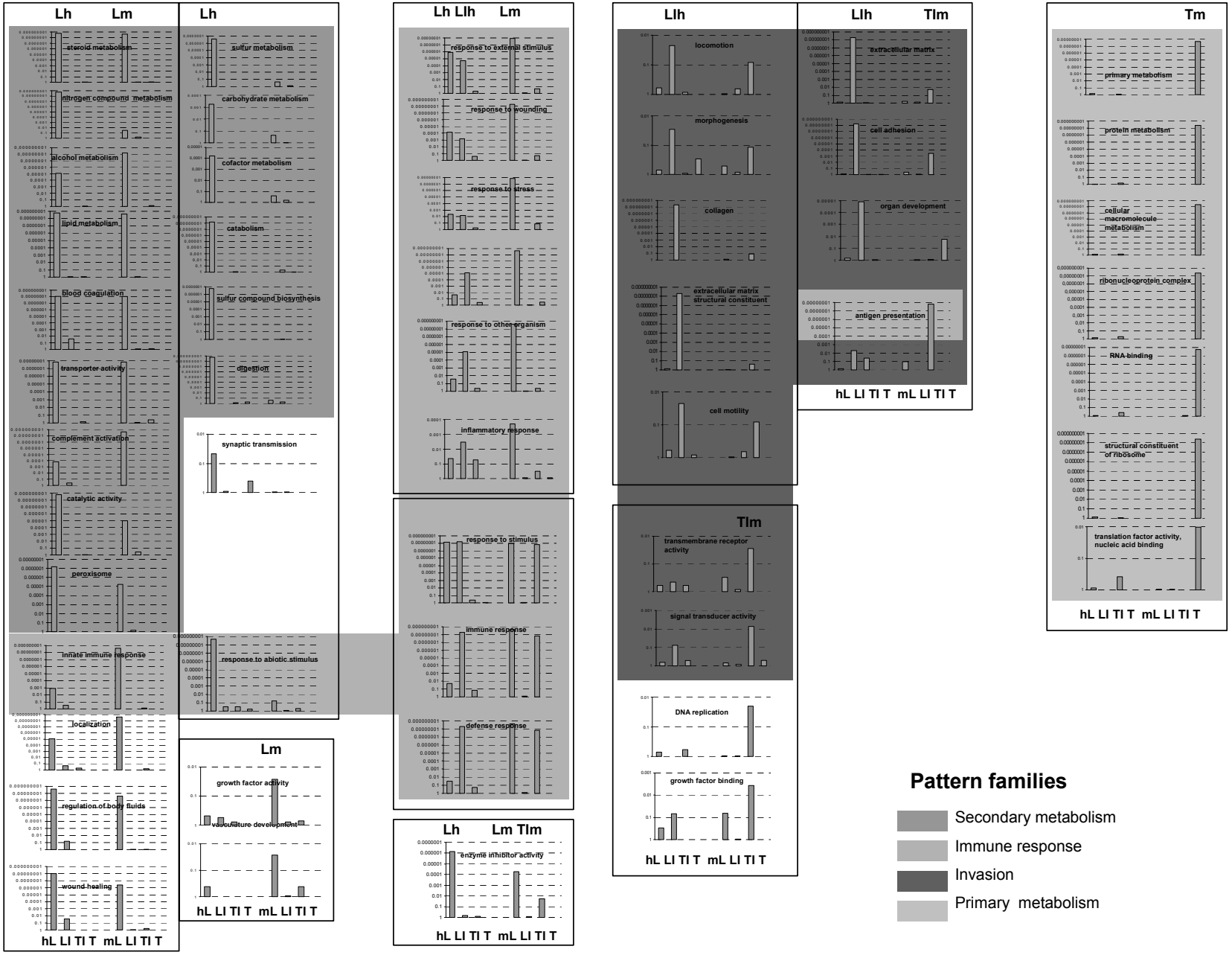
Lh
Lm
steroid metabolism
nitrogen compound metabolism
alcohol metabolism
lipid metabolism
blood coagulation
transporter activity
complement activation
catalytic activity
peroxisome
innate immune response
localization
regulation of body fluids
wound healing
hL LI TI T mL LI TI T
Lh
sulfur metabolism
carbohydrate metabolism
cofactor metabolism
catabolism
sulfur compound biosynthesis
digestion
synaptic transmission
response to abiotic stimulus
Lm
growth factor activity
vasculature development
hL LI TI T mL LI TI T
Lh Llh Lm
response to external stimulus
response to wounding
response to stress
response to other organism
inflammatory response
response to stimulus
immune response
defense response
Lh Lm Tlm
enzyme inhibitor activity
hL LI TI T mL LI TI T
Llh
locomotion
morphogenesis
collagen
extracellular matrix structural constituent
cell motility
Tlm
transmembrane receptor activity
signal transducer activity
DNA replication
growth factor binding
hL LI TI T mL LI TI T
Llh Tlm
extracellular matrix
cell adhesion
organ development
antigen presentation
hL LI TI T mL LI TI T
Tm
primary metabolism
protein metabolism
cellular macromolecule metabolism
ribonucleoprotein complex
RNA-binding
structural constituent of ribosome
translation factor activity, nucleic acid binding
hL LI TI T mL LI TI T
Pattern families
Secondary metabolism
Immune response
Invasion
Primary metabolism

Figure 5: Compartmental distribution of compartment specifically over-represented GO-terms.

GO-terms were selected as described in the text. GO-term-diagrams are ordered in columns according to their compartmental distribution. The respective significant compartments are indicated in bold. Each diagram consists of 4 human compartments (to the left) and 4 murine compartments (to the right).

Abbreviations: Lh=human liver, LIh=human liver invasion, TIh=human tumor invasion, T=human tumor, suffix “m” indicates murine compartments respectively.

Groups of GO terms with identical compartmental distribution are framed. Pattern families are indicated by different grey scales (see insert)

A. Secondary metabolism

The syn-compartmental interspecies evaluation revealed a huge number of GO-terms belonging to secondary metabolism among the liver compartments in both species (Figure 5, column 1, dark grey). In contrast, none of the other three compartments showed over-representation of any secondary metabolism term indicating that this pattern family is liver specific. In addition, the human liver displayed some more metabolism terms that were not found to be statistically significant in the murine liver (Figure 5, column 2). Some additional terms, not belonging to the secondary metabolism family were found to be over-represented in murine and human livers separately or in combination.

B. Immune response

GO-terms positioned either upstream or downstream of the marker term “Immune response” were distributed along the liver, liver invasion and tumor invasion compartments in both species (Figure 5, light grey). Only the tumor compartment did not show any significant “immune response” -related patterns. Different compartments seemed to be involved in innate and acquired immune response: The GO-terms “Innate immune response” (Figure 5) as well as “neutrophil activation” and “phagocytosis” (not shown) were over-represented in the liver compartments but not in any invasion front compartments. In contrast, the GO terms “antigen presentation” (Figure 5), and “antigen processing” (not shown) typical for the acquired immune response were over-represented in the invasion front compartments in both species, but not in the liver compartments.

C. Invasion

GO-terms which have earlier been detected in a nude mouse model to be typical for invasion (Bandapalli et al 2006) were over-represented in both species in the invasion front compartments but not in any of the other compartments (Figure 5, darkest grey). Some terms such as “locomotion”/”cell motility” were over-represented in human liver invasion only, and others such as “signal transducer activity” were over-represented in murine tumor invasion only, while not reaching statistical significance in the other invasion compartments. Several GO-terms such as “extracellular matrix, “cell adhesion” and “differentiation”/”development” were over-represented in the human liver invasion compartment and in the murine tumor invasion compartment. This finding indicates that the invasion compartments, in addition to immune response patterns (see above), display typical invasion-related patterns. Surprisingly only the murine tumor compartment and the human liver compartment displayed over-represented invasion terms. This phenomenon may indicate a high degree of similarity of human and murine tumor invasion on the pattern level, which, however, remains only true if the invasion front is examined as a whole.

D. Primary metabolism

In the murine but not in the human tumor compartment, a prominent “primary metabolism” cluster was found (Figure 5, lightest grey). This finding will be commented in the discussion section.

In summary, these data indicate that GO-terms can be condensed by applying an inclusion algorithm and by simple biological reasoning to reveal four pattern families that include most GO-patterns and that seem to represent expected biological functions, at least in liver and invasion front compartments.

4.1.4 Single-gene overlap within overlapping patterns

Finally the data was examined to see, whether the observed low overlap on the single-gene level (Table 5, first panel) would still hold true if the constitutive genes of

actually overlapping GO-patterns were compared between the species. In addition, compartment-specific up-regulation of overlapping genes was confirmed on the mRNA level by qPCR.

For the determination of single-gene overlaps within the “secondary metabolism” family two main metabolism sub-terms: “lipid metabolism” and “nitric compound metabolism” were chosen. As indicated in Table 3 (first panel), 16.1 % of human “lipid metabolism” genes and 17.8 % of human “nitrogen compound metabolism” genes were identical among the human and murine liver compartments.

Table 3: Interspecies overlap of single genes underlying specific GO-terms

	Human	*Murine*	*Overlap*	
	No.	*No.*	*No.*	*%*
Secondary metabolism				
Lipid metabolism	59 ± 5.7	63.5±2.1	9.5±2.1	16.1
Nitrogen compound metabolism	53.5±10.6	24 ±1.4	9.5±2.1	17.8
Immune response				
Innate immune response	10.5±2.1	18±0	5±1.4	47.6
Antigen presentation	6 ±0	12±2.8	2±0	33.3
Invasion				
Cell Adhesion	23±4.2	40.5±3.5	2±1.4	8.4
Extracellular Matrix	20±4.2	21.5±2.1	3±1.4	15

Upper three GO-terms from both liver compartments lower three GO-terms from human liver invasion and murine tumor invasion. Overlaps as total number and in percent of human genes.

Compartment-specific up-regulation was verified on the arbitrarily selected *apolipoprotein F* gene from the “lipid metabolism” pattern. The gene showed the highest levels of mRNA in the liver compartment in both species (Table 4). Gene activity decreased with increasing distance from the liver compartment in both species.

For the determination of single-gene overlaps within the “immune response” family two immune response terms: “innate immune response” and “acquired immune response” were chosen. As shown in Table 3 (second panel), 47.6 % of human “innate immune response” genes and 33.3 % of human “antigen presentation” genes were identical among the human and murine liver compartments.

For the determination of single-gene overlaps within the “invasion” family the terms: “cell adhesion” and “extracellular matrix” were chosen. As shown in Table 3 (third panel), 8.7 % of human “cell adhesion” genes and 15 % of human “extracellular matrix” genes were identical between the human liver invasion compartment and the murine tumor invasion compartments.

Compartment-specific up-regulation was verified on arbitrarily selected genes from the “cell adhesion” and the “extracellular matrix” patterns. Both genes, *thrombospondin-2* and *procollagen V-alpha 2* showed the highest level of mRNA in the human liver invasion compartment and the murine tumor invasion compartment respectively (Table 4).

Table 4: Gene expression of selected genes typical for specific compartments

Gene Name	*GO-term*		*L*	*LI*	*TI*	*T*
Apolipoprotein F	*Lipid metabolism*	*Human*	**100%**	41.75%	17.4%	16.1%
		Murine	**100%**	26.5%	22%	7.9%
Thrombospondin-2	*Cell adhesion*	*Human*	21.6%	**100%**	22.7%	8.2%
		Murine	4%	7.2%	**100%**	18.1%
Procollagen V-alpha 2	*Extracellular matrix*	*Human*	12%	**100%**	73.5%	28.7%
		Murine	4%	20.6%	**100%**	14%

RNA-levels in percent of gene expression of the compartment with highest RNA levels (=100%).

Single-gene overlap of any “primary metabolism” patterns was not found because the GO-terms did not reach statistical significance in any of the other compartments.

Altogether, these data indicate that single genes underlying overlapping GO-terms display interspecies identity to a varying degree. In addition, up-regulation on microarrays was validated by independent qPCR on arbitrarily selected genes.

4.2 Global gene expression profiles of host tissue at the invasive front of colorectal liver metastases

Invasion of tumor cells is dependent on a permissive host environment on the primary invasive site as well as on the site of metastasis.

This study examined the potential change in gene expression profiles of the host invasive front in response to the invading tumor tissue in a xenograft mouse model (LS174T), where human colon adenocarcinoma cells growing in the livers of nude mice. Colorectal liver metastases are a particularly interesting target. From a therapeutic point of view this disease is of special interest because liver metastases often remain the only manifestation of the disease after removal of the primary tumor (Curley et al., 2004 and Grem et al., 1991) such that cure is possible if the metastases can be prevented or eradicated. Brand et al and Elezkurtaj et al have examined host cell targeting strategies for the treatment of colorectal liver metastases by liver cell directed over-expression of tissue inhibitor of metalloproteinases-1 and -2 (TIMP-1, TIMP-2) targeting the tumour host interaction (impregnation concept) (Brand et al., 2000 and Elezkurtaj et al., 2004). Although they observed dramatic reductions of metastatic tumor load, the precise nature of the anti-metastatic mechanism remains to be based on circumstantial evidence. It is therefore the hope of this study that the examination of global gene expression patterns will shed some light onto the black box between hypothesis driven therapeutic experiments and the observed preclinical or clinical efficacy.

This study has the following aims:

1) To examine whether a xenograft nude mouse model of colorectal liver metastases would deliver reliable and valid data,

2) To provide a comprehensive and unbiased study of the components of the host reaction upon tumor invasion and

3) To deliver potential target genes for the development of host cell directed therapeutics.

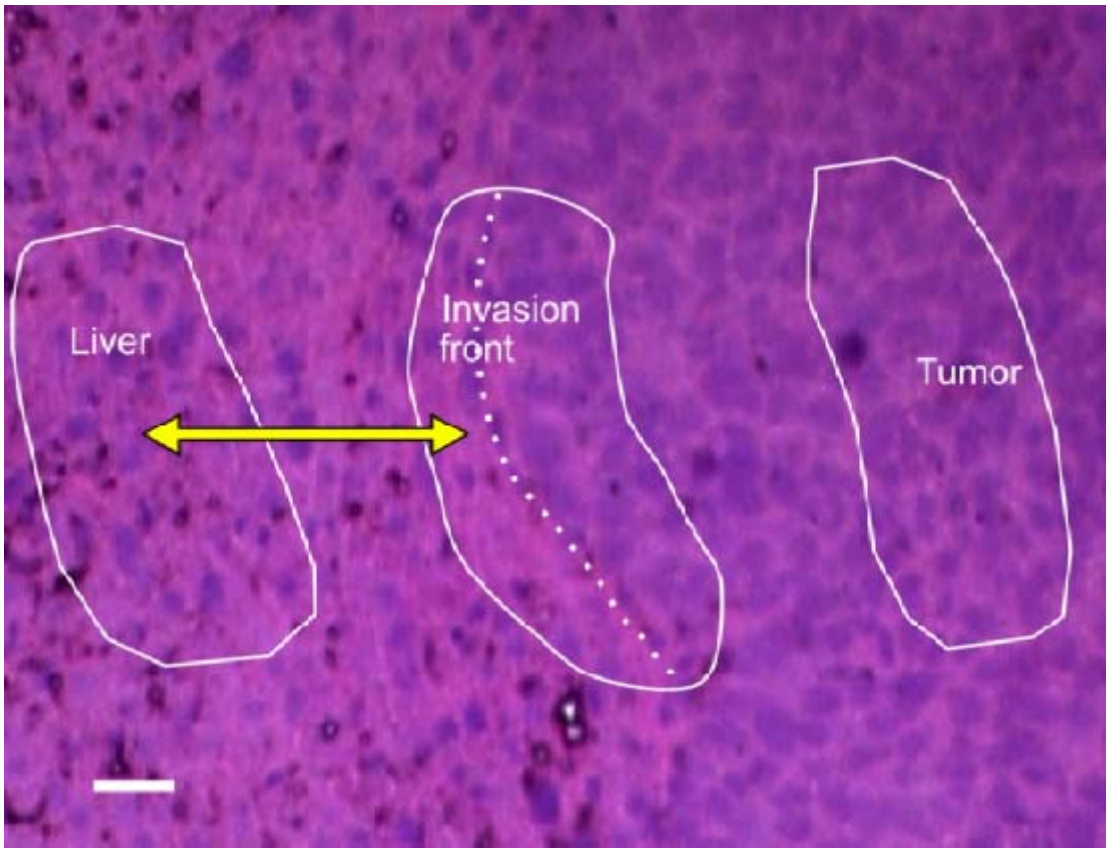

Figure 6: Areas subjected to microdissection

Dotted line indicates demarcation for liver part of invasion front, which was used for qPCR. Bar=50 µm

4.2.1 Gene expression profiles of host tissue in response to tumor invasion: Over-represented GO terms at the invasive front

First goal for the global analysis of gene expression in the invasion front was to achieve patterns of gene expression which would either confirm known processes or provide additional insights into patterns of the biological processes in this region.

To this extent minimal number of consistent gene expression patterns were defined by grouping all those genes, which are either up- or down-regulated in the host part of the invasion front.

The GO tree with its branches “biological process”, “cellular component” and “molecular function” served as the first matrix. The distribution of genes which were found to be at least 2 fold up-regulated in the liver part of the invasion front (test group) was compared to the distribution of a reference group which contained the whole group of all genes which were present in at least one of the tissues under examination (Change Call comparison, Table 5, columns to the left). Four different experiments resulting from four sets of separately microdissected material were analyzed separately. In addition, the distribution of genes which were present in the host part of the invasion front was compared to the distribution of genes which were either present in the host part of the invasion front or in the unaffected host tissue (Absolute Call comparison, Table 5 columns to the right). The Change Call comparison will reveal GO terms which are significantly over represented in the group of differentially up-regulated genes. The Absolute Call comparison will reveal GO terms which represent genes which are switched on in the invasion front while remaining inactive in the unaffected liver tissue. In all these analyses, cross reactive genes were eliminated as described in Bandapalli et al (Bandapalli et al., 2006).

Statistical significance of differential representation of GO terms between test group and reference group was analysed by the GOSSIP software (Bluthgen et al., 2005) (http://gossip.gene-groups.net) which uses Fisher’s exact test corrected for multiple testing effects. Single-test p-values are included for completeness whenever the term was significant in at least one experiment after multiple testing corrections (FDR, false discovery rate).

The above described analysis revealed lists of GO terms which were over represented in the respective test groups (Table 5).

These GO terms were then manually clustered by first grouping together all terms within one track and then combining tracks from the three different main branches which belong together due to biological reasoning.

By following these algorithms, 7 distinct groups of GO terms were defined which included 66 out of 68 significant GO terms resulting from the analyses (Table 5).

The group of terms with the overall highest level of significance is best represented by the cellular component “extracellular matrix” and the related molecular function “extracellular matrix structural constituent” which displayed the highest level of

significance in all four Change Call experiments. These results indicate that there is an abundance of transcripts of extracellular matrix (ECM) components in the host part of the invasion front as compared to unaffected host tissue. In addition, ECM components are significantly over represented among those genes which are only present in the invasion front indicating that there is an activation of otherwise silent genes by the host upon tumor invasion. Among the genes, which are responsible for this finding, are collagens which seem also to be responsible for the overrepresentation of constituents of the basal membrane.

The second group of GO terms which is consistently up-regulated in all 4 Change Call analyses is best represented by the biological process of “cell communication” which indicates increased interplay between the cells of the invasive front as compared to unaffected liver. Accordingly, “cell adhesion” / “cell adhesion molecule activity” are dramatically increased in the invasive front as well as “signal transduction”.

Table 5: GO terms consistently up regulated in the liver part of the invasion front

GO #	GO Term	Change Call				Absolute Call			
	Experiment	1	2	3	4	1	2	3	4
5575	Cellular component (CC)		*	*					
5576	Extracellular (CC)	***	***	***	**	*		•	
5615	extracellular space (CC)	***	***	**	•	*		•	
5578	extracellular matrix (CC)	***	***	***	***	°	°	*	°
5604	..basement membrane (CC)	**	***	***	*			°	
5605	....basal lamina (CC)	•		*	•				
5581	..collagen (CC)	***	***	***	***			•	
5201	extracellular matrix structural constituent (MF)	***	***	***	***	*	•	•	
30020	..extracellular matrix structural constituent conferring tensile strength activity	***	***	***	***				

	(MF)								
5539	glycosaminoglycan binding (MF)	•	*	•					
9987	cellular process (BP)	***	**	*	***				
7154	cell communication (BP)	***	***	***	***				
7155	..cell adhesion (BP)	***	***	***	***				
7160	....cell-matrix adhesion (BP)		*						
5194	cell adhesion molecule activity (MF)	***	***	***	***				
5886	..plasma membrane (CC)	•	°		*				
7165	..signal transduction (BP)	***			**				
1637	….G-protein chemoattractant receptor activity (MF)	*							
9605	response to external stimulus (BP)	***			*	**	°	*	*
42330	….taxis (BP)	**	°						
6935	……chemotaxis (BP)	**	°						
42221	……..response to chemical substance (BP)	*							
9607	..response to biotic stimulus (BP)	***			**	**	°	*	*
6952	....defense response (BP)	***			**	**	•	*	*
6955	.....immune response (BP)	***			**	*	°	•	•
19884	.....antigen presentation, exogenous antigen (BP)	**	**	*	•				
19886	……..antigen processing, exogenous antigen via MHC class II (BP)	***	**	*	•				
45087	……..innate immune response (BP)	*		•	•				
6954	……inflammatory response (BP)	**		•	•				
19956	….chemokine binding (MF)	*							

4950	……chemokine receptor activity (MF)	*							
45012	……..MHC class II receptor activity (MF)	**	**	*	•				
9611	..response to wounding (BP)	*		•	•				
					•				
5856	….Cytoskeleton (CC)	*	***		•				
15629	……actin cytoskeleton (CC)	*	*						
15630	……microtubule cytoskeleton (CC)		**						
5875	……..microtubule associated complex (CC)		**						
5871	……kinesin complex (CC)		*						
5198	structural molecule activity (MF)	**	***	**	°				
5200	structural constituent of cytoskeleton (MF)		**	*					
5488	binding (MF)	***		°	*				
5515	protein binding (MF)	***			*				
8092	..cytoskeletal protein binding (MF)	***	•		°				
3779	..actin binding (MF)	***	•		•		°	*	*
3782	….F-actin capping activity (MF)	*	•						
7010	……cytoskeleton organization and biogenesis (BP)		•	°					
46872	metal ion binding (MF)	***	•		*				
5509	..calcium ion binding (MF)	***	***	•	***				
6816	..calcium ion transport (MF)	*			°				
8283	..cell proliferation (BP)	°			*				*
7049	….cell cycle (BP)	*			*				
910	….cytokinesis (BP)				*				

16049	..cell growth (BP)	***	***	•	*				
1558	….regulation of cell growth (BP)	**	**		°				
19838	..growth factor binding (MF)	•	**						
5520	….insulin-like growth factor binding (BP)	•	**		°				
7275	development (BP)			*	°				
30154	cell differentiation (BP)		•	•	°				
9653	morphogenesis (BP)	°		•	*				
9887	..organogenesis (BP)			*	•				
7517	….muscle development (BP)		**						
45765	…….regulation of angiogenesis (BP)	*		°					
30234	enzyme regulator activity (MF)	°			•	•	°	*	*
4857	..enzyme inhibitor activity (MF)					**	°	*	•
30414	….protease inhibitor activity (MF)			°		**		*	*
4866	…….endopeptidase inhibitor activity (MF)			°		**		*	*
19835	….cytolysis (BP)	*		°					
5102	receptor binding (MF)		°	*					

GO distribution of genes up regulated in the liver part of the invasion front as compared to the control group (Change Call comparison, columns to the left). Distribution of genes solely present in the invasion front as compared to unaffected liver tissue (Absolute Call comparison, columns to the right). Number of asterisks indicates level of significance of GO term overrepresentation. Levels of significance (after multiple testing correction, FDR): $^{***}p<0.0005$, $^{**}p<0.005$, $^{*}p<0.05$,
Single-test p-values were included for completeness ($^{\bullet}p< 0.02$, $^{\circ}p<0.05$), whenever the term was significant in at least one experiment after multiple testing corrections. Change Call and Absolute Call comparisons were examined independently.
Different font (normal or italic) of GO numbers and term names indicate GO clusters obtained by biological reasoning.

Hierarchical levels are indicated by number of dots in front of GO terms.
Abbreviations in brackets behind the GO terms indicated main GO branches; CC=cellular component, MF=molecular function, BP= biological process.

The central term of the third GO cluster seems to be “response to biological stimulus” as the most significantly up-regulated node of the branch “response to external stimulus” which in addition is supported by “taxis” and “response to wounding”. Several immunological processes are up regulated in the invasive front. This GO group shows the highest overrepresentation among the Absolute Call comparisons of all 7 groups indicating that either cell populations which are not present in the unaffected tissue invade the invasion front or otherwise silent genes are expressed.

A fairly large fourth group is formed by cytoskeletal molecules stemming from the microfilamental (actin) as well as the microtubular network.

The fifth group consists of “cell proliferation” and “cell growth” including several sub nodes.

The sixth group is headed by the main biological process “development” and consists of the sub node “cell differentiation” as well as “morphogenesis” with its related sub node “regulation of angiogenesis”.

The seventh group consists of molecules with “enzyme regulator activity” including the molecular function “endopetidase inhibitor activity”.

Only two terms, namely “cytolysis” and “receptor activity” could not clearly be assigned to one of the seven major groups by biological reasoning.

To further rule out any major bias, which might have been introduced into the data set by excluding cross reactive genes from the analysis, Change Call comparisons were performed for experiment 1 with and without elimination of cross reactive genes. All GO terms, which had been significantly over represented in the invasion front in the cross reactive-negative data set, were confirmed in the cross positive-positive data set (data not shown). These results indicate that cross-reactive genes do not participate in differential gene regulation to an extent which would severely disturb the results of statistical analysis.

4.2.2 Gene expression profiles of host tissue in response to tumor invasion: Under-represented GO terms at the invasive front

In a similar fashion as described above for up-regulated genes, Change call and Absolute call comparisons were performed for down-regulated genes. A huge number of GO terms were found by this type of analysis, namely 23 for “cellular component”, 86 for “molecular function” and 85 for “biological process”. Among these terms the most reliably down-regulated terms were selected by including only those terms which are significantly down-regulated in at least three out of the eight analyses (Change call comparison and Absolute Call comparison) and which in addition display at least 5 asterisks in sum) as indicators of significance (Table 6).

Among the significant GO terms as depicted in Table 6 , “mitochondrion” (cellular component, Table 6), “oxidoreductase activity” (molecular function, Table 6), and “electron transport” (biological process) are highly significantly down-regulated and in their combination clearly indicate a severely impaired respiratory chain in the cells of the invasion front. These terms are underscored by the significantly down-regulated terms “energy pathways” and “carrier activity” (Table 6, molecular function, Table 6, biological process).

Nearly all areas of metabolism seem to be severely reduced in the invasion front like “lipid metabolism” (Table 6 c, biological process), “amino acid metabolism”, “aromatic compound metabolism”, “organic acid metabolism”, “amine metabolism”, “alcohol metabolism” and “monosaccharide metabolism” (Table 6c, biological process). Accordingly, several types of “catalytic activity” (Table 6b, molecular function) were significantly down regulated in several of the experiments although they did not reach the set threshold (except “lyase activity”). These data indicate that metabolic functions (“metabolism”, Table 6 b, molecular function) and “catalytic activity” (Table 6 c, biological process) were very broadly down regulated in the invasion front.

This pattern of GO terms suggests an impairment of hepatocellular functions and/or an under-representation of hepatocytes in the invasion front. Due to their physiologic function, hepatocytes are among the metabolically most active cells in the human body, and an impairment of hepatocellular functions or just a reduced number of hepatocytes may explain the very extensive overrepresentation of genes with catalytic activity and metabolism genes including those of mitochondrial metabolism

among the down-regulated genes in the invasion front. In addition, some typical hepatocellular functions were found to be down regulated although not always above the threshold for inclusion into Table 6. Examples are “blood coagulation”, (BP)/ “blood coagulation factor activity“(MF)/”complement activity” (MF), “alcohol metabolism” (BP, Table 6)/”alcohol dehydrogenase activity” (MF), “steroid metabolism” (BP, Table 6)/”steroid biosynthesis” (BP), “gluconeogenesis” (BP), “urea cycle” (BP) and “phenylalanine metabolism” (BP, Table 6)“/phenylalanine catabolism”.

Table 6: GO terms consistently down regulated in the liver part of the invasion front

GO #	GO Term	Change Call				Absolute Call			
	Experiment	1	2	3	4	1	2	3	4
	CELLULAR COMPONENT								
5737	...cytoplasm	***			***	***	*	•	***
5739	....mitochondrion	***	**	***	***	***	**	*	***
42579	….microbody	***	***	***	*	*			•
5777	……peroxisome	***	***	***	*	*			•
5783	….endoplasmic reticulum	*	*	•	**	*	°		**
267	..cell fraction	**	***	***	*	*		*	**
5624	..membrane fraction	***	***	***	**	*	°	**	**
42598	….vesicular fraction	***	***	***	***	**	*	•	***
5792	......microsome	***	***	***	***	**	*	•	***
	BIOLOGICAL PROCESS							•	
3824	.Catalytic Activity	***	***	***	***	***	**	•	**
16491	..Oxidoreductase Activity	***	***	***	***	**	**	•	***
16705	…Oxidoreductase Activity acting on paired donors	***	***	***	**	*			•
6614	…oxidoreductase activity, acting on CH-OH group of donors	*	***	**	*				

4497	…Mono Oxygenase activity	***	***	***	***	*	•		**
16712	….oxidoreductase activity, acting on paired donors, with incorporation or reduction of molecular oxygen*	**	***	***	**				
16616	….oxidoreductase activity, acting on the CH-OH group of donors, NAD or NADP as acceptor	°	***	**	*				
16829	..Lyase Activity	*	***	**	**	*			*
5386	..Carrier Activity				**	**	*		*
	MOLECULAR FUNCTION								
8152	.metabolism	**	***	***	**	***	•	°	*
6118	..electron transport	***	***	***	***	*	*	•	***
6082	..organic acid metabolism	***	***	***	***	*	°	•	*
19752	….carboxylic acid metabolism	***	***	***	***	*	°	•	*
6629	..lipid metabolism	***	***	***	*	**	°		*
6631	….fatty acid metabolism	*	***	**	•	*			
8202	….steroid metabolism		**	**		•			**
6725	..aromatic compound metabolism	**	***	**	**	*	*		*
6519	..amino acid and derivative metabolism	***	***	***	***				*
6520	….amino acid metabolism	***	***	***	***				
9063	……amino acid catabolism	***	***	**	***				
9072	……aromatic amino acid family metabolism	**	***	**	***				
6558	……L-phenylalanine metabolism	*	**	*	*				
6570	……tyrosine metabolism	**	**	*	**				
9308	..amine metabolism	***	***	***	***				
9310	….amine catabolism	***	***	**	***				

5996	….monosaccharide metabolism		**	**	*				
19318	……hexose metabolism		**	**	*				
9058	..biosynthesis	*	•	**	**	***	°		***
8610	...lipid biosynthesis	*	**	**	°	•			*
6066	..alcohol metabolism	*	***	***	*	°	•		*
6091	..energy pathways		*	*	**				*

GO distribution of genes down regulated in the liver part of the invasion front as compared to control group (Change Call comparison, columns to the right). Distribution of genes solely present in the unaffected liver tissue as compared to the invasion front (Absolute Call comparison, columns to the right). Number of asterisks indicates level of significance of GO term overrepresentation. Levels of significance (after multiple testing correction, FDR): $^{***}p<0.0005$, $^{**}p<0.005$, $^{*}p<0.05$,
Single-test p-values were included for completeness ($^{\bullet}p< 0.02$, $^{\circ}p<0.05$), whenever the term was significant in at least one experiment after multiple testing correction. Change Call and Absolute Call comparisons were examined independently.
Different font (normal or italic) of GO numbers and term names indicate GO clusters obtained by biological reasoning.
Hierarchical levels are indicated by number of dots in front of GO terms.

4.2.3 Confirmation of stellate cell activation at the invasive front

In order to confirm the suspected activation and myoblastic transdifferentiation status of HSC in the invasion front, qPCR and immunohistochemistry was performed with several genes which have been described to participate in these processes. The commonly HSC activation marker α-SMA showed in real time PCR a 2.9 fold difference in crossing points between liver and liver part of the invasion front which corresponds to a 7.9 fold higher gene expression in the invasion front as compared to unaffected liver (Table 7). In addition, histological sections were stained against α-SMA. As shown (Figure 7a), α-*SMA* activity seems to originate mainly from cells with elongated nuclei which are directly lining the central part of the invasion front i.e. the border between tumor and liver tissue. A similar immunohistochemical pattern (Figure 7b) was found for the cytoskeletal protein transgelin which was up regulated 6.5 fold in the qPCR (Table 7A). *Procollagen type I* was up regulated 4.5 fold in the qPCR (Table 7A). The protein seems to be predominantly localized to cells with small nuclei

(Figure 7c), which probably correspond to HSC. Staining seems however to extend a little further into the liver tissue. This tendency is even stronger with cRBP-1 which is clearly not only expressed in the invasion front but also in unaffected liver (Figure 7d). In addition, besides HSC, hepatocytes seem to express cRBP-1 as well, which has been described before (Schmitt-Graff et al., 2003). According to the qPCR, *cRBP-1* is up regulated 4.9 fold.

Altogether, these data confirm the up-regulation of several HSC genes in the invasion front by two independent methods. In addition to the several other genes which are up regulated at the invasion front of liver compared to the liver were confirmed qPCR (Table 7B)

Table 7: Determination of differentially regulated gene levels in liver and liver part of the invasion front

A

Gene	Liver	Liver invasion front	ΔCrossing points	Fold change (EΔcp)
Smooth muscle α-actin				
Exp. 1	32.2	28		
Exp. 2	32.2	28		
Raw value (mean)	32.2	28	4.3	
Normalized on GapDH and efficiency corrected	31.5	28.7	2.9	7.5
Transgelin (SM 22 α				
Exp. 1	26.5	23.9		
Exp. 2	25.1	23.5		
Raw value (mean)	25.8	23.7	2.1	
Normalized on GapDH and efficiency corrected		23.1	3.3	8.6
Cellular retinol binding protein (cRBP-1)				
Exp. 1	28	26.1		
Exp. 2	24.8	24.2		
Raw value (mean)	26.4	25.1	1.3	
Normalized on GapDH and efficiency corrected	27	14.5	2.5	5.7

B

Gene Name	Gene Symbol	Upregulation (Fold Change)
Cathepsin C	Ctsc	5.3
Cathepsin S	Ctss	5.8
Cystatin B	Cstb	8.5
Endoglin	Eng	1.6
Tyrosine kinase receptor 1	Tie1	2.9
FMS-like tyrosine kinase 1	Flt1	3
Guanylate nucleotide binding protein 1	Gbp1	22.3
Guanylate nucleotide binding protein 2	Gbp2	6.4
Guanylate nucleotide binding protein 3	Gbp3	2.5
Endothelial-specific receptor tyrosine kinase	Tek	3
Eph receptor B4	Ephb4	1.95
Ephrin B2	Efnb2	2.9
Chemokine (C-X-C motif) receptor 2	CXCR2	1.4

Total RNA of microdissected liver and liver part of the invasion front were isolated as described for hybridization experiments. 1.5 ng of total RNA were used for quantification. Obtained raw values of crossing points were normalized by GapDH values to correct for RNA quality. In addition, differences in PCR amplification efficiencies of GapDH and candidate genes were accounted for by calculation of the respective efficiencies in serial two-fold dilutions of non-microdissected tissue-RNA and normalization to the obtained ratio. The observed differences in crossing points were transcribed into fold changes according to efficiency values.

In order to examine whether activation of HSC is accompanied by increased relative number of HSC in particular in relation to hepatocytes, HSC were stained against desmin, which has been reported to stain quiescent as well as activated HSC. Hepatocytes were stained with the antibody Hep-Par-1. Immunostaining revealed gradual differences in cellular distribution in the invasion front, the two extremes of which are displayed in the two upper panels of Figure 8. Staining against hepatocytes reveals areas of direct contact between hepatocytes and tumor cells as well as regions where these two groups of cells seem to be separated by a narrow and cell poor strip containing cells of different morphology (Figure 8, B, E). These patterns were hardly distinguishable by ordinary HE staining (Figure 8, A, D).

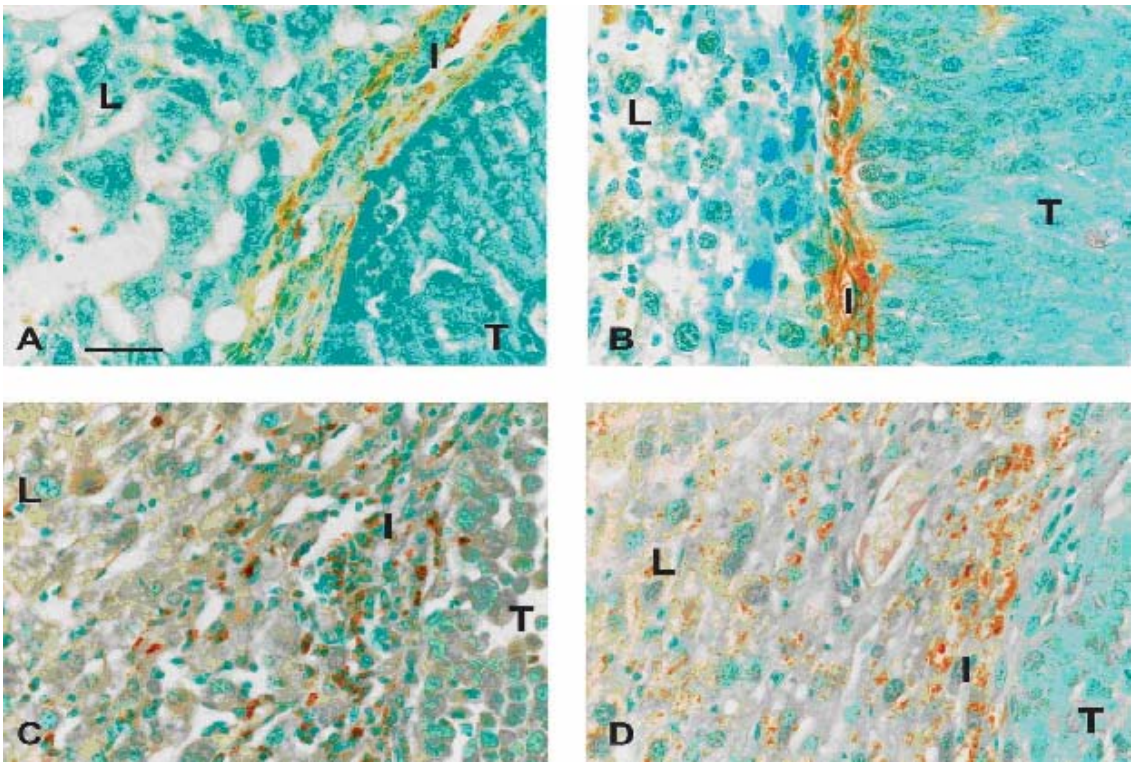

Figure 7: Immunohistochemistry for detection of activated HSC

Slides were stained against α-SMA (A), transgelin (B), procollagen type I (C) and cRBP-1 (D) and counterstained with methyl green.
T= tumor, L=liver, I= invasion front, V=blood vessel. Bar=50 µm

Staining against desmin shows that the areas of close contact of hepatocytes and tumor cells do not show any net increase of HSC in the invasion front as compared to unaffected liver. Here, HSC seem to cover a significant but minor portion in the invasion front and liver and even seem to populate the tumor. In contrast, HSC seem to be the main population in the area where tumor cells and hepatocytes are separated by a cell poor strip. These results underscore the crucial role of HSC for the deposition of ECM as indicated by our gene expression analysis.

In addition, the lower panel of figure 8 shows that HSC apparently take part in structuring the tumor tissue as they are lining intratumoral septi.

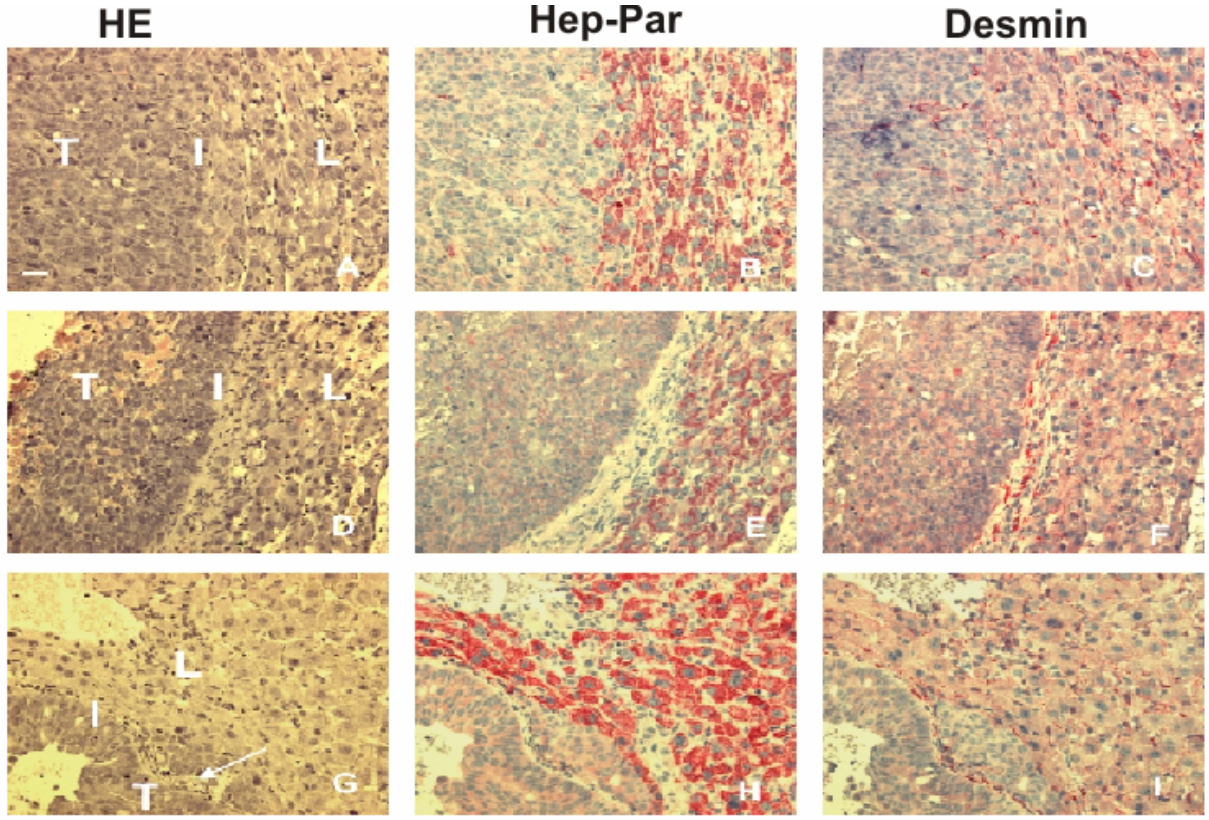

Figure 8: Immunohistochemistry for detection of hepatocytes and HSC

Representative sections were stained with HE routine stain or alternatively immunostained against a mitochondrial hepatocyte marker or against the HSC marker desmin and counterstained with hemalaun.
Upper panel (A-C): area of close contact of hepatocytes and tumor cells
Middle panel (D-F): area of separation of hepatocytes and tumor cells by a cell poor strip
Lower panel (G-I): area which includes an intratumoral fibrous septum
T= tumor, L=liver, I= invasion front. Bar=50 µm

4.3 Gene expression profiles of tumor cells in vitro, in vivo and at the invasion front of colorectal liver metastasis

Metastatic tumor epithelia encounter specific host reactions during metastatic invasion into host tissue. This study was focused to examine how gene expression changes if cells from cell culture are grown *in vivo* in the inner parts of a tumor and in the invasive margin

The transcriptional changes in human LS174T colon adenocarcinoma cells grown orthotopically in the livers of nude mice were investigated to better mimic the environment of human liver metastasis. To gain further insight into the contributions of various factors in the microenvironment of liver metastasis, gene expression

profiles of cells grown *in vitro* were compared with profiles of orthotopically implanted tumors and with profiles at the invasion front of tumor. Use of xenograft mouse model helped to distinguish between host and tumor part of the invasion front by deleting cross reactive genes.

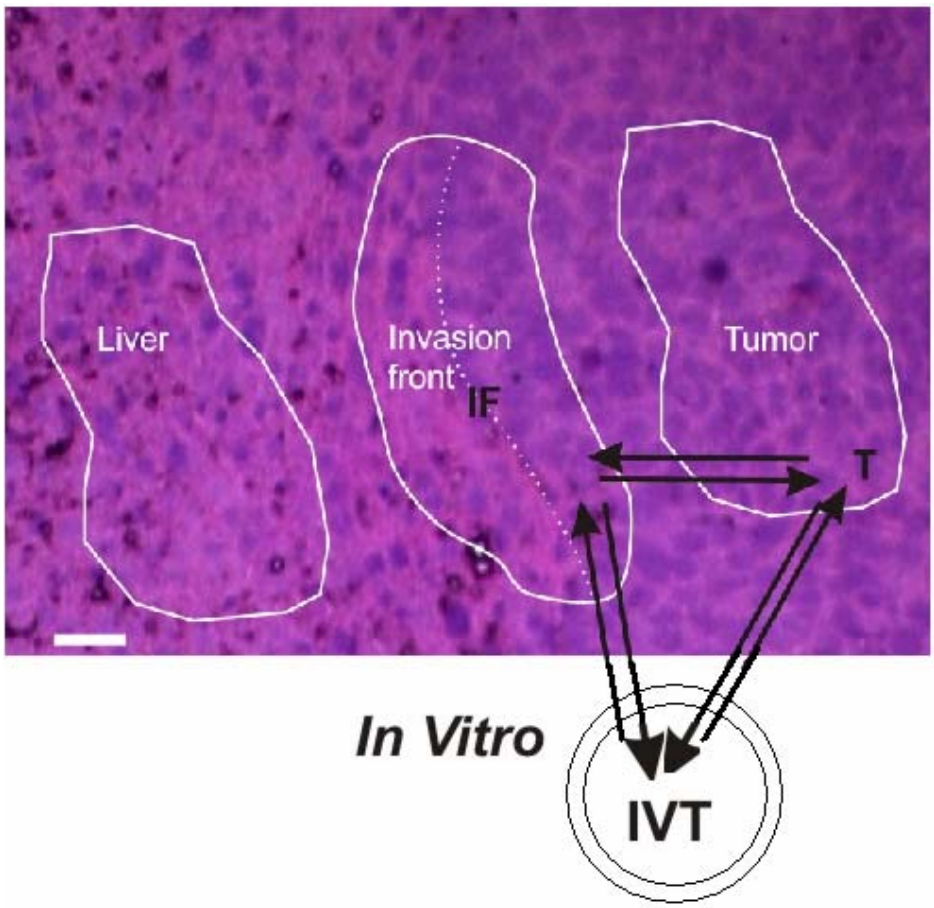

Figure 9: Areas subjected to microdissection

Dotted line indicates demarcation for tumor part of invasion front which was used for qPCR. Bar=50 µm

4.3.1 Elimination of cross reacting genes leads to a tolerable loss of genes

By applying a human tumor cell line growing in murine liver, species differences of gene sequence for discrimination of differential gene expression of host (murine) and tumor (human) genes was used. A critical determinant for the usefulness of the xenograft model was the level of cross reactivity of the murine tissue on the human chips which should be as low as possible. Invasion liver tissue was not used for determination of cross reactivity of murine samples on human chips because the

invasion liver tissue although predominantly consisting of liver cells consists in part of tumor epithelia of human origin which would obscure real cross reactivity if hybridized on human chips. Therefore RNA from liver cells was used as the representative samples for examination of cross hybridization of mouse liver tissue on human chips. The percentage of cross-reactive Affymetrix-IDs was 7% (Table 8).

Table 8: Murine tissue (Liver) cross reacting with human chips

Call	Present	Marginal	Present + Marginal	Absent	Total
Number of IDs	2679	498	3177	41643	44820
Percentage (of total IDs on chip)	6%	1%	7%	93%	100%

Number and percentage of present calls resulting from hybridisation of RNA from nude mouse liver tissue on U 133A and B human genome chips. Quality of cross reacting sample was examined on test chips.

Because of this level of cross hybridization, we next evaluated to which extent the elimination of cross reactive genes would reduce the gene pool still available for further analysis of differential gene expression. Before deletion of cross reactive IDs, the first criteria that IDs have to be present at least in *in vitro*,Tumor or invasion front was applied (Table 9, upper and upper line). Then, cross reactive genes (transcripts from liver cells hybridising on human chips) were subtracted from the resulting pool of IDs (Table 9, upper and middle line). As expected from the small fraction of cross reactive genes, only 14.6% (on average) of murine genes hybridizing on human chips had to be deleted due to cross hybridization of their human counterparts (Table 9, lower line). This analysis indicates that deletion of cross hybridizing genes leads to a tolerable loss of IDs for further analysis.

Table 9: Elimination of cross reactive gene (presernt or marginal in liver)

Criteria Compartment	Invasion front	Tumor	*In vitro*
Cross reactive genes included	12991	15607	12361
Cross reactive genes excluded	10858	13461	10066
Percent reduction	16%	14%	14%

Elimination of cross reactive genes leads to an only moderate reduction of the gene pool for further analysis

4.3.2 Degree of tumor cell Specialization increases with increased contact to host cells

First goal for the global analysis of gene expression was to examine gene expression changes when cells from cell culture are grown *in vivo* and in the invasive margin.

To this extent, minimal number of consistent gene expression patterns were defined by grouping all those genes that are up- or down-regulated between the compartments (*in vitro* to *in vivo* to invasion front and vice versa).

The distribution of genes which were found to be at least 2 fold up-regulated in the specific compartment (test group) was compared to the distribution of a reference group which contained the whole group of all genes which were present in at least one of the tissues under examination (Bandapalli et al., 2006).

Comparison of global gene expression profiles using gene ontology terms and GOSSIP software revealed an overall increase of cellular specialization from the *in vitro* to the *in vivo* situation and a further increase of specialization from tumor to invasion front. The analysis resulted in overrepresentation of 28 GO terms in *in vivo* and 41 in the Invasion front compared to *in vitro* The number of GO terms overrepresented between *in vivo* to the invasion front were 18. There was no under representation of GO terms from the invasion front to the tumor where as 4 GO terms were found to be under represented from invasion front and tumor respectively to *in vivo* (Figure 10).

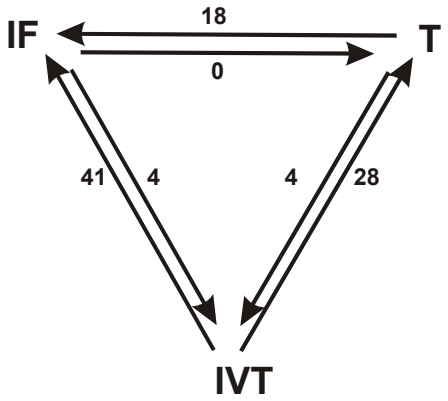

Figure 10: Number of GO-terms over represented in pair wise comparisons

Genes which were at least two fold up-regulated between the respective pair wise compartmental comparisons were subjected to pattern analysis with Gossip software (Microdiscovery GmbH, Berlin). The direction of the arrow indicates the compartment with the up-regulated genes.
IF= invasion front, T=tumor, IVT= cells in vitro

These GO terms were then manually clustered by biological reasoning. Among the patterns specific for the *in vivo* situation are “cell adhesion” and “actin cytoskeleton organisation (Figure 11A). An invasion specific and *in vivo* specific pattern is “signal tranducer activity” (Figure 11C).

Further examination of the GO terms revealed *in vitro* specificity of “ribosome” and “protein biosynthesis” (Figure 11B) patterns. Invasion specificity of “signal transducer activity” is due to G-Protein coupled receptors (GPCR) but not tyrosine kinase receptors as they are *in vivo* specific (Figure 11C lower panel). A purely invasion specific pattern is “cell communication” (Figure 11D). The group of terms with the overall highest level of significance is best represented in *in vivo* pattern (cell adhesion) followed by *in vivo* and invasion pattern (cell communication).

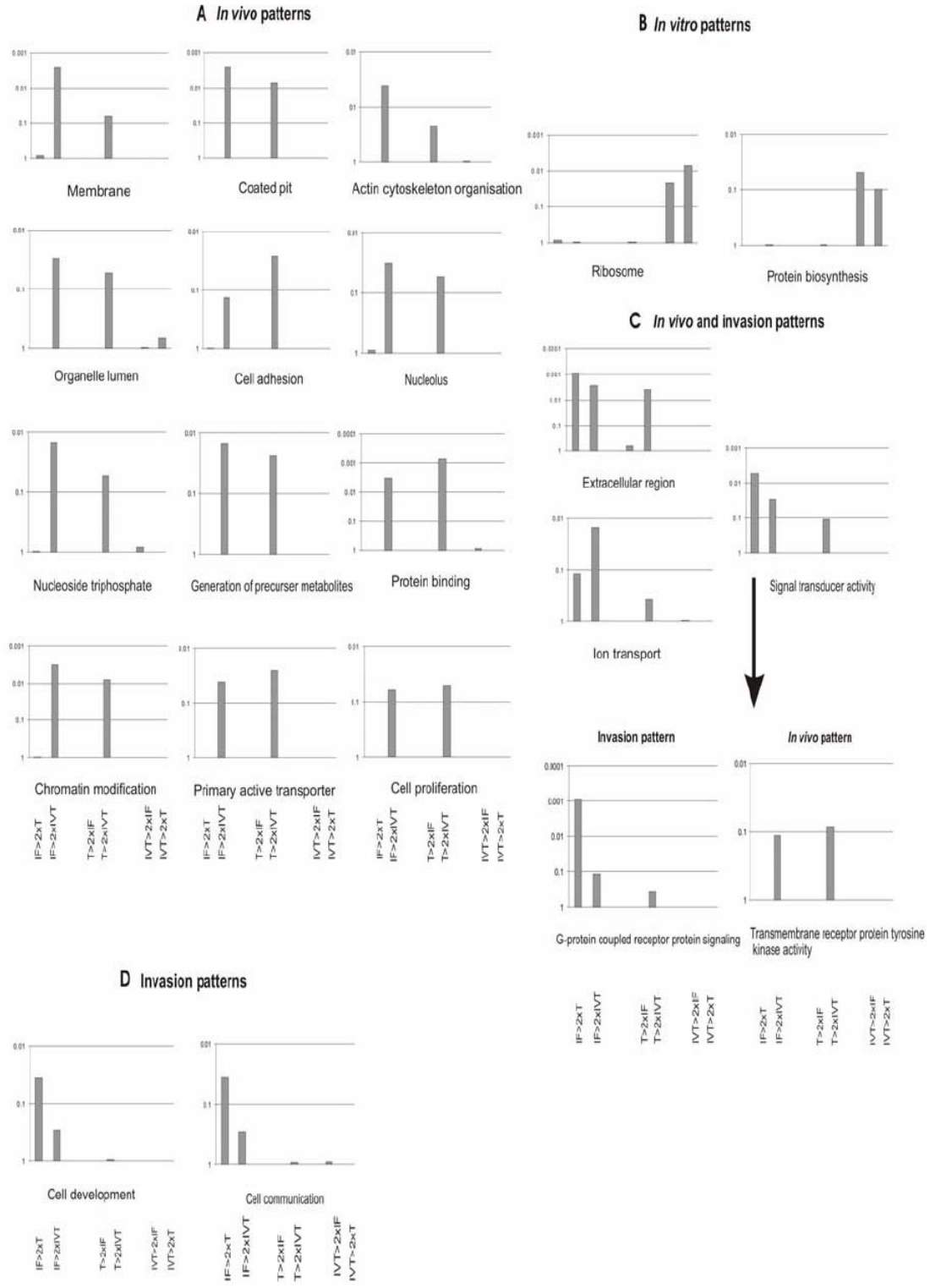

Figure 11: Levels of significance (p-values) of GO-terms over represented in pair wise comparisons.

A: in vivo pattern, B: In vitro pattern, C: in vivo and invasion pattern and D: Invasion patterns Genes which were at least two fold up-regulated between the respective pair wise compartmental comparisons were subjected to pattern analysis with Gossip software (Microdiscovery GmbH, Berlin).

4.3.3 Regulation of Pro-angiogeneic CXC chemokines

A particularly important question from a basic scientific and particularly from a (gene) therapeutic point of view is the cellular origin of differentially expressed genes. Using GO-based GOSSIP software all secreted genes were determined in the epithelium of the tumor part of the invasion front and the epithelium of the inner parts of the tumor which have been reported to be associated with vasculature development. All growth factor-like genes were examined for differential gene expression**.** Most of the well known classical pro-angiogenic molecules were present in invasion front and tumor core but were not differentially regulated (Table 10).

Table 10: Presence of angiogenic growth factors in tumor cells and their respective receptors in host cells

Angiogeneic growth factor (tumor cells)	**Change call**	**Receptor (host)**	**Change call**
VEGF	NC	FLT1,KDR	NC/NC
P(L)GF	NC	FLT1,KDR	NC/NC
Angiopoietin-1	NC	TIE-2	NC
PD-ECGF-1	NC		
Angiogenin	NC		

Examination of gene expression between tumor cells of the invasion front and those from the inner parts of the tumor or between host cells of the invasion front and those of the liver further away from the invasion front reveals the lack of differential gene expression (no change, NC). The lack of differential gene expression of VEGF has been confirmed by qPCR (not shown).

In contrast, one class of pro-angiogenic molecules, the ELR+CXC chemokines was differentially regulated. All pro-angiogenic members of that family including potent pro-angiogenic CXCL8 (IL-8) were up regulated in the tumor cells of the invasion front as compared to the tumor core (Table 11). Moreover, angiostatic CXC chemokines like CXCL9, 10, 11 do not seem to be expressed by the tumor cells or at least not at a higher level in the invasion front (data not shown).

Table 11: Pro-angiogenic CXC chemokines in tumor cells

CXC chemokine (tumor cells)	Change call	Fold change
CXCL1	Increase	19.6
CXCL2	Increase	2.8
CXCL3	Increase	1.7
CXCL5	Increase	6.8
CXCL8	Increase	2.7

All five chemokines have been found to be up-regulated in the tumor cells of the invasion front as compared to the tumor cells of the inner part of the tumor.

These results may indicate that, ELR+CXC chemokines as compared to other pro-angiogenic molecules may have a more specific role during the early steps of angiogenesis e.g. for the recruitment of endothelial cells into the tumor stroma.

4.3.4 Targeted down-regulation of CXCL1 and CXCL8 expression using shRNA

As ELR+CXC chemokine expression was elevated at the invasion front as compared to the inner parts of the tumor in the xenograft model, a shRNA–based approach to down-regulate CXC Chemokine expression in LS174 cells was used to determine if this played a contributory role in determining their invasive phenotype and angiogenesis. Appropriate shRNA and nontargeting control plasmids were constructed and transfected into LS174T cells, and puromycin-resistant colonies were expanded and tested for CXC chemokine expression. shRNA transfected clones (shCXCL1&ShCXCL8) showed inhibition of CXCL1 & CXCL8 expression as judged by quantitative real-time PCR using gene specific primers, whereas clones transfected with a non-targeting control vector (NTC) showed similar levels of CXCL1 and CXCL8 expression as the parental LS174T cells. These data were further confirmed by Western blotting (Figure 12). Thus, stable targeted down regulation of

CXCL1 and CXCL8 expression using shRNA plasmids can be achieved with a high degree of inhibition.

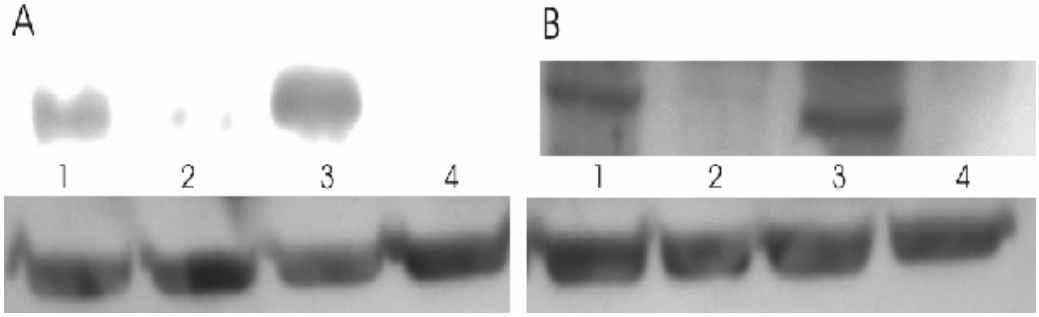

Figure 12: Inhibition of CXCL1 and CXL8 expression in LS174T cells.

Upper Panel:
A. CXCL1: 1) shNTC; 2) shCXCL1#1; 3) LS174T cells; 4) shCXCL1#2 B.
CXCL8 (IL-8): 1) shCXCL8#1, 2) shNTC; 3) Ls174 T cells; 4) shCXCL8#2
Lower panel:
ß- actin of the respective samples

Confirmation of up regulated genes in the invasion front of tumor compared to the inner parts of tumor by qPCR

Table 12: Conformation of differentially regulated gene levels in tumor and tumor part of the invasion front

Gene Name	Gene Symbol	Upregulation (Fold Change)
Apoptosis Protease activating Factor	APAF	2.7
E-Cadherin	CHD1	4
Myristoylated Alanine-Rich protein Kinase C Substrate	MARCKS	15.9
MAP/microtubule affinity-regulating kinase 3	MARCK3	6.9
Myelin protein zero-like 1	MPZL1	2.8
Ephrin receptor 2	EpBH2	7.5
Epiregulin	EREG	2.5
Beta Catenin	CTNNB1	3.4
Lectin, Galactoside-binding, Soluble, 1	LGALS	2.9
Ras Homolog gene family, member B	RHOB	4.3

Total RNA of microdissected liver and liver part of the invasion front were isolated as described for hybridization experiments. 1.5 ng of total RNA were used for quantification. Obtained raw values of crossing points were normalized by GapDH values to correct for RNA quality. In addition, differences in PCR amplification efficiencies of 18sRNA and candidate genes were accounted for by calculation of the respective efficiencies in serial two-fold dilutions of non-microdissected tissue-RNA and normalization to the obtained ratio. The observed differences in crossing points were transcribed into fold changes according to efficiency values.

Normalization of qPCR

To normalize qPCRs, standard curves for □-catenin (Gene of interest) and 18s RNA (reference) were established. For this purpose, serial dilutions of mRNA were prepared. Serial dilutions of gene of interest and reference gene were amplified on the LightCycler (Figure 13). Standard curve slopes were –3.980 for 18s RNA and

–3.535 for ß-catenin resulting in PCR efficiencies (E) of 1.78 and 1.92, respectively (Figure 13A).

Melting curve analysis confirmed specificity of PCR reactions. Melting of 18sRNA and ß -catenin PCR products resulted in single melting-peaks for 18sRNA and ß -Catenin (Figure 13B).

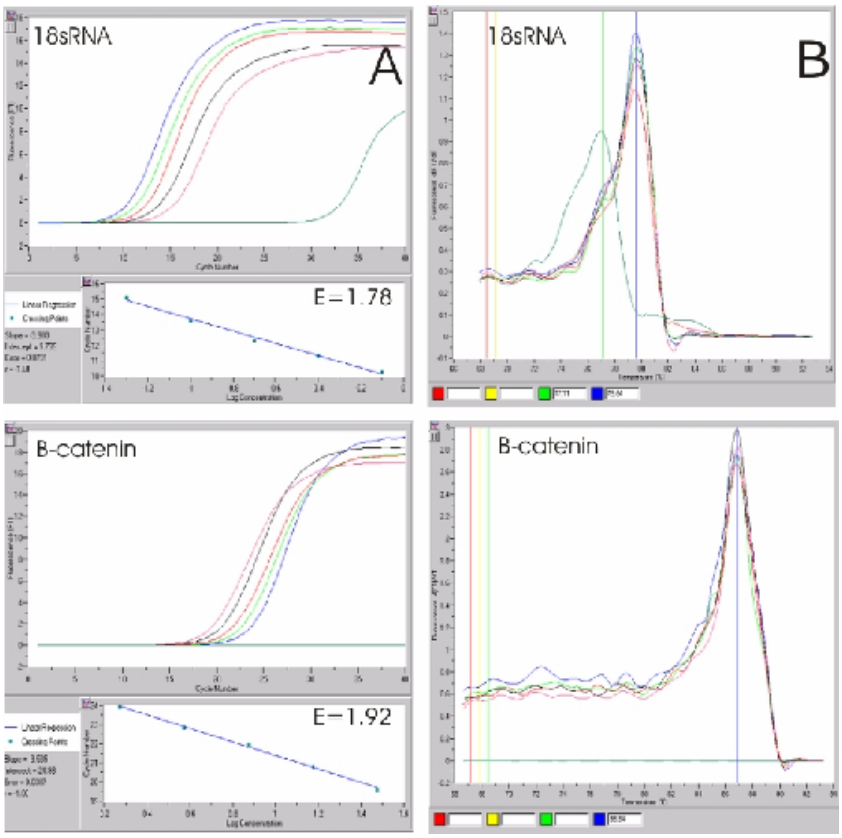

Figure 13: Calibration of quantitative RT-PCR.

Standard curves for 18sRNA and β -catenin; (B) Melting curve analysis of 18sRNA and ß -catenin indicating the specificity of both PCR reactions. Unspecific primer-dimers occurred in no template control of 18sRNA.

4.3.5 Activation of the β-catenin promoter in the invasion front of colorectal liver metastases

All adhesion related genes were examined for differential gene expression**.** Well known classical pro-oncogenic molecule □-catenin was found to be up regulated in the invasion front compared to the inner parts of the tumor. To address transcriptional regulation of β-catenin the established *in vivo* model of colorectal liver metastases from human LS174T colon carcinoma cells growing in the nude mouse was used which allowed to evaluate micro environmental influences on tumor development (Bandapalli et al., 2006). Influence of a complex environment on β-catenin expression was studied by comparison of β-catenin expression in tumor cells *in vitro*, in the interior of the tumor and at the invasion front. The dual species nature of the model allowed to monitor gene expression in tumor cells irrespective of contaminating stromal cells (Bandapalli et al., 2006). The LS174T colorectal

carcinoma cell line that was used in this animal model harbours a stabilizing β-catenin mutation at codon 45 (Rowan et al., 2000). Accordingly, β-catenin protein was readily detected by Western blotting in LS174T cell lysates (Figure 14a, left band) and by immunohistochemistry *in vitro* (Figure 14b). A marked increase of the β-catenin level was detected once the tumor cells grew *in vivo* (Figure 14a, right band). A further increase was seen in tumor cells growing at the invasion front (Figure 14 c, d). This is the first report of increased β-catenin levels *in vivo* in comparison to cell culture. According to yet unpublished data (manuscript in preparation) on global gene expression of tumor cells in the animal model, a distinct *in vivo* pattern of genes, to which β-catenin apparently belongs to, exists at the tumor invasion front. In addition to the increased □-catenin mRNA level redistribution of β-catenin to the nucleus at the invasion front was observed however, not at a comparable degree as described before (Brabletz et al., 2001).

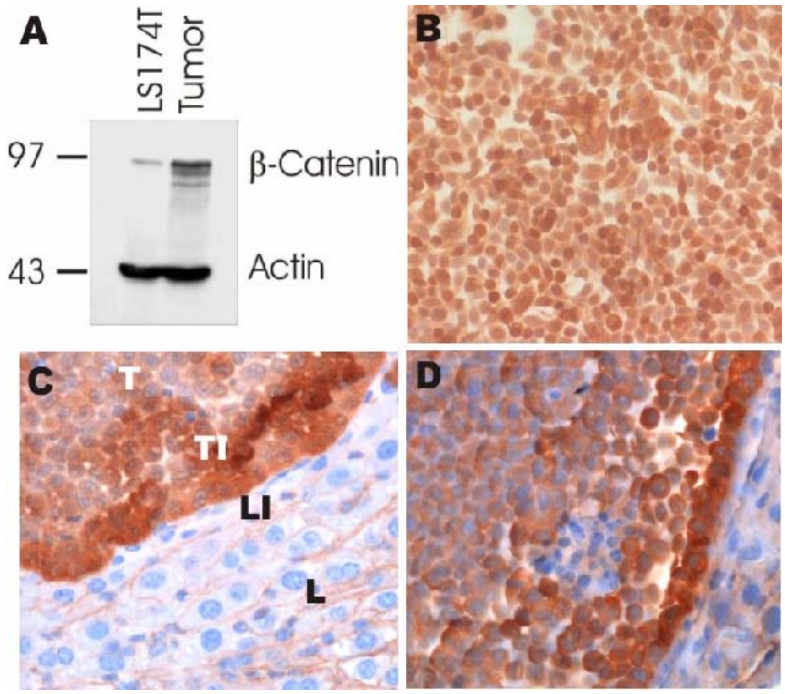

Figure 14: Elevated levels of β-catenin in vivo.

A. Elevated levels of β-catenin in vivo
A. Western blotting: Increased levels of β-catenin in the interior of the tumor in vivo (right band) compared to cells grown in cell culture (left band).
B, C, D. Immunohistochemistry: LS174 cells cultured in vitro (B) and in vivo (C,D). Increased ß -catenin staining occurs at the invasion front of the tumor (IT).

To examine whether mRNA levels paralleled protein, qPCR was performed from microdissected samples. As shown in Figure 15 a, β-catenin mRNA was elevated 2.7-fold in tumor cells grown *in vivo* versus cells grown *in vitro* and another 3.4-fold at the invasion front compared to the interior of the tumor. In total, ß-catenin mRNA levels were increased 9.6 fold at the invasion front versus those *in vitro*. Our data indicate that ß-catenin is up regulated on the transcriptional level in response to changes in the tumor microenvironment. Increased mRNA levels of β-catenin have been reported to occur in a number of human cancers as compared to the respective normal tissue of origin (El-Bahrawy et al., 2001& Mann et al., 1999, Ebert et al., 2002, Cui et al., 2001 & Saito et al., 2002) However, this is the first report demonstrating a response of cancer cells to the *in vivo* situation or the situation of being confronted with host tissue of the invasion front.

To examine whether increased mRNA levels were indeed due to transcriptional up-regulation, LS174 T cells were stably transfected with the human alkaline phosphatase reporter gene under the control of two different β-catenin promoter fragments which have been described before (Nollet et al., 1996). Activity of the two promoter fragments was evaluated by determination of both, reporter protein by luminescent activity and reporter gene mRNA levels by qPCR. As assessed by SEAP-mediated luminescence, the two fragments displayed a β-catenin promoter activity of 147 fold (fragment 1, position -298 to +139) and 190 fold (fragment 2, position -4700 to +1300) above background in LS174T cells *in vitro* (Figure 15 b). Because SEAP protein activity cannot be measured in microdissected samples from *in vivo* experiments, the suitability of qPCR for assessment of promoter activity was examined. As shown in Figure 15 c, SEAP mRNA levels were 831 fold (fragment 1) and 1448 fold (fragment 2), respectively above background. These data indicate that levels of reporter protein (Figure 15 b) were paralleled by levels of mRNA as assessed by qPCR specific for SEAP mRNA (Figure 15 c). Using either method, fragment 2 was shown to be more active than fragment 1 and the ratio of fragment 2 to fragment 1 regarding the fold changes above background is 1.3 for protein and 1.7 for mRNA respectively indicating comparability of the methods. Our data are in good agreement with the initial report by Nollet et al. (Nollet et al., 1996) who had used a murine epithelial cell line (NMe), although in LS174T cells the difference on the protein level was not as prominent which may be ascribed to species differences. In addition, according to our results, promoter activity is apparently better reflected on

the mRNA level (higher values) than on the protein level, which might reflect posttranslational modifications of the protein.

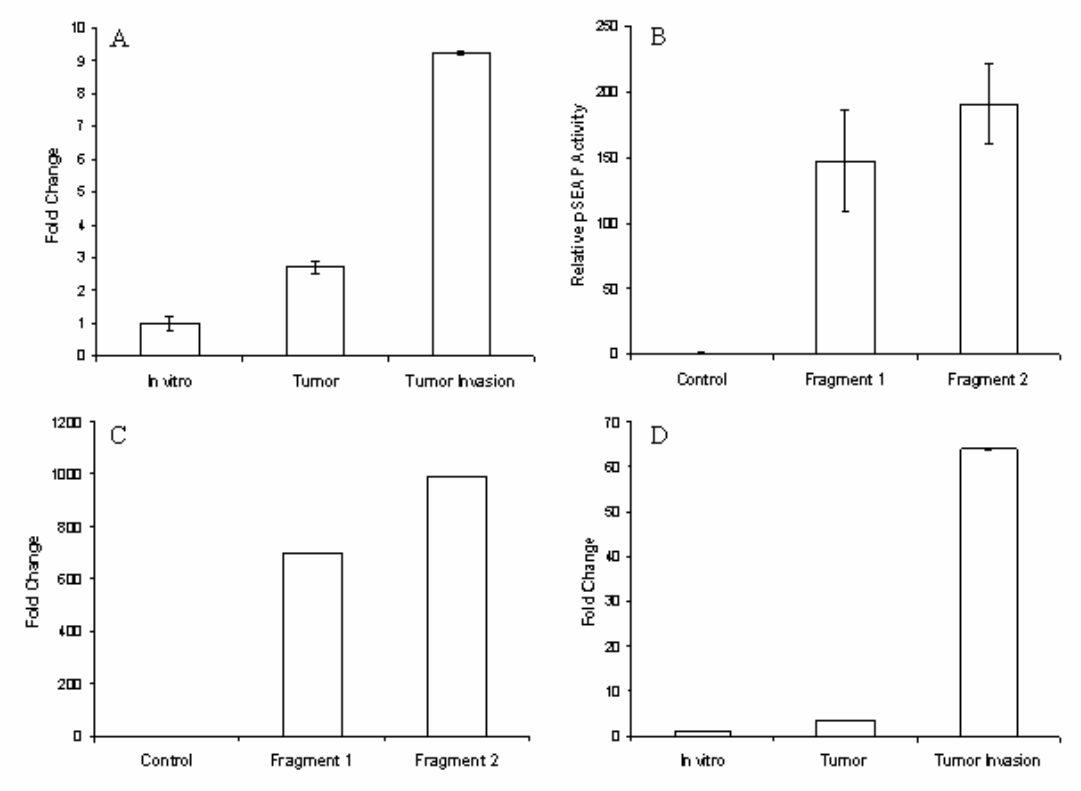

Figure 15: β-catenin promoter activity in vitro and in vivo.

A: Levels of β-catenin mRNA in LS 174 T tumor cells in vitro, in the interior of the tumor and in the invasion front.

B, C: β-catenin promoter activity in vitro

D: Activity of the β-catenin promoter in LS 174 T tumor cells in vitro, in the interior of the tumor and in the invasion front.

To examine promoter activity *in vivo*, liver metastases were induced with genetically modified cells (one cell clone harbouring fragment 2) and control cells as described above. To determine promoter activity, tumor invasion front and tumor compartments were microdissected as described above. Quantification of promoter activity was performed with qPCR specific for human alkaline phosphatase mRNA. As shown in Figure 15 d, SEAP reporter gene mRNA was elevated 3.5-fold in cells grown in the tumor versus *in vitro* growth and another 18.4 -fold in cells grown at the invasion front compared to cells in the interior of the tumor. In total, this reflects a 64 -fold activation of the □-catenin promoter in cells grown at the invasion front versus those *in vitro*. In principle, reporter gene mRNA levels (Figure 15 d) parallel β-catenin mRNA levels (Figure 15a) and protein levels (Figure 14), indicating that activation of the β-catenin promoter is responsible for increased mRNA and protein levels, at least in part.

However, the dramatic promoter activation at the invasion front does not seem to be entirely reflected by β-catenin RNA and protein levels indicating some posttranscriptional and/or posttranslational modifications.

5 Discussion

5.1 Interspecies comparison of gene and gene expression profiles in a mouse model of colorectal liver metastasis and in clinical specimens

Murine models represent a necessary tool in cancer research. However, there is always an uncertainty about the extent to which findings in the animal can be related to the human situation. In this study global, gene expression profiling in addition to standard histopathologic examination was used in judging the suitability of a murine model of colorectal liver metastases for the detection of invasion front target genes. The central observation was a decrease in overlap from the level of pattern families through single gene ontology patterns to the single gene level. Although the central processes are fairly similar between the species, the percentage of overlapping potential target genes in interspecies syn-compartmental comparisons was at maximum 8.2% of the up-regulated genes among respective invasion front compartments in our system. In other words, there is only a limited chance that invasion relevant genes that are detected in clinical samples will display a similar regulation in exactly the same compartment in a standard animal model of tumor cell injection. If, conversely, a target gene validation project starts with the animal model, one cannot necessarily expect that target genes arising from the murine invasion front are really relevant for exactly the same clinical situation. The number of overlapping genes can be significantly increased if those invasion relevant genes are included which show cross-compartmental overlap or are even up-regulated in liver compartments. In addition, relaxation of inclusion criteria leads to an increase of potential target genes. However, both modifications of the initial targeting strategy decrease specificity of the approach.

Histopathology, pattern analysis and single-gene analysis in our system turned out to be complementary methods to achieve some understanding of differences and similarities between the clinical and the animal model situation.

5.1.1 Inherent species differences

Differences of liver tissue compartments far from the invasion front may represent the degree of dissimilarity between the species of only marginally affected organs. Data indicate that the biology of human livers as compared to the livers of Balb/C mice is not exactly the same as only 16.7% up-regulated genes were found to be

overlapping. It is likely that these inherent dissimilarities of the host tissue will have a severe impact on the mechanisms in the invasion front.

Although this present approach is to our knowledge the first whole genome interspecies approach for invasion, several other interspecies comparisons on a more or less genome- wide scale have been performed. It is however difficult to compare data due to differences in methods and models. Sometimes, an encouraging similarity between the species is reported such as in a microarray meta-analysis of the complex biological phenotype of aging. Here, the authors identified an expression signature common to the aging transcriptomes of mouse, man and rat at least within some organs (Wennmalm et al., 2005). A nice correlation of gene expression data from a rat liver cancer model with clinical cytogenetic abberration profiles resulted in the identification of several pathways involved in human liver cancer (Fang et al., 2005) In contrast, even on the level of one single-cell type *in vitro*, marked interspecies differences have been observed in a massive parallel signature-sequencing approach, which identified only a small (core) set of conserved genes between human and murine embryonic stem cells (Wei et al., 2005). These data indicate that, depending on the biological context; the animal model can be closer or more deviant from the clinical situation. Obviously, the type of analysis determines the degree of interspecies overlap as well. The number of potential target genes in the invasion front compartments could easily increase to 50% and more (Table 2, lowest panel) if human up-regulated genes only had to be present (but not necessarily up regulated in the respective murine compartments). It is, however, unlikely that such target genes would indeed represent the targeted biological pathway in the animal model.

5.1.2 Tumor model

Only 1.6% of exclusively up-regulated genes were overlapping among the tumor compartments, which obviously has a severe impact on the mechanisms in the invasion front. No overlapping GO-terms between the tumor compartments were detected. The murine tumor displayed more features of uniqueness than its human counterpart (51 vs. 11 GO terms, data not shown). Most of these terms were associated with primary metabolism. In contrast to secondary metabolism, which produces and breaks down compounds that are essential for the whole organism, primary metabolism contains all pathways necessary to keep the cell alive. While the

liver is known to be the classical site of secondary metabolism (see above), it is more difficult to explain why only the murine tumor compartment displays such a huge number of primary metabolism terms. Primary metabolism is also defined as normal anabolic and catabolic processes that result in assimilation, respiration, transport, and differentiation and which directly function in the processes of growth and development. A closer look at the sub-terms reveals that several belong to protein biosynthesis so that it can be predicted that the tumor compartment in the murine model is mainly occupied with maintaining its primary functions represented e.g. protein biosynthesis. Histologically, both examined cancer types were adenocarcinomas of colorectal origin. However, the murine tumor is a lowly differentiated to undifferentiated carcinoma whereas the human specimens manifest moderate to low differentiation. These histological differences may partly explain low overlap of tumor compartments.

5.1.3 Misleading histology

Another reason for limited single-gene overlaps in the invasion front compartments may be due to the fact that mechanisms involved in invasion do not appear to respect boundaries as estimated by standard histopathologic observation; the most striking observation was the relatively high degree of overlap between human liver invasion and murine tumor invasion which was 6.25% (versus 2.8% with murine liver invasion) on the single-gene level and 16.5% (vs. 0% for murine liver invasion) on the pattern level. Despite different tissue of origin, typical invasion front patterns such as “cell adhesion”, “extracellular matrix”, “organ development” and “antigen presentation” were present in human liver invasion and murine tumor invasion, which indicate that these compartments may be functionally similar. In addition, liver compartments displayed strong immune response patterns that may be a part of a host counterattack against the invading tumor. Liver immune response consisted mainly of innate immune response whereas invasion-related immune response was characterized by acquired immune response.

From these data one can conclude that when mining for invasion target genes, one should consider the invasion front as a whole and even take tissue further away from the invasion front like the liver compartments into consideration.

5.1.4 Functional redundancy

A fourth reason for the limited overlap of target genes is the redundancy of gene regulation within biological processes. Neoplastic processes that are targeted by drugs include proliferation, apoptosis, invasion and several more. These processes are on the descriptive level of pattern families or patterns. Many animal models for target gene determination or validation are chosen according to whether they exhibit these pattern-like functions. As data shows, the degree of similarity on the pattern family level between clinical samples and the animal model can be fairly high, but it decreases dramatically with an increase of specificity of the underlying processes (single GO- terms) down to that low degree of overlap on the single-gene level. The liver compartments, for example, displayed a high degree of similarity on the level of patterns families as the “secondary metabolism” family was composed of 15 core GO-terms which are over-represented in both species and only 8 species-specific core GO-terms (Figure 5, columns 1 and 2). In contrast, on the level of single GO terms including those with less than 10 genes (those which are usually closer to the small branches of the GO tree) the overlap was only 28%. Finally, overlap on the single-gene level (all genes) was only 16.7%, which corresponds to the degree of overlap of the genes underlying overlapping GO-terms (17.8 % for the “lipid metabolism” term (Table 3)). In other words, although the liver compartments of both species apparently carry out typical liver functions related to secondary metabolism and even sub-terms like “lipid metabolism” are significantly over-represented in the liver of both species, only a minor portion of the actual underlying genes are identical. Due to reasons described above the situation is even more complicated for invasion front and tumor compartments. That ultimately means that targeted biological processes are by nature represented by a variety of perhaps similar, perhaps alternative or even redundant genes.

The problem of functional redundancy can probably be circumvented if the animal model is chosen *a priori* to have the same molecular defect as the human counterpart tumor. A recent publication argues in favor of this approach. A good correlation of gene expression profiles for a mouse model of KRAS2-induced lung cancer and KRAS2-mutated human lung carcinoma was reported (Sweet-Cordero et al.,2005).

It is notable that in that same study (Sweet-Cordero et al.,2005), the gene expression signature of KRAS2 activation was not identifiable by analysis of human tumors

alone, but only by integration of mouse and human data. This integration indicates that a murine model, in addition to displaying molecular similarity, could uncover patterns or pathways relevant to human cancer that are obscured in the human data. Similarly in the current study, only through interspecies gene expression profiling, high degree of unspecific immune response in the liver away from the invasion front was uncovered, which would probably not have gained attention if only one species would have been used.

5.2 Gene expression profiles of host tissue at the invasive front of colorectal liver metastases

The crucial importance of the host reaction on metastatic invasion has been increasingly recognized. The results from the analysis of expression profiles of host tissue at the invasive front present the first global analysis of differential gene expression with emphasis on gene regulation of the host without severe interference by tumor cells. The findings indicate that 1) a xenograft model of colorectal tumor cells of human origin growing in the liver of nude mice can be reliably and repeatedly used for this purpose, 2) the patterns of gene expression in the host part of the invasion front are characterized by dramatically increased cellular communication and deposition of ECM and at the same time dramatically decreased metabolic functions and 3) activation and probably migration or proliferation of HSC in the invasive front are at least partly responsible for the observed phenomena.

The difficulty to discriminate between desired and undesired cells upon microdissection of a histologic specimen is a common problem in the field of global molecular analysis of tissues (Maitra et al., 2001). Ways to solve this problem are either the performance of very time consuming and difficult microdissection procedures on the single cell level or extensive morphological validation of over-expressed genes following microarray analysis. This problem can be circumvented by the xenograft model which allows successful hybridization of the desired host tissue of murine origin on Affymetrix mouse microarrays while any contaminations by invading tumor cells of human origin will hybridize to a dramatically lower extent on this murine chip. In addition, to eliminate any residual signals resulting from cross hybridizing human transcripts, all cross hybridizing genes were deleted prior to data analysis. Fortunately, this fraction comprises only 15.3 % of all genes that remain

after data tailoring such that the introduced bias might be tolerable at least for gross analysis of gene expression.

The biological processes in the invasive front of liver metastases have not been systematically examined before. An unbiased, non hypothesis driven examination of the differences in global and single gene expression patterns between the host part of the invasion front and unaffected liver tissue lead to groups of up-regulated and down-regulated genes. The GO distribution of these groups was compared to the distribution of a reference group comprising all genes that are present either in the invasion front or the unaffected liver tissue.

Genes of the ECM were found to be most strikingly up regulated in the invasion front. In principle, this finding supports earlier suggestions that remodelling of the ECM, which is confined to the immediate pericellular environment of the cell seems to be a necessary step in local invasion (Liotta et al., 1989& Werb et al., 1991). However, the dramatic up regulation was somewhat unexpected particularly because routine morphological HE staining did not suggest massive ECM deposition. Subsequent immunostaining against hepatocytes revealed that besides areas of close association of hepatocytes and tumor cells, regions with a narrow cell poor gap between these two populations exist where ECM seems to be deposited. Such a deposition of fibrotic material has been reported in activated cultured myofibroblast (Ooi et al., 1995) as well as for human metastases of colorectal origin where the formation of fibrotic capsules surrounding the tumor has been found in 20% within a group of 69 examined cases (Lunevicius et al., 2001). On one hand, such ECM deposition may have an anti-tumor defensive function as indicated by the better prognosis if capsules have formed around colorectal liver metastases (Lunevicius et al., 2001) or the fact that less liver metastases are formed in cirrhotic livers (Pereira-Lima et al., 2003). On the other hand, ECM deposition seems to provide proinvasive signals (De Wever et al., 2002& 2003). Tenascin that is upregulated in the invasion front in the current model provides proinvasive signals to colon cancer cells (De Wever et al., 2004). Finally, the differentially up-regulated ECM molecules fibronectin and collagen IV have proangiogenic properties (Jain et al., 2003).

The most likely candidate cells responsible for ECM production are HSC that are transformed into myofibroblasts upon activation by profibrogenic signals (De Wever et al., 2002& 2003). Their role in hepatic fibrosis has been described to a significant

extent and HSC have been described to be the major source of ECM in the liver (Armendariz-Borunda et al., 1989 & Schmitt-Graff et al., 1991).

Five HSC genes belong to the class of actin genes or actin-binding genes, namely *actinin α (1),* the *tropomyosins 1* and *4, transgelin (SM22α)* and *α-smooth muscle actin (α-SMA). α-SMA* is a typical and widely used HSC activation marker, which seems to be expressed if HSC acquire contractile and refractile features typically described during the development of liver fibrosis (Schmitt-Graff et al., 1991). Dramatic up regulation of *α-SMA* and *transgelin* were confirmed the in the invasion front by qPCR and immunohistochemistry. Similar results of HSC specific immunoreactivity have been found for human specimen (Lunevicius et al., 2001& Ooi et al., 1997).

The tropomyosins stabilize actin fibers and the α-actinins are actin-cross linking proteins that are responsible for the formation of contractile bundles. They are concentrated in stress fibres, which they hold in contact to the plasma membrane. Transgelin is an actin cross-linking protein as well but is rather responsible for the construction of actin networks (gelling). The up regulation of these cytoskeletal genes is paralleled by the significant overrepresentation of cytoskeleton related GO terms such as " structural molecule activity", "cytoskeleton" and "actin cytoskeleton" (Table 5). The up regulation of cytoskeletal genes in the invasion front and their activation status in HSC most likely results from the required modulations of cell shape, motility and adhesion. In addition, α-actinin and tropomyosin dependent reorganisation of the actin cytoskeleton has been reported to occur upon retinol treatment of HSC (Mermelstein et al., 2001). In our model, one additional protein involved in retinoid metabolism, retinol binding protein 1 (cRBP-1) was found to be up-regulated as well. HSC are the main cell type responsible for retinol metabolism and storage in the liver (Hendriks et al., 1987). In addition to their already described roles the up-regulated genes *α-SMA, RBP-1* and *transgelin* are myoblastic differentiation genes. They are supplemented by *galectin-1* whose gene product is a member of the family of beta-galactoside-binding proteins implicated in modulating cell-cell and cell-matrix interactions up-regulated in the invasion front. Interestingly, these HSC differentiation genes are paralleled by significant overrepresentation of the GO term "morphogenesis" which is the major sub term of "cell differentiation".

The further analysis of the GO distribution of genes with overrepresentation in the invasion front reveals several more interesting patterns which are however less specific for HSC.

It is obvious that deposition of ECM requires repeated cycles of detachment and attachment to the surrounding structures by the involved cells and that such an area of intensive cellular interplay will require a lot of cellular communication. These phenomena are reflected in this xenograft model by a very prominent overrepresentation of the GO terms “cell communication”, “cell adhesion” and “cell adhesion molecule activity” in the invasive front. Further localisation and more mechanistic studies are however required to pinpoint the specific roles of host cell adhesion molecules in this model e.g. proangiogenic integrins on endothelial cells (Jain et al., 2003), cadherins like N-cadherin on myofibroblasts for interaction with and paving the way for cancer cells (De Wever et al., 2003&2004) or adhesion molecules for the initial attachment of circulating cancer cells (Zetter et al., 1993, Cavallaro et al., 1996 & Brand et al., 2001).

Host cells in the invasion front are apparently intensively responding to the external stimuli initiated by tumor invasion since the GO terms “response to external stimulus” and “response to biotic stimulus” are over represented. Interestingly, immune response genes seem to account for most of these up-regulated transcripts. The high level of significance of MHC II restricted antigen processing genes argues for macrophages, most likely the resident Kupffer cells as one main source of immune response genes. Several other significant GO terms such as “chemotaxis” and “inflammatory response”, or “chemokine receptor activity” indicate paracrine effects leading to the recruiting of circulating cells, perhaps neutrophils to the invasion front. Macrophages (Lin et al., 2001), neutrophilic granulocytes (Obermueller et al., 2004) and mast cells (DeClerck et al., 2004) have been shown to exhibit tumor-supporting effects. On the other hand, an inflammatory immune response is a well known anti-tumor host reaction. Therefore, it will be very interesting to evaluate under which circumstances the described prevention of physical contact between inflammatory cells and cancer cells by myofibroblasts and their surrounding ECM (Lieubeau et al., 1999) will be beneficial or not.

The significantly over represented terms “cell growth” and “cell proliferation” indicate that the cells of the invasion front are more active than unaffected liver with respect to

cell division. On one hand, this fits to the observed differences in the cellular composition of these two areas and particularly to morphological data, which indicates a decrease of hepatocytes and an increase of HSC in the invasion front. On the other hand, at least cancer cells in the invasion front can be higher (Dissanayake et al., 2003) as well as lower (Jung et al., 2001) in proliferation than their counterparts in the inner parts of the tumor allowing them to concentrate on their specific roles in the process of invasion. This may hold true for some host cells as well but not for others (like endothelial cells). Further studies like single cell microdissection and protein localisation are required to determine the responsible cell populations.

The examination of the genes and GO terms which are down-regulated in the invasion front as compared to the unaffected liver revealed a dramatic overrepresentation of metabolism related genes. Several of the major metabolic pathways seem to be impaired in the invasion front which is particularly interesting as not one single metabolic pathway was found to be increased in the invasion front. The most dramatically reduced GO term among the metabolic functions was “electron transport” represented by “oxidoreductase activity” which takes place in “mitochiondria”. In addition, several GO terms representing typical hepatocellular functions e.g. “urea cycle” or “steroid biosynthesis” were found to be over represented among the genes down-regulated in the invasion front. These findings can be interpreted as indicators of severely impaired physiological functions mainly of hepatocytes upon confrontation with invading tumor cells. In addition, immunohistochemistry revealed that hepatocytes might be under-represented in number within the microdissected samples of the invasion front.

In summary, the global genomic analysis of the host reaction of the liver tissue on tumor infiltration indicates dramatic changes of the cellular composition and activation status of the different types of parenchymal and non-parenchymal liver cells.

5.3 Gene expression profiles of tumor cells in vitro, in vivo and at the invasion front of colorectal liver metastases

Using a combination of microarrays and real time quantitative PCR fifteen genes have been identified to be up regulated at the invasion front compared to the inner parts of the tumor which might be invasion and metastasis associated. As a starting point for the evaluation of the cross talk of tumor cells and host cells regarding

angiogenesis in the invasion front, gene expression data was examined for genes involved in angiogenesis. Surprisngly one class of pro-angiogenic molecules, the ELR+CXC chemokines were differentially regulated. All pro-angiogenic members of that family including potent pro-angiogenic CXCL8 (IL-8) were up regulated in the tumor cells of the invasion front as compared to the tumor core. Moreover, angiostatic CXC chemokines like CXCL9, 10, 11 do not seem to be expressed by the tumor cells or at least not at a higher level in the invasion front (data not shown). The possible role of CXC chemokines in colorectal liver metastasis will be discussed in the following sections. β-catenin which appeared to be the most interesting candidate gene was chosen for further studies. These results will be discussed in section 4.3.2.

5.3.1 CXC Chemokines

A. Role of chemokines and their receptors in tumor biology

Although chemokines were initially characterized as attractants of leukocytes, it is now widely recognized that any cell type can express chemokines and chemokine receptors. In particular, their expression by tumor cells has attracted much attention, and the prevailing hypothesis implicates chemokines as road signs for tumor cell invasion and metastasis. However, chemokines appear to function more than as attractants, and increasing evidence indicates that interactions between chemokines and their receptors are important in virtually every step of tumor development, including tumor growth, progression, and metastasis, as reviewed by Tanaka et al., 2005. Emerging evidence indicates that chemokines are directly involved in the transformation, survival and growth of tumor cells. For instance, several chemokines, including CXCL1/ Groα/MGSAα and CXCL8/IL-8, bind not only to their natural receptor, CXCR2, but also to the G-protein-coupled receptors (Tanaka et al., 2005).

B. Chemokines enhance invasion

Invasion is in fact a physiological function that leukocytes constantly execute in inflammation. The direction of leukocyte migration is towards increasing chemokine concentrations. Chemokines, while attracting leukocytes, often activate the production of cytoskeletal motor proteins, secreted proteinases and glycanases and the expression of adhesion molecules, including mucins, selectins, integrins and immunoglobulin family receptors. Whereas chemokine actions have been mainly

studied in immune responses, these activities have also been observed in specific tumor models. For instance, prostate tumor cells, responding to IL-8/CXCL8 through CXCR2 are more invasive in vitro (Reiland et al., 1999) and chemokines induce migrational responses (chemotaxis and cytoskeletal changes) in various human breast carcinoma cell lines (Youngs et al., 1997). In vivo, the invasive phenotype may be assisted by tumor-derived chemokines. Indeed, expression of IL -8/CXCL8 mRNA in ovarium carcinoma is correlated with histological grading (Davidson et al., 2002). In many models, xenografting with chemokine expressing cancer cells has been used to show chemokine action (i.e. tumor infiltration of leukocytes and proteinase induction) (Melani et al., 1995). It needs to be noticed that in most of these settings a strong immune response is elicited and thus the tumor may eventually grow, but often is rejected by the workings of the hosts immune response (vide infra).

C. Chemokines provide paracrine growth advantages via angiogenesis

Angiogenesis has been well studied in the biology of organ development, tissue repair and cancer growth and invasion. Vessel growth, relevant for cancer, varies widely (e.g. blood and lymph vessels) and is governed by many factors that stimulate (e.g. angiogenesis by vascular endothelial growth factors) or dampen (e.g. angiostatin) proliferation of the various types of endothelial cells (Folkman, 1995).

After local growth and crossing tissue barriers, the tumor cells may enter blood or lymph vessels. This forms the first phase of tumor cell entry during the process of metastasis. In many ex vivo studies, the expression of chemokines has been associated with higher clinical tumor staging. Along this line, studies are available on IL- 8/CXCL8 in cutaneous melanoma, malignant melanoma, ovarian carcinoma, non-Hodgkin lymphoma, breast carcinoma and lung cancer (Opdenaakker et al., 2004). Whether the process of vessel entry is determined by enzyme induction, by the process of angiogenesis, by both or by still other mechanisms must await further experimentation, e.g. by using specific knockout models or by specifically blocking proteinases or chemokines with monoclonal antibodies.

Because chemokines and chemokine receptors are important in tumor progression and metastasis, disrupting these interactions may prove to be a useful approach for treating cancers. However, given the complex nature of carcinogenesis and

metastasis formation, let alone the heterogeneity of different cancers, it is not likely that any single inhibitor or functional modulator of chemokines or chemokine receptors will become a 'cure' for cancer. It is more probable that, when used in conjunction with other therapeutic regimens, newly discovered chemokine- or chemokine-receptor-based agents will contribute significantly to the control of tumor cell invasion and metastasis. Such an approach may lead to many cancers becoming dormant and clinically manageable. An increased understanding of the mode of action of chemokines on tumor cells and their microenvironment will help us meet this goal.

5.3.2 Activation of the β-catenin promoter in the invasion front of colorectal liver metastases

Activation of the β -catenin promoter finding supports earlier assumptions originating from promoter studies (Nollet et al.,1996 & Li et al.,2004) and observations of elevated mRNA levels (El-Bahrawy et al., 2001& Mann et al., 1999, Ebert et al., 2002, Cui et al., 2001 & Saito et al., 2002) in tumors, suggesting that β-catenin may be regulated on the transcriptional level in addition to the well studied post-translational regulation. It should however be mentioned that in our model micro environmental changes, which are most likely not genetically fixed, are probably responsible for promoter activation. It has to be determined whether this holds true for the reported elevated β-catenin mRNA in tumor tissue resulting from the comparison with normal tissue.

In LS174T xenograft model the most prominent promoter activity was seen in cells at the invasion front. Some increase was seen between the *in vitro* and the *in vivo* situation. Therefore it can be assumed that the interaction between invading tumor cells and host cells is responsible for promoter activation but which signals are involved will be subject of future investigation.

Since increased promoter activity is converted into increased mRNA levels and finally into increased protein content, once can assume that transcriptional regulation plays a dominant role for protein content at least in LS174T xenograft model. Increased protein levels at the invasion front of colorectal liver metastases have occasionally

been reported (Brabletz et al., 2001) but seem to be inconsistent and not generally occurring.

Among the regulating proteins involved in activation of the β-catenin promoter, β-catenin itself might play a role in this model. Since LS174T cell line is characterized by high levels of β-catenin protein even in cell culture, and a TCF/LEF site has recently been detected in the β-catenin promoter (Li et al.,2004) a positive feed back loop between increased β-catenin protein and increased transcription of its gene is likely to occur. This hypothesis is supported by the fact that particularly high mRNA levels of β-catenin in desmoid tumors (Saito et al., 2002) and in gastric carcinomas (Ebert et al., 2002) were correlated to high levels of mutated β-catenin. It will be interesting to examine whether increased promoter activity is associated with the subset of colorectal cancers harbouring oncogenic β-catenin mutations. If this holds true, an a priori increased rate of β-catenin transcription might facilitate the binding of other transcription factors that are specific for the *in vivo* situation, particularly at the invasion front.

Conclusions

The overall aim of this thesis is to provide candidate genes for small molecule inhibitors and gene therapeutics for the treatment of colorectal liver metastases with special emphasis on the invasion front because this area is only poorly described although it is of crucial relevance for metastatic invasion. Initial experiments involved the microdissection and gene expression profiles of three to four distinct areas of the invasion front and the surrounding tissue namely unaffected liver, liver invasion, tumor invasion and tumor further away from the invasion front towards a more general understanding of the regulatory processes during invasion.

Differential gene expression was examined in three model systems: A syngeneic mouse model (CT26/Balb/C mouse, a xenograft mouse model (LS174/nude mouse) and several clinical specimens. Initial results regarding these three different models yielded similar gene expression patterns in the invasion front of colorectal liver metastases. For candidate gene evaluation, the xenograft mouse model was used: This model is a human tumor growing in the liver of mice has the advantage that one can discriminate between host derived and tumor cell derived genes. This helped to confirm differentially regulated genes from global gene expression studies by real time PCR using species-specific primers.

Use of laser captured microdissection and xenograft mouse model enabled to perform mRNA analysis between liver, liver invasion tumor and tumor invasion front.

Histology and gene expression patterns are valuable to understand cancer-relevant processes and to judge on the suitability of animal models. However, due to inherent species differences and functional redundancy the number of actual target genes that are similarly regulated in both the clinical situation and the animal model has to be determined individually in standard grafted models. Invasion relevant genes in a murine model may not be relevant in exactly the same compartment and in exactly the same tumor entity (but probably in several others) in the human situation.

The results from the xenograft model of colorectal liver metastasis indicate that the tumor host interface is characterized by extensive cellular communication accompanied by remodelling of the extracellular matrix. The predominant cell type in that area which is probably responsible for many of the observed processes was

found to be activated HSC. Further experimentation will address two important remaining issues:

1. The discrimination between truly up-regulated genes and those genes whose increased transcript detection is rather due to an increase of the respective cellular subpopulation?

2. The precise cellular origin of up-regulated transcripts.Studies on transcriptional profiles of cells grown *in vitro* with profiles of orthotopically implanted tumors show an intricate molecular interplay between the tumor and host microenvironments that likely regulates important aspects of tumor biology. Concerns regarding the potential confounding effect of mouse tissue when profiling xenograft tumors using human arrays to determine (human) cancer cell expression patterns are alleviated by the findings of tissue-specific and cytokine-induced responses of cells to the microenvironment. We may expect that different cell lines respond differently to the *in vivo* microenvironment. Consequently, xenograft tumor profiling studies on a larger scale may be highly informative with respect to the extent to which these cell lines when grown *in vivo* may exhibit different properties compared with their *in vitro* growth. However, cell lines grown *in vitro* remain a powerful model for studying cancer; this study indicates that novel therapeutic targets or biomarkers may be found by superseding *in vitro* models and looking initially at *in vivo* models.

Further experimentation on CXC chemokines will answer the following questions

1. Histomorphologic angiogenesis picture of the invasion front in our model.

2. Role of putative pro-angiogenic CXC cytokines during neo-angiogenesis.

3. Whether CXC cytokines are the main soluble molecules secreted by tumor cells during early angiogenesis?

Further experiments on β-catenin activation will solve two important questions

Generality and clinical importance of transcriptional activation of the β-catenin promoter.

Mechanism of β-catenin promoter activation *in vivo* and particularly in the invasion front

References

Addison CL, Daniel TO, Burdick MD, Liu H, Ehlert JE, Xue YY, Buechi L, Walz A, Richmond A, Strieter RM. The CXC chemokine receptor 2, CXCR2, is the putative receptor for ELR+ CXC chemokine-induced angiogenic activity. J Immunol 2000;*165(9)*:5269-77

Addison CL, Belperio JA, Burdick MD, Strieter RM. Overexpression of the duffy antigen receptor for chemokines (DARC) by NSCLC tumor cells results in increased tumor necrosis. BMC Cancer 2004; *4(1):*28.

Armendariz-Borunda J, Greenwel P, Rojkind M. Kupffer cells from CC1 (4)-treated rat livers induce skin fibroblast and liver fat-storing cell proliferation in culture. Matrix 1989; *9*: 150-8.

Ausubel Frederick M, B. R., Kingston Robert E., Moore David D., Seidman J. G., Smith John A., Struhl Kevin Current Protocols in Molecular Biology, Current Protocols: Greene Publishing Associates, Inc. and John Wiley & Sons, Inc., 1994; 1

Bandapalli, O. R., Geheeb, M., Kobelt, D., Kuehnle, K., Elezkurtaj, S., Herrmann, J., Gressner, A. M., Weiskirchen, R., Beule, D., Bluthgen, N., Herzel, H., Franke, C., and Brand, K. Global analysis of host tissue gene expression in the invasive front of colorectal liver metastases. Int J Cancer, 2006; *118*: 74-89.

Bandapalli, O. R., Schirmacher, P., Brand, K. Comparison of global gene expression profiles of tumor cells growing in cell culture and in vivo in the inner parts and in the invasion front of colorectal liver metastases. Pathology Research and Practice, 2006; 202: 321.

Belperio JA, Keane MP, Arenberg DA, Addison CL, Ehlert JE, Burdick MD, Strieter RM. CXC chemokines in angiogenesis. J Leukoc Biol 2000; *68(1):*1-8.

Bissell MJ, Radisky D. Putting tumours in context. Nat Rev Cancer 2001;*1*:46-54.

Bluthgen N, Kielbasa SM, Herzel H. Inferring combinatorial regulation of transcription in silico. Nucl Acids Res 2005; *33*: 272-9.

Borkham-Kamphorst E, Herrmann J, Stoll D, Treptau J, Gressner AM, Weiskirchen R. Dominant-negative soluble PDGF-beta receptor inhibits hepatic stellate cell activation

and attenuates liver fibrosis. Lab Invest 2004; *84*: 766-77.

Brabletz, T., Jung, A., Reu, S., Porzner, M., Hlubek, F., Kunz-Schughart, L. A., Knuechel, R., and Kirchner, T. Variable beta-catenin expression in colorectal cancers indicates tumor progression driven by the tumor environment. Proc Natl Acad Sci U S A, 2001; *98:* 10356-10361.

Brabletz, T., Jung, A., Spaderna, S., Hlubek, F., and Kirchner, T. Opinion: migrating cancer stem cells - an integrated concept of malignant tumour progression. Nat Rev Cancer, 2005; *5:* 744-749.

Bramhall SR, Hallissey MT, Whiting J, Scholefield J, Tierney G, Stuart RC, Hawkins RE, McCulloch P, Maughan T, Brown PD, Baillet M, Fielding JW. Marimastat as maintenance therapy for patients with advanced gastric cancer: a randomised trial. Br J Cancer 2002; *86:* 1864-70.

Brand K, Baker AH, Perez-Canto A, Possling A, Sacharjat M, Geheeb M, Arnold W. Treatment of colorectal liver metastases by adenoviral transfer of tissue inhibitor of metalloproteinases-2 into the liver tissue. Cancer Res 2000; *60:* 5723-30.

Brand K, Lubbe AS, Justus DJ. Hyperthermia decreases cytokine-mediated adhesion molecule expression on human umbilical vein endothelial cells. Int J Hyperthermia 1996; *12:* 527-38.

Brattain, M. G., Strobel-Stevens, J., Fine, D., Webb, M., and Sarrif, A. M. Establishment of mouse colonic carcinoma cell lines with different metastatic properties. Cancer Res, 1980; *40:* 2142-2146.

Brazma A, Hingamp P, Quackenbush J, Sherlock G, Spellman P, Stoeckert C, Aach J, Ansorge W, Ball CA, Causton HC, Gaasterland T, Glenisson P,. Minimum information about a microarray experiment (MIAME)-toward standards for microarray data. Nat Genet 2001; *29:* 365-71.

Brembeck, F. H., Rosario, M., and Birchmeier, W. Balancing cell adhesion and Wnt signaling, the key role of beta-catenin. Curr Opin Genet Dev, 2006; *16:* 51-59.

Carmeleit P., Jain R. K. Angiogenesis in cancer and other diseases. Nature, 2000, *407:* 249-57.

Cavallaro U, Christofori G. Cell adhesion in tumor invasion and metastasis: loss of the glue is not enough. Biochim Biophys Acta 2001; *1552*: 39-45.

Costa AM, Tuchweber B, Rubbia-Brandt L, Peyrol S, Chevallie M, Adham M, Gabbiani G, Rosenbaum J, Desmouliere A. Early activation of hepatic stellate cells and perisinusoidal extracellular matrix changes during ex vivo pig liver perfusion. J Submicrosc Cytol Pathol 2001; *33:* 231-40.

Cui, J., Zhou, X., Liu, Y., and Tang, Z. Mutation and overexpression of the beta-catenin gene may play an important role in primary hepatocellular carcinoma among Chinese people. J Cancer Res Clin Oncol, 2001; *127:* 577-581.

Cullen, B. and M. Malim. Secreted placental alkaline phosphatase as a eukaryotic reporter gene. Methods in Enzymol. 1992; *216*:362-368.

Curley SA, Izzo F, Abdalla E, Vauthey JN. Surgical treatment of colorectal cancer metastasis. Cancer Metastasis Rev 2004; *23:* 165-82.

Davidson, B., Reich, R., Kopolovic, J., Berner, A., Neslkand, J.M., Kristensen, G.B., Trope, C.G., Bryne, M., Risberg, B., Van De Putte, G. and Goldberg, I. Interleukin-8 and vascular endothelial growth factor mRNA and protein levels are down-regulated in ovarian carcinoma cells in serous effusions. Clin. Exp. Metastasis. 2002;*19:*135-144.

De Wever O, Mareel M. Role of myofibroblasts at the invasion front. Biol Chem 2002; *383:* 55-67.

De Wever O, Mareel M. Role of tissue stroma in cancer cell invasion. J Pathol 2003; *200:* 429-47.

De Wever O, Nguyen QD, Van Hoorde L, Bracke M, Bruyneel E, Gespach C, Mareel M. Tenascin-C and SF/HGF produced by myofibroblasts in vitro provide convergent pro-invasive signals to human colon cancer cells through RhoA and Rac. FASEB J 2004; *18:* 1016-8.

De Wever O, Westbroek W, Verloes A, Bloemen N, Bracke M, Gespach C, Bruyneel E, Mareel M. Critical role of N-cadherin in myofibroblast invasion and migration in vitro stimulated by colon-cancer-cell-derived TGF-beta or wounding. J Cell Sci 2004; *117(Pt 20):* 4691-703.

DeClerck YA, Mercurio AM, Stack MS, Chapman HA, Zutter MM, Muschel RJ, Raz A, Matrisian LM, Sloane BF, Noel A, Hendrix MJ, Coussens L, Proteases, extracellular matrix, and cancer: a workshop of the path B study section. Am J Pathol 2004; *164*: 1131-9.

Debois J. M. (Ed.) TxNxM1 The Anatomy and Clinics of Metastatic Cancer, , 2002; Kluwer Academic Publishers, Boston, Dordrecht, London

Dissanayake U, Johnson NW, Warnakulasuriya KA. Comparison of cell proliferation in the centre and advancing fronts of oral squamous cell carcinomas using Ki-67 index. Cell Prolif 2003; *36:* 255-64.

Dong G, Chen Z, Li ZY, Yeh NT, Bancroft CC, Van Waes C. Hepatocyte growth factor/scatter factor-induced activation of MEK and PI3K signal pathways contributes to expression of proangiogenic cytokines interleukin-8 and vascular endothelial growth factor in head and neck squamous cell carcinoma. Cancer Res 2001; *61(15):*5911-8.

Dunnington DJ, Buscarino C, Gennaro D, Greig R, Poste G. Characterization of an animal model of metastatic colon carcinoma. Int J Cancer 1987; *39:* 248-54.

Ebert, M. P., Fei, G., Kahmann, S., Muller, O., Yu, J., Sung, J. J., and Malfertheiner, P. Increased beta-catenin mRNA levels and mutational alterations of the APC and beta-catenin gene are present in intestinal-type gastric cancer. Carcinogenesis, 2002; *23*: 87-91.

El-Bahrawy, M. A., Poulsom, R., Jeffery, R., Talbot, I., and Alison, M. R. The expression of E-cadherin and catenins in sporadic colorectal carcinoma. Hum Pathol, 2001; *32:* 1216-1224.

Elezkurtaj S, Kopitz C, Baker AH, Perez-Canto A, Arlt MJ, Khokha R, Gansbacher B, Anton M, Brand K, Kruger A. Adenovirus-mediated overexpression of tissue inhibitor of metalloproteinases-1 in the liver: efficient protection against T-cell lymphoma and colon carcinoma metastasis. J Gene Med 2004; *6:* 1228-37.

Evans JD, Stark A, Johnson CD, Daniel F, Carmichael J, Buckels J, Imrie CW, Brown P, Neoptolemos JP. A phase II trial of marimastat in advanced pancreatic cancer. Br J Cancer 2001; *85*: 1865-70.

Fang, H., Tong, W., Perkins, R., Shi, L., Hong, H., Cao, X., Xie, Q., Yim, S. H., Ward,

J. M., Pitot, H. C., and Dragan, Y. P. Bioinformatics approaches for cross-species liver cancer analysis based on microarray gene expression profiling. BMC Bioinformatics, 2005; *6: Suppl 2:* S6.

Folkman, J. Angiogenesis in cancer, vascular, rheumatoid and other disease. Nat Med. 1995; *1*:27-31.

Frederick MJ, Clayman GL. Chemokines in cancer. Expert Rev Mol Med. 2001: *18*; 1-18

Freshney, R. I. Culture of Animal Cells-A Manual of Basic Technique:

Wiley-Liss, 1987.

Geerts A, Eliasson C, Niki T, Wielant A, Vaeyens F, Pekny M. Formation of normal desmin intermediate filaments in mouse hepatic stellate cells requires vimentin. Hepatology 2001; *33*: 177-88.

Grem JL. Current treatment approaches in colorectal cancer. Semin Oncol 1991; *18(1 Suppl 1)*: 17-26.

Hendriks HF, Brouwer A, Knook DL. The role of hepatic fat-storing (stellate) cells in retinoid metabolism. Hepatology 1987; *7:* 1368-71.

Huelsken, J. and Behrens, J. The Wnt signalling pathway. J Cell Sci, 2002; *115*: 3977-3978.

Jain RK. Molecular regulation of vessel maturation. Nat Med 2003; *9:* 685-93.

Jung A, Schrauder M, Oswald U, Knoll C, Sellberg P, Palmqvist R, Niedobitek G, Brabletz T, Kirchner T. The invasion front of human colorectal adenocarcinomas shows co-localization of nuclear beta-catenin, cyclin D1, and p16INK4A and is a region of low proliferation. Am J Pathol 2001; *159:* 1613-7.

Lamps LW, Folpe AL. The diagnostic value of hepatocyte paraffin antibody 1 in differentiating hepatocellular neoplasms from nonhepatic tumors: a review. Adv Anat Pathol 2003; *10:* 39-43.

Li, Q., Dashwood, W. M., Zhong, X., Al-Fageeh, M., and Dashwood, R. H. Cloning of the rat beta-catenin gene (Ctnnb1) promoter and its functional analysis compared with

the Catnb and CTNNB1 promoters. Genomics, 2004; *83:* 231-242.

Li A, Dubey S, Varney ML, Dave BJ, Singh RK. IL-8 directly enhanced endothelial cell survival, proliferation, and matrix metalloproteinases production and regulated angiogenesis. J Immunol 2003; *170(6)*:3369-76.

Lieubeau B, Heymann MF, Henry F, Barbieux I, Meflah K, Gregoire M. Immunomodulatory effects of tumor-associated fibroblasts in colorectal-tumor development. Int J Cancer 1999; *81:* 629-36.

Lin EY, Nguyen AV, Russell RG, Pollard JW. Colony-stimulating factor 1 promotes progression of mammary tumors to malignancy. J Exp Med 2001; *193:* 727-40.

Liotta LA, Steeg P, Rojkind M. Cancer metastasis and liver fat-storing cell proliferation in culture. Cell 1989; *9:* 150-8.

Liotta LA, Kohn EC. The microenvironment of the tumour-host interface. Nature 2001; *411:* 375-9.

Lunevicius R, Nakanishi H, Ito S, Kozaki K, Kato T, Tatematsu M, Yasui K. Clinicopathological significance of fibrotic capsule formation around liver metastasis from colorectal cancer. J Cancer Res Clin Oncol 2001; *127:* 193-9.

Luo L, Salunga RC, Guo H, Bittner A, Joy KC, Galindo JE, Xiao H, Rogers KE, Wan JS, Jackson MR, Erlander MG. Gene expression profiles of laser-captured adjacent neuronal subtypes. Nat Med 1999; *5:* 117-22.

Luster AD. Chemokines--chemotactic cytokines that mediate inflammation. N Engl J Med 1998; *338(7):*436-45.

Luzzi V, Holtschlag V, Watson MA. Expression profiling of ductal carcinoma in situ by laser capture microdissection and high-density oligonucleotide arrays. Am J Pathol 2001; *158:* 2005-10.

Maitra A, Wistuba II, Gazdar AF. Microdissection and the study of cancer pathways. Curr Mol Med 2001; *1:* 153-62.

Mann, B., Gelos, M., Siedow, A., Hanski, M. L., Gratchev, A., Ilyas, M., Bodmer, W. F., Moyer, M. P., Riecken, E. O., Buhr, H. J., and Hanski, C. Target genes of beta-catenin-T cell-factor/lymphoid-enhancer-factor signaling in human colorectal carcinomas. Proc

Natl Acad Sci U S A, 1999; *96:* 1603-1608.

Mareel M. M., Van Roy F. M., Bracke M. E. How and when do tumor cells

metastasize? Crit Rev Oncol, 1993, *4:* 559-94.

Mareel M., Leroy A. Clinical, cellular, and molecular aspects of cancer invasion. Physiol Rev. 2003; *83(2):*337-76.

Mareel M M., Physiopathology of liver metastasis. Acta Chir Belg. 2003; *103 (5):*444-7

Mareel M. M., Bracke M. E. Molecular mechanisms of cancer invasion. Bertino J. R. (ed.) Encyclopedia of Cancer, Academic Press, 2002; *2(3):* 221-33.

Mariani L, McDonough WS, Hoelzinger DB, Beaudry C, Kaczmarek E, Coons SW, Giese A, Moghaddam M, Seiler RW, Berens ME. Identification and validation of P311 as a glioblastoma invasion gene using laser capture microdissection. Cancer Res 2001; *61*: 4190-6.

Melani, C., Pupa, S.M., Stoppaciaro, A., Menard, S., Colnaghi, M.I., Parmiani, G. and Colombo, M.P. An in vivo model to compare human leukocyte infiltration in carcinoma xenografts producing different chemokines. Int J Cancer. 1995; *62*:572-578.

Mermelstein CS, Guma FC, Mello TG, Fortuna VA, Guaragna RM, Costa ML, Borojevic R. Induction of the lipocyte phenotype in murine hepatic stellate cells: reorganisation of the actin cytoskeleton. Cell Tissue Res 2001; *306:* 75-83.

Murdoch C, Monk PN, Finn A. CXC chemokine receptor expression on human endothelial cells. Cytokine 1999; *11(9):*704-12.

Müller A., Homey B., Soto H. Involvement of chemokine receptors in breast cancer metastasis. Nature, 2001; *410:* 50-6.

Nollet, F., Berx, G., Molemans, F., and van Roy, F. Genomic organization of the human beta-catenin gene (CTNNB1). Genomics, 1996; *32:* 413-424.

Nor JE, Christensen J, Liu J, Peters M, Mooney DJ, Strieter RM, Polverini PJ. Up-Regulation of Bcl-2 in microvascular endothelial cells enhances intratumoral angiogenesis and accelerates tumor growth. Cancer Res 2001; *61(5):*2183-8.

Obermueller E, Vosseler S, Fusenig NE, Mueller MM. Cooperative autocrine and

paracrine functions of granulocyte colony-stimulating factor and granulocyte-macrophage colony-stimulating factor in the progression of skin carcinoma cells. Cancer Res 2004; *64:* 7801-12.

Ooi LP, Crawford DH, Gotley DC, Clouston AD, Strong RW, Gobe GC, Halliday JW, Bridle KR, Ramm GA. Evidence that myofibroblast-like cells are the cellular source of capsular collagen in hepatocellular carcinoma. J Hepatol 1997; *26:* 798-807.

Ooi LP, Preaux AM, Mallat A, Clouston AD, Rosenbaum J. Human myofibroblastlike cells are the fibrogenic cells in the liver. J Hepatol 1995; *22:* 788-97.

Opdenakker G, Van Damme J. The counter current principle in invasion and metastasis of cancer cells. Recent insights on the roles of chemokines. Int J Dev Biol. 2004; *48(5-6)*:519-27.

O'Reilly M. S., Holmgren L., Shing Y. Angiostatin: a novel angiogenesis inhibitor that mediates the suppression of metastases by a Lewis lung carcinoma. Cell, 1994; *79:* 315-28.

Paddison, P Cloning of short hairpin RNAs for gene knockdown in mammalian cells. Nature Methods 2004; *1(2):* 163-167.

Paget S. The distribution of secondary growths in cancer of the breast. Lancet, 1889; *1:* 571-3.

Paweletz CP, Charboneau L, Bichsel VE, Simone NL, Chen T, Gillespie JW, Emmert-Buck MR, Roth MJ, Petricoin IE, Liotta LA. Reverse phase protein microarrays which capture disease progression show activation of pro-survival pathways at the cancer invasion front. Oncogene 2001; *20:* 1981-9.

Pereira-Lima JE, Lichtenfels E, Barbosa FS, Zettler CG, Kulczynski JM. Prevalence study of metastases in cirrhotic livers. Hepatogastroenterology 2003; *50:* 1490-5.

Radinsky R, Ellis LM. Molecular determinants in the biology of liver metastasis. Surg Oncol Clin N Am 1996; *5:*215–29.

Reiland, J., Furcht, L.T. and Mc Carthy, J.B. CXC-chemokines stimulate invasion and chemotaxis in prostate carcinoma cells through the CXCR2 receptor. Prostate. 1999; *41 (2):*78-88.

Roesch A, Vogt T, Stolz W, Dugas M, Landthaler M, Becker B. Discrimination between gene expression patterns in the invasive margin and the tumour core of malignant melanomas. Melanoma Res 2003; *13:* 503-9.

Rowan, A. J., Lamlum, H., Ilyas, M., Wheeler, J., Straub, J., Papadopoulou, A., Bicknell, D., Bodmer, W. F., and Tomlinson, I. P. APC mutations in sporadic colorectal tumors: A mutational "hotspot" and interdependence of the "two hits". Proc Natl Acad Sci U S A, 2000; *97:* 3352-3357.

Ryu B, Jones J, Hollingsworth MA, Hruban RH, Kern SE. Invasion-specific genes in malignancy: serial analysis of gene expression comparisons of primary and passaged cancers. Cancer Res 2001; *61*: 1833-8.

Saito, T., Oda, Y., Kawaguchi, K., Tanaka, K., Matsuda, S., Tamiya, S., Iwamoto, Y., and Tsuneyoshi, M. Possible association between higher beta-catenin mRNA expression and mutated beta-catenin in sporadic desmoid tumors: real-time semiquantitative assay by TaqMan polymerase chain reaction. Lab Invest, 2002; *82*: 97-103.

Salcedo R, Resau JH, Halverson D, Hudson EA, Dambach M, Powell D, Wasserman K, Oppenheim JJ. Differential expression and responsiveness of chemokine receptors (CXCR1-3) by human microvascular endothelial cells and umbilical vein endothelial cells. Faseb J 2000; *14(13):*2055-64.

Schmitt-Graff A, Ertelt V, Allgaier HP, Koelble K, Olschewski M, Nitschke R, Bochaton-Piallat ML, Gabbiani G, Blum HE. Cellular retinol-binding protein-1 in hepatocellular carcinoma correlates with beta-catenin, Ki-67 index, and patient survival. Hepatology 2003; *38:* 470-80.

Schmitt-Graff A, Kruger S, Bochard F, Gabbiani G, Denk H. Modulation of alpha smooth muscle actin and desmin expression in perisinusoidal cells of normal and diseased human livers. Am J Pathol 1991; *138:* 1233-42.

Silva, J Second-generation shRNA libraries covering the human and mouse genomes Nature Genetics 2005; *37:11,* 1281-88.

Strieter RM, Polverini PJ, Kunkel SL, Arenberg DA, Burdick MD, Kasper J, Dzuiba J, Van Damme J, Walz A, Marriott D, The functional role of the ELR motif in CXC

chemokine-mediated angiogenesis. J Biol Chem 1995;*270(45)*:27348-57.

Strieter RM, Belperio JA, Phillips RJ, Keane MP. CXC chemokines in angiogenesis of cancer. Semin Cancer Biol 2004; *14(3):*195-200.

Sweet-Cordero, A., Mukherjee, S., Subramanian, A., You, H., Roix, J. J., Ladd-Acosta, C., Mesirov, J., Golub, T. R., and Jacks, T. An oncogenic KRAS2 expression signature identified by cross-species gene-expression analysis. Nat Genet, 2005; *37:* 48-55.

Tanaka T, Bai Z, Srinoulprasert Y, Yang BG, Hayasaka H, Miyasaka M. Chemokines in tumor progression and metastasis. Cancer Sci. 2005; *96(6):*317-22

Towbin, H.; Staehelin, T. & Gordon, J. electrophoretic transfer of proteins from polyacrylamide gels to nitrocellulose sheets: procedure and some applications. Proc. nat. Acad. Sci. (Wash.), 1979; *76:* 4350-4354.

Ueberham E, Low R, Ueberham U, Schonig K, Bujard H, Gebhardt R. Conditional tetracycline-regulated expression of TGF-beta1 in liver of transgenic mice leads to reversible intermediary fibrosis. Hepatology 2003; *37:* 1067-78.

Wei, C. L., Miura, T., Robson, P., Lim, S. K., Xu, X. Q., Lee, M. Y., Gupta, S., Stanton, L., Luo, Y., Schmitt, J., Thies, S., Wang, W., Khrebtukova, I., Zhou, D., Liu, E. T., Ruan, Y. J., Rao, M., and Lim, B. Transcriptome profiling of human and murine ESCs identifies divergent paths required to maintain the stem cell state. Stem Cells, 2005; *23:* 166-185.

Wennerberg AE, Nalesnik MA, Coleman WB. Hepatocyte paraffin 1: a monoclonal antibody that reacts with hepatocytes and can be used for differential diagnosis of hepatic tumors. Am J Pathol 1993; *143:* 1050-4.

Wennmalm, K., Wahlestedt, C., and Larsson, O. The expression signature of in vitro senescence resembles mouse but not human aging. Genome Biol2005; *6:* R109.

Werb Z. ECM and diseased human livers. Cell 1991; *91:* 439-42

.Zetter BR. Adhesion molecules in tumor metastasis. Semin Cancer Biol 1993, *4:* 219-29.

LEBENSLAUF

Name	Obul Reddy Bandapalli
Geburstdatum	01.06.1977
Geburtsort	Madanapalli, Indien
Nationalität	Indisch

STUDIUM

1997-1999	Master of Science (Biotechnology), G.G.University, Bilaspur, India.
1994-1997	Bachelor of Science (Sciences), S.V.University, Tirupati, India.
1992-1994	Intermediate (10+2) Board of Intermediate Education, Sri Dwarakanatha Junior College, Madana Palli, India.
1982-1992	Primary Education (10), Board of Secondary Education, Chinnatippa Samudram, India

BERUFSTÄTIGKEIT

Master thesis work, Jawaharlal Nehru University, New Delhi, India.

Thema: Cloning of cyclodextrin glycosyl transferase (CGTase) gene from *Bacillus species*.

PROMOTION

Seit Oktober 2003	Promotionstudium – am Institute of Biologie, Humboldt Universität, PD. Dr. Karsten Brand.

CURRICULUM VITAE

NAME : Obul Reddy Bandapalli

DATE OF BIRTH : 01 June 1977

NATIONALITY : Indian

WORK EXPERIENCE: PhD student from Jan. 2005 at **Uni. Clinic Heidelberg**

PhD student from Oct.2003 to Dec. 2004 at **Humboldt Uni. Berlin**

Scientific Co-worker from Dec.2002 to Oct.2003 at **Custos Biotechnologie GmbH,** Berlin

Junior&Senior Research Fellow from Jun.2000 to Sep.2002 at **Central Food Technological Research Institute** Mysore, India

DBT Research Fellow from Nov.1999 to Jun.2000 at **Dabur Research Foundation**, New Delhi.

PhD THESIS

Analysis of global gene expression profiles and invasion related genes of colorectal liver metastasis.

SCIENTIFIC EDUCATION

MSc Biotechnology	Guru Ghasidas University, Bilaspur, MP, India.
Years of study	1997-1999
Class obtained	FISRT
Title of Thesis	Cloning of Cyclodextrin Glycosyl Transferase (CGTase) gene from *Bacillus* sp.
BSc	Sri Venkateswara University, Tirupati, India
Year of study	1994-1997
Class obtained	FISRT

EDUCATION

10 years + 2 years passed with distinction (Above 70%)

PUBLICATIONS

Obul Reddy Bandapalli, Geheeb M, Kobelt D, Kuehnle K, Elezkurtaj S, Herrmann J, Gressner AM, Weiskirchen R, Beule D, Bluthgen N, Herzel H, Franke C, Brand K. Global analysis of host tissue gene expression in the invasive front of colorectal liver metastases. (**Int J Cancer. 2006 Jan 1; 118(1): 74 – 89**)

T Rajasekaran, G A Ravishankar and **B Obul Reddy** In vitro growth of Tagetes patula L. hairy roots, production of thiophenes and its mosquito larvicidal activity .**(Indian Journal of Biotechnology, 2004;3:92-96**).

Sudha C.G, **Obul Reddy.B**, Ravishankar.G.A and Seeni.S. Production of Ajmalicin and Ajmalin in hairy root cultures of Rauvolfoa micrantha Hook f. a rare endemic medicinal plant. (**Biotechnol Lett. 2003 Apr; 25(8): 631-6**)

Rajasekharan T, Ravishankar G A and **Obul Reddy.B** Enhanced production of Thiophenes from Callus cultures of Tagetes patula and its mosquito larvicidal activities. **(Indian Journal of Experimental Biology, 2003; 41:63-68**).

Giridhar P., Vijayaramu D., **Obul Reddy B**., Rajasekharan T., Ravishankar G.A- Influence of phenyl acetic acid on clonal propagation of Decalepis hamiltonii Wight & Arn. an endangered shrub. (**In Vitro Cell & Dev. Biol. Plant 2003 39: 1-6).**

Obul Reddy.B, Giridhar.P and Ravishankar.G.A Effect of triacontanol on the micropropagation of Capsicum frutescens.L and Decalepis hamiltonii W&A (Plant Cell Tissue & Organ Culture 2002; 71: 253-258)

Obul Reddy.B, Giridhar.P and Ravishankar. G.A In vitro rooting of Decalepis hamiltonii W & A, an endangered shrub influenced by auxins and root promoting agents (Current Science 2002; 81: 101-103)

Giridhar.P, **Obul Reddy.B** and Ravishankar. G.A. Silver nitrate influences in vitro shoot multiplication and root formation in Vanilla planifolia Andr. (**Current Science 2002; 81: 1166-1170**)

COMMUNICATED PAPERS

Obul Reddy Bandapalli , Christoph Kahlert, Victoria Hellstern, Peter Schirmacher, Jürgen Weitz, Karsten Brand; Cross-species comparison of gene expression patterns and underlying genes in a mouse model of colorectal liver metastasis and in clinical specimen

MANUSCRIPTS UNDER PREPARATION

Obul Reddy Bandapalli , Susanne Dihlmann, Peter Schirmacher, Karsten Brand; Activation of b-catenin promoter in the invasion front of colorectal liver metastasis

Obul Reddy Bandapalli , Peter Schirmacher, Karsten Brand; Comparison of global gene expression profiles of tumor cells growing in cell culture, *in vivo* in the inner parts of the tumor and in the invasion front of colorectal liver metastases

POSTERS

Comparison of global gene expression profiles of tumor cells growing in cell culture and *in vivo* in the inner parts and in the invasion front of colorectal liver metastasis at 90th annual conference of the **German Society of Pathology** in Berlin between 19-21 April 2006.

Differential regulation of gene and gene expression profiles in the tumor epithelium of the invasionfront of colorectal liver rmetastasis at 22nd Annual conference of the **German Association for the Study of Liver** in Leipzig between 20-21 January 2006.

Global analysis of host tissue gene expression in the invasive front of colorectal liver metastases at 21st Annual conference of the **German Association for the Study of Liver** in Ulm between 28-29 January 2005.

Differential regulation of gene and gene expression profiles in the invasive front of colorectal liver metastasis at annual conference of the **Arbeitsgemeinschaft Gastroenterologische Onkologie** (AGO), Aachen, March 2005.

Micropropagation of *Gardenia*, *Vanilla platifolia*, *Beeta vulgaris* and *Decalepis hamiltonii* at **New Origins in Biotechnology** 2002, organized by The Department of Applied Botany and Biotechnology, University of Mysore, India .

Micropropagation and acclimatization of *Decalepis hamiltonii* an endangered shrub to plains which normally grow in high altitudes - Organized by The **Society of Plant Physiology** 2001, Muzaffar Nagar, India.

ACADEMIC HONOURS

Poster prize from the German Society for the Study of Liver 2005 (Shared with PD.Dr.Karsten Brand)

Poster prize from the Arbeitsgemeinschaft Gastroenterologische Onkologie (AGO) Jahrestagung der AGO, Aachen, 2005 (Shared with PD.Dr.Karsten Brand)

Senior Research Fellowship (SRF) from Council of Scientific and Industrial Research (CSIR), India Jan 2002.

Prize for presentation of Master thesis work from The Society of Biological Chemists (I), Central Food Technological Research Institute (CFTRI), Mysore, India Sept. 2000.

Department of Biotechnology **(DBT) fellowship** for biotech industrial research program, at Dabur Research Foundation from Nov. 1999 to May 2000.

EXTRACURRICULAR ACTIVITIES:

Member of the Organisation Committee: Society of Biological Chemists, India 2001

Regional Coordinator: International Foundation for prevention of birth disorders

Obul Reddy Bandapalli